



Application of Alpha-Repeat Proteins as Antiviral Molecules Against HIV-1 Targeting Viral Assembly or Maturation

Sudarat Hadpech

► To cite this version:

Sudarat Hadpech. Application of Alpha-Repeat Proteins as Antiviral Molecules Against HIV-1 Targeting Viral Assembly or Maturation. Virology. Université de Lyon; Mahāwitthayālai Chāng Mai, 2017. English. NNT : 2017LYSE1139 . tel-01628207

HAL Id: tel-01628207

<https://theses.hal.science/tel-01628207>

Submitted on 3 Nov 2017

HAL is a multi-disciplinary open access archive for the deposit and dissemination of scientific research documents, whether they are published or not. The documents may come from teaching and research institutions in France or abroad, or from public or private research centers.

L'archive ouverte pluridisciplinaire **HAL**, est destinée au dépôt et à la diffusion de documents scientifiques de niveau recherche, publiés ou non, émanant des établissements d'enseignement et de recherche français ou étrangers, des laboratoires publics ou privés.



N°d'ordre NNT : 2017LYSE1139

THESE de DOCTORAT DE L'UNIVERSITE DE LYON

opérée au sein de

l'Université Claude Bernard Lyon 1

Ecole Doctorale ED341-E2M2

Evolution Ecosystèmes - Microbiologie Modélisation

et

University of Chiang Mai

Faculty of Associated Medical Sciences

Diplôme de Doctorat

Soutenue publiquement le 18 Juillet 2017

par :

Mlle Sudarat HADPECH

**Nouveaux agents antiviraux dérivés de protéines cellulaires à motifs répétés
et ciblant l'assemblage du VIH**

Devant le jury composé de :

M. le Professeur ANDRE Patrice

Examineur

Mme. la Professeure CHAICAMPA Wanpen

Rapporteure

M. le Professeur MINARD Philippe

Rapporteur

Dr. KITIDEE Kuntida

Rapporteure

Dr. YASAMUT Umpa

Examinatrice

Dr. NANGOLA Sawitree

Co-Directrice de Thèse

Dr. HONG Saw-See

Directrice de Thèse

M. le Professeur TAYAPIWATANA

Directeur de Thèse

UNIVERSITE CLAUDE BERNARD - LYON 1

Président de l'Université	M. le Professeur Frédéric FLEURY
Président du Conseil Académique	M. le Professeur Hamda BEN HADID
Vice-président du Conseil d'Administration	M. le Professeur Didier REVEL
Vice-président du Conseil Formation et Vie Universitaire	M. le Professeur Philippe CHEVALIER
Vice-président de la Commission Recherche	M. Fabrice VALLÉE
Directrice Générale des Services	Mme Dominique MARCHAND
COMPOSANTES SANTE	
Faculté de Médecine Lyon Est – Claude Bernard	Directeur : M. le Professeur G.RODE
Faculté de Médecine et de Maïeutique Lyon Sud – Charles Mérieux	Directeur : Mme la Professeure C. BURILLON
Faculté d'Odontologie	Directeur : M. le Professeur D. BOURGEOIS
Institut des Sciences Pharmaceutiques et Biologiques	Directeur : Mme la Professeure C. VINCIGUERRA
Institut des Sciences et Techniques de la Réadaptation	Directeur : M. X. PERROT
Département de formation et Centre de Recherche en Biologie Humaine	Directeur : Mme la Professeure A-M. SCHOTT

COMPOSANTES ET DEPARTEMENTS DE SCIENCES ET TECHNOLOGIE	
Faculté des Sciences et Technologies	Directeur : M. F. DE MARCHI
Département Biologie	Directeur : M. le Professeur F. THEVENARD
Département Chimie Biochimie	Directeur : Mme C. FELIX
Département GEP	Directeur : M. Hassan HAMMOURI
Département Informatique	Directeur : M. le Professeur S. AKKOUCHE
Département Mathématiques	Directeur : M. le Professeur G. TOMANOV
Département Mécanique	Directeur : M. le Professeur H. BEN HADID
Département Physique	Directeur : M. le Professeur J-C PLENET
UFR Sciences et Techniques des Activités Physiques et Sportives	Directeur : M. Y.VANPOULLE
Observatoire des Sciences de l'Univers de Lyon	Directeur : M. B. GUIDERDONI
Polytech Lyon	Directeur : M. le Professeur E.PERRIN
Ecole Supérieure de Chimie Physique Electronique	Directeur : M. G. PIGNAULT
Institut Universitaire de Technologie de Lyon 1	Directeur : M. le Professeur C. VITON
Ecole Supérieure du Professorat et de l'Education	Directeur : M. le Professeur A. MOUGNIOTTE
Institut de Science Financière et d'Assurances	Directeur : M. N. LEBOISNE

Résumé de la thèse en Français

Au cours de notre programme de thèse, nous avons isolé et caractérisé des molécules protéiques à activité antivirale intracellulaire dirigée contre le VIH-1. Ces protéines, appelées α Rep, ont été obtenues par criblage d'une banque de protéines artificielles de nouvelle génération, construites de façon combinatoire à partir de protéines naturelles constituées de motifs alpha-hélicoidaux répétés. La cible virale (ou "appât") utilisée pour ce criblage est une région de la polyprotéine Gag du VIH-1 identifiée comme une cible privilégiée de nouvelles thérapeutiques antivirales, car essentielle à l'assemblage viral, l'empaquetage du génome viral et le clivage de maturation de Gag aboutissant à la formation de virions infectieux. Deux molécules d' α Rep à forte affinité pour la cible virale, l' α Rep4E3 (32 kDa; 7 motifs répétés) et l' α Rep9A8 (28 kDa; 6 motifs répétés) ont ainsi été isolées, clonées et caractérisées. L'étude de l'activité anti-VIH intracellulaire de ces α Rep a été réalisée dans différents systèmes d'expression cellulaire, nécessitant la construction de lignées stables de cellules d'insecte et de cellules épithéliales humaines, et leur infection par différents types de vecteurs viraux recombinants, baculovirus ou lentivirus, porteurs du gène rapporteur luciférase. Mais surtout, notre étude a été menée sur des cellules lymphocytaires-T (SupT1), cibles naturelles du virus, exprimant ces α Rep et infectées par du VIH-1 naturel infectieux. Nos résultats ont montré que l' α Rep4E3 et l' α Rep9A8 ont toutes deux un effet négatif significatif sur le cycle réplcatif du VIH-1, mais ciblent des fonctions virales différentes. L' α Rep4E3 bloque l'empaquetage du génome viral, tandis que l' α Rep9A8 inhibe la maturation et diminue l'infectivité virale. De plus, l' α Rep9A8, exprimée de façon constitutive dans les cellules SupT1, leur confère une résistance au VIH: une lignée de SupT1 chroniquement infectée par le VIH-1 a pu être ainsi isolée et maintenue en culture pendant plusieurs semaines, sans effet cytopathique viro-induit apparent. Ces nouvelles données auront des implications non-négligeables dans le choix et la conduite de futures stratégies de thérapie cellulaire anti-VIH.

Mots-clés: VIH-1; antivirals; designed molecular scaffolds; HEAT-like repeat; α Rep protéine

ABSTRACT

Human immunodeficiency virus type 1 (HIV-1) infection is a long-term disease which required a long-life treatment. Besides the standard highly active retroviral therapy (HAART) regiment, HIV-1 gene therapy is one of a promising alternative strategy which give rise to hope for better HIV-1 treatments. In addition, protein-based therapeutics represent another promising approach which show the high impact results in curing various types of diseases. Nowadays, it has already become a significant part of the current medical treatments. In this study, we focused on α Rep proteins, the non-immunoglobulin scaffold proteins which were designed to target nucleocapsid (NC) domain of HIV-1 Pr55Gag polyprotein precursor and investigated their possible roles as intracellular therapeutic agents. Phage display technology was used for the specific isolation of α Rep against a critical C-terminal region of the HIV-1 Pr55Gag (CA₂₁-SP1-NC) from a large and diverse α Rep phage library. Several strong α Rep binders were thus isolated, but only two binders, referred to as α Rep4E3 and α Rep9A8, were further characterized. The α Rep4E3 contains 7 internal repeat motifs (32 kDa), whereas α Rep9A8 has 6 repeat motifs (28 kDa). Both α Rep proteins were expressed at high level in a conventional bacterial expression system, and were recovered at high yields in soluble form. Their potential antiviral activity was investigated using different cell systems. The baculovirus system was used for determining the antiviral effects on virus-like particle (VLP) production of both α Rep scaffold molecules. Sf9 cells stably expressing N-myristoylated α Rep4E3 and α Rep9A8 fused to the GFP reporter protein at their C-termini were infected with a recombinant baculovirus carrying the gene encoding the HIV-1 Pr55Gag polyprotein (AcMNPV^{gag}), and the antiviral effects were evaluated by quantitative and qualitative methods. The results showed that N-myristoylated α Rep4E3 and α Rep9A8 qualitatively altered the particle formation and were coencapsidated with Pr55Gag into the VLPs released into the culture supernatant. The different patterns of particle morphology were observed by electron microscopy. The α Rep4E3-expressing cells mainly produce aberrant VPLs, while α Rep9A8 expression induces the accumulation of Pr55Gag at the plasma membrane of

AcMNPV^{gag}-infected Sf9 cells. In the human T cell line system, α Rep4E3 and α Rep9A8 proteins were expressed intracellularly by transducing SupT1 cell with SIN CGW lentiviral vector carrying the α Rep genes fused to the EGFP coding sequence at their 3'-end. These stable SupT1 cell lines were then challenged with HIV-1_{NL4-3}. The results indicated that both α Rep4E3 and α Rep9A8 displayed antiviral effects, which occurred at the late steps of the HIV-1 life cycle, with no effect on proviral DNA integration. Reduction and delay in the viral progeny production were found in infected SupT1 expressing α Rep4E3-EGFP and α Rep9A8-EGFP. Difference in the antiviral mechanism was observed between these two α Rep proteins: α Rep4E3-EGFP mainly interferes with the packaging of the viral genomic RNA, while α Rep9A8-EGFP interferes with the proteolytic processing of Pr55Gag polyprotein, and performs as a protease inhibitor to prevent the HIV-1 protease cleavage which is required for the production of newly infectious mature virions. Interestingly, SupT1 expressing α Rep9A8-EGFP is able to survive to chronic HIV-1 infection up to 38 days after infection, with a low level of noninfectious HIV-1 particle production. Taken together, our results suggested that α Rep, a new type of scaffold protein, could serve as a promising alternative antiviral agent which would influence the future strategies and candidates of antiviral molecules to be used in anti-HIV-1 cell therapy.

Keywords: HIV-1; antivirals; designed molecular scaffolds; HEAT-like repeat; α Rep proteins

บทคัดย่อ

การติดเชื้อไวรัสเอชไอวี 1 ก่อให้เกิดโรคติดเชื้อเรื้อรังที่ต้องรักษาตลอดชีวิต นอกเหนือไปจากการรักษาด้วยยาต้านไวรัสซึ่งเป็นการรักษามาตรฐานในปัจจุบันแล้ว การรักษาด้วยยีนถือเป็นอีกหนึ่งแนวทางใหม่ที่จะช่วยเพิ่มความหวังในการรักษาให้ดีขึ้น โดยทำการออกแบบยีนที่กำหนดการสร้างโมเลกุลที่มีประสิทธิภาพในการยับยั้งการแบ่งตัวของเชื้อไวรัส ในการศึกษาครั้งนี้เป็นครั้งแรกที่ใช้ยีนสำหรับสร้างโปรตีนแอลฟารีฟิทซึ่งเป็นโปรตีนโครงสร้างพิเศษที่แตกต่างไปจากแอนติบอดี มาทดสอบการยับยั้งวงจรชีวิตของไวรัสเอชไอวี 1 โดยทำการคัดเลือกโปรตีนแอลฟารีฟิทที่สามารถจับได้กับบริเวณนิวคลีโอแคพซิด ซึ่งเป็นส่วนหนึ่งของโปรตีนโครงสร้างของเชื้อไวรัสโดยเทคนิคฟาจดิสเพลย์ พบว่าสามารถคัดเลือกโปรตีนแอลฟารีฟิทโคลนที่จับอย่างจำเพาะได้ 2 โคลนคือ ลีอีสาม (α Rep4E3) และเก้าเอแปด (α Rep4E3) ซึ่งโปรตีนแอลฟารีฟิทดังกล่าวนี้ประกอบไปด้วยจำนวนรีฟิท 7 รีฟิท มีขนาดโมเลกุล 32 กิโลดาลตัน และ 6 รีฟิท มีขนาดโมเลกุล 28 กิโลดาลตัน ตามลำดับ โปรตีนทั้งสองโมเลกุลมีระดับการแสดงออกที่สูงและมีความคงตัวสูงในเซลล์หลายชนิดทั้งในแบคทีเรีย เซลล์แมลง และเซลล์มนุษย์ จากนั้นนำยีนของโปรตีนทั้งสองโคลนนี้เข้าสู่เซลล์เพื่อทดสอบฤทธิ์ในการยับยั้งวงจรชีวิตของเชื้อไวรัสภายในเซลล์ ทั้งในเซลล์แมลงชนิดเอสเอฟเก้า (SF9) และในเซลล์เม็ดเลือดขาวของมนุษย์ชนิดทีเซลล์ (SupT1) ซึ่งการทดสอบผลของแอลฟารีฟิททั้งสองในการรบกวนการผลิตอนุภาคเสมือนไวรัส (VLP) โดยใช้เซลล์แมลงนั้น ได้ทำการออกแบบให้โปรตีนแอลฟารีฟิทมีการแสดงออกในรูปแบบที่มีโมริสติกแอซิดติดอยู่ด้านหางปลายอะมิโนและเชื่อมต่อโปรตีนเรืองแสงสีเขียว (GFP) เข้าไปทางด้านปลายคาร์บอกซิลิก จากนั้นจึงติดเชื้อเซลล์ดังกล่าวด้วยแบคทีริโอไฟต์ไวรัส AcMNPV^{gag} ที่ทำหน้าที่ในการนำส่งยีนกำหนดการสร้างโปรตีนแกก (Gag) ของไวรัสเอชไอวี 1 และติดตามผลการรบกวนการสร้าง VLP ในเซลล์ดังกล่าว จากผลการทดลองพบว่าโปรตีนแอลฟารีฟิททั้งสองมีผลทำให้การประกอบอนุภาคของไวรัสแปรเปลี่ยนไปในเชิงคุณภาพ พบรูปแบบที่แตกต่างกันทางสัณฐานวิทยาของ VLP ซึ่งเป็นผลมาจากฤทธิ์ของโปรตีนแอลฟารีฟิทเมื่อศึกษาโดยใช้กล้องจุลทรรศน์อิเล็กตรอน โดยสังเกตพบว่า α Rep4E3 มีฤทธิ์ส่งเสริมให้มีการผลิต VLP ที่มีรูปร่างผิดปกติ ในขณะที่ α Rep9A8 มีผลทำให้เกิดการสะสมของโปรตีน Gag ที่ผนังเซลล์ SF9 และพบอีกว่าโปรตีนแอลฟารีฟิททั้งสองถูกบรรจุเข้าไปในอนุภาค VLP จากนั้นจึงทำการศึกษาฤทธิ์ของโปรตีนแอลฟารีฟิทต่อในเซลล์เม็ดเลือดขาวของมนุษย์ชนิด SupT1 โดยได้ออกแบบโปรตีนแอลฟารีฟิททั้งสองให้มีการแสดงออกภายในเซลล์ได้อย่างต่อเนื่องโดยได้เชื่อม

EGFP ไว้ทางด้านปลายปลายคาร์บอกซิลิกของโปรตีน จากนั้นทำการติดเชื้อเซลล์ที่มีการแสดงออกของโปรตีนแอลฟารีฟิทั้งสองชนิดด้วยไวรัสเอชไอวีที่ 1 สายพันธุ์ NL4-3 ที่ 1 MOI ติดตามผลการทดลองพบว่าโปรตีนแอลฟารีฟิทั้งสองตัวมีความสามารถในการด้านการเพิ่มจำนวนของไวรัสและพบอีกว่าโปรตีนแอลฟารีฟิทั้งสองออกฤทธิ์ในช่วงท้ายของวงจรชีวิตของเอชไอวีโดยที่ไม่มีผลในการยับยั้งการฝังตัวของดีเอ็นเอของไวรัสในโครโมโซมของเซลล์ติดเชื้อ นอกจากนั้นพบว่าไวรัสตัวใหม่สร้างได้น้อยลงและช้าลงในเซลล์ที่มีการแสดงออกของโปรตีนแอลฟารีฟิทั้งสอง และยังพบอีกว่ากลไกในการยับยั้งไวรัสนั้นแตกต่างกันระหว่างโปรตีนแอลฟารีฟิทั้งสองตัว โดย α Rep4E3 มีฤทธิ์ในการรบกวนการบรรจุอาร์เอ็นเอจีโนมเข้าไปในอนุภาคไวรัส ในขณะที่ α Rep9A8 พบว่ามีการรบกวนกระบวนการสร้างไวรัสที่สมบูรณ์ (maturation) โดยทำหน้าที่เสมือนเป็นตัวขัดขวางเอ็นไซม์โปรติเอสไม่ทำให้สามารถเข้าตัดโปรตีน Gag ได้ ซึ่งขั้นตอนดังกล่าวนี้มีความจำเป็นสำหรับการผลิตไวรัสตัวเต็มวัยตัวใหม่ อีกทั้งยังพบประเด็นที่น่าสนใจว่าเซลล์ SupT1 ที่มีการแสดงออกของ α Rep9A8 สามารถรอดชีวิตนานถึง 38 วันในสถานะที่เป็นการติดเชื้อเรื้อรัง พบการสร้างไวรัสตัวไม่เต็มวัยและไม่สามารถในการติดเชื้อออกมาในน้ำเพาะเลี้ยงในระดับต่ำ จากการศึกษาทั้งหมดนี้สามารถกล่าวได้ว่าโปรตีนแอลฟารีฟิเป็นโปรตีนชนิดใหม่ซึ่งถือเป็นทางเลือกที่น่าสนใจสำหรับการนำมาใช้ในการพัฒนาเป็นโมเลกุลต้านไวรัสและสามารถนำมาต่อยอดเพื่อการพัฒนาเซลล์ต้านไวรัสเอชไอวีเพื่อใช้ในการรักษาได้

ACKNOWLEDGEMENTS

This thesis is the story which has been arisen for several years in my Ph.D. study. I would say that it is such a great and wonderful memories. However, I will never forget experiencing many important lessons, hard examinations, late night experiments and the stressful I have when I wrote this thesis. During my study program, I have had a very great honor to work with a large number of amazing people. It would not have been possible to finish this thesis without their warm help, support, guidance, and friendship. It also would not have been possible to finish this thesis without financial support throughout my education. I would like to take this opportunity to express that this thesis is the result of many experiences I have encountered from dozens of remarkable individuals who I wish to acknowledge.

First and foremost I wish to express my deepest gratitude and sincere appreciation to my thesis supervisor, Prof. Dr. Chatchai Tayapiwatana, for giving me a great opportunity to be a Ph.D. student under his supervision. It has been a great honor to be his student, not only because of his tremendous academic support but also because he is one of the great teachers and researchers I have ever met in my life. His guidance helped me in all the time of studying and writing of this thesis. He has always made himself available to clarify my doubts despite his busy schedules. I could not have imagined having a better advisor and mentor for my Ph.D. study. He is the type of person called "polymath" which means "a man can do all things if he would like to". I really wish that someday I could be as enthusiastic and energetic as Prof. Chatchai and to someday be able to command an audience as well as he can.

I am extremely grateful to express my gratitude and appreciation to Dr. Saw-See Hong and Prof. Pierre Boulanger, my thesis advisors from UMR754, UCBL, and my parents in Lyon for their support, guidance, and taking care of me. They are the beginning of alpha repeat proteins project, the beginning of this thesis work. Dr. Saw-See is the one that changed my perspective on life. I see things more in a positive way after I know her. I have learned to be more kind, sweet, and be a positive thinking person than I was.

Prof. Pierre is a rare type of man I know, I mean it in a good way. He is like a big mobile library with a large storage capacity. He always makes me surprise that how can one man packs all that knowledge inside the brain, not only about sciences but also many others; history, archeology, architecture, and politic, and everything. I must thank you for all of your kind, supportive, encouragement, insightful comments and hard questions during thesis writing and manuscript preparation. Finally, I would like to thank you for taking care of me like a family, without you two, living in France for two years could not be this happy.

I take this opportunity to sincerely acknowledge Prof. Dr. Watchara Kasinrerker for valuable advice, kindly providing monoclonal antibodies, and support laboratory equipment. I also thanks to Dr. Supansa Pata, and other members of Prof. Dr. Watchara Kasinrerker's laboratory for their technical support and kind help.

I must express my grateful thanks to Dr. Sawitree Nangola from Division of Clinical Immunology and Transfusion Sciences, School of Allied Health Sciences, the University of Phayao. I remember well that she is my first teacher who teaches me how to work in the laboratory since I started working as research assistance 6 years ago before register to graduate school. Since that she is still and will always be my teacher. I would like to thank for her valuable advice, suggestion, support, encouragement, and kindness. This thesis work would not have been completed without her help even in the last experiment that I thought it was impossible, but she makes it possible.

I additional need to express my appreciation to Dr. Kuntida Kitidee from Center of Development and Technology Transfer, Faculty of Medical Technology, Mahidol University for her advice, suggestion, supportive, understanding and personal attention which have provided good and smooth basis for my Ph.D. tenure.

I would like to express my appreciation to Dr. Supachai Sakkhachornphop at Research Institute for Health Sciences (RIHES), Chiang Mai University for cell culture, viral propagation, and flow cytometer facility. I am also thankful Miss Chansunee Panto for technical assistance and her friendship

I would like to extend an individual special acknowledge to many people. All of fellow labmates in CT lab, Mr. Somphot Saoin, Miss Wannisa Khamaikawin, Miss Kannaporn Intachai, Mr. Warachai Praditwongwan, Miss Tanchanok Wisitponchai, Miss Supattra Suwanpairoj, Miss Wannarat Jinathep, Miss Kanokwan Samerjai, Mr. Koolawat Chupradit and Mr. Supirat Moonmuang for their warm friendship and taking care me as brother as sister. I would express my special thanks to Miss Weeraya Thongkum for her supportive, encouragement, and taking care of me. I also would like to thank to Mrs. Kongkham patumwan for her kindness. I would like to special thank Mrs. Tuanjai Ponsung for the best services in official document preparations.

I would like to express my grateful to Madame Sylvie Farget for her constant secretarial aid and her kindness and friendly, Madame Marie-Pierre Confort for her skillful technical assistance and friendship, Madame Elisabeth Errazuriz and Madame Christel Cassin (Centre d'Imagerie Quantitative de Lyon-Est) for their valuable assistance in electron microscopy. Moreover, I must extend an individual special acknowledge to all of my friends, Mr. Wilhelm Furnon, Miss Najate Ftaich, Miss Maryline Gomes, Miss Claire Cancia, Mr. Franck Touret, Miss Margot Enguehard, Miss Emma Reungoat, Mr Nicolas Baillet, and Miss Cyrielle Vituret for their warm welcome and friendship.

The work in Thailand was supported by the Centre of Biomolecular Therapy and Diagnostics (CBTD), the Ph.D. Franco-Thai scholarship program (2013) of the French Government, the 50th CMU Anniversary Ph.D. Program, and the Faculty of Pharmaceutical Sciences, Burapha University. The work in Lyon was financed by the Ministry of Foreign Affairs, and the Cystic Fibrosis French Association.

Last but not the least, I would like to thank my family: my parents Mr. Sumrit Hadpech, Mrs. Nongyao Hadpech and to my brothers Mr. Warayut Hadpech for supporting me spiritually throughout writing this thesis and my life in general. Thank you for always believing in me and support my decision. I would like to thank my beloved cats Cookie and Candy for their love.

Sudarat Hadpech

CONTENTS

	Page
Abstract in French	3
Abstract in English	4
Abstract in Thai	6
Acknowledgements	8
List of Tables	15
List of Figures	16
List of Abbreviations	18
Statement of originality in English	23
Chapter 1 Introduction	24
1.1 Literature review	26
1.1.1 Human immunodeficiency virus type 1 (HIV-1)	26
1.) HIV life cycle	26
2.) HIV-1 structural proteins	29
3.) Matrix (MA)	31
4.) Capsid (CA)	31
5.) Nucleocapsid (NC)	32
6.) Spacer peptides 1 and 2 (SP1 and SP2)	32
7.) p6 protein	34
8.) HIV-1 genome	34
9.) HIV-1 Antiviral Therapy	37
10.) Entry inhibitors	37
11.) Nucleoside reverse transcriptase inhibitors	38
12.) Non-nucleoside reverse transcriptase inhibitors	38

13.) Integrase strand transfer inhibitors	38
14.) Protease inhibitors	39
15.) Assembly and Maturation inhibitors	39
1.1.2 Scaffold proteins	42
1.) α Rep proteins	43
1.1.3 Phage-display technology	47
1.1.4 Baculovirus	50
1.1.5 Lentivirus vectors	55
Objectives	59
Chapter 2 Materials and Methods	60
2.1 Chemicals and equipments	60
2.2 <i>E. coli</i> strains	60
2.3 Plasmids and vectors	60
2.4 Cells	61
2.5 Construction of α Rep library	61
2.6 Screening of α Rep phage library on the viral targets	62
2.7 Production of α Rep proteins	63
2.7.1 Construction of pQE-31 expression vectors for soluble α Rep proteins production	63
2.7.2 Expression and purification of α Rep proteins	63
2.8 Western immunoblotting	65
2.9 Construction of Sf9 stable cell lines stably expressing α Rep proteins fused to GFP	65
2.9.1 Construction of pIB vectors expressing (Myr+) α Rep4E3-GFP and pIB_(Myr+) α Rep9A8-GFP	65
2.9.2 Establishment of Sf9 cells stable expressing (Myr+) α Rep4E3-GFP and pIB_(Myr+) α Rep9A8-GFP	66
2.10 Luciferase-based quantitative assay of α Reps on HIV-1 VLP assembly	66
2.11 Electron microscopy analysis of HIV-1 Gag assembly into VLPs in Sf/(Myr+) α Rep4E3GFP or Sf/(Myr+) α Rep9A8GFP	68
2.12 Construction of lentiviral vectors	68

2.13 Production of VSV-G-pseudotyped lentiviral vectors	69
2.14 Construction of SupT1 stable cell lines stably expressing α Rep proteins	70
2.15 Flow cytometry	72
2.16 Confocal microscopy	72
2.17 HIV-1 stock	73
2.18 Evaluation of antiviral activity of α Rep proteins in SupT1 stable cell lines	73
2.18.1 Determination of p24 level by p24 antigen ELISA	74
2.18.2 Quantitation of integrated proviral DNA by SYBR RT-PCR-based integration assay	74
2.19 Infectivity Assay of HIV-NL4-3 derived from SupT1 cells lines stably expressing α Rep proteins	74
2.20 ELISA based HIV-1 Pr55Gag maturation assay	75
2.21 Generation of HIV-1 target proteins	75
2.22 Protein pull-down assays	77
Chapter 3 Results	78
3.1 A new scaffold protein library and the CA ₂₁ -SP1-NC domain of the Gag polyprotein precursor as target	78
3.2 Selection of CA ₂₁ -SP1-NC binders from a library of phage displayed α Rep proteins	80
3.3 Biochemical and biophysical characterization of CA ₂₁ -SP1-NC binders	82
3.4 Effects of α Rep4E3 and α Rep9A8 on HIV-1 virus-like particle assembly	86
3.4.1 Construction of Sf9-derived cell lines stably expressing α Rep proteins	86
3.4.2 Biological effects of α Rep4E3 and α Rep9A8 on HIV-1 virus-like particle production in heterologous system: quantitative aspects	88
3.4.3 Biological effects of α Rep4E3 and α Rep9A8 on HIV-1 VLP production in heterologous system: qualitative aspects	91

3.4.4 Co-encapsidation of (Myr+)αRep4E3-GFP and (Myr+)αRep9A8-GFP into VLPs	94
3.5 Expression of αRep4E3-GFP and αRep9A8-GFP proteins in HeLa cells using a lentiviral vector	96
3.6 Construction of SupT1 cell lines stably expressing αRep proteins	98
3.7 αRep4E3- and αRep9A8-mediated protection of SupT1 cells against HIV-1 infection	100
3.7.1 Determination of HIV-1 production by CAp24-ELISA	100
3.7.2 HIV-1 proviral DNA detection	103
3.7.3 Status of the extracellular HIV-1 genomic RNA molecules	103
3.7.4 Cell viability and αRep protein expression in HIV-1 infection SupT1 cells	106
3.8 Molecular mechanisms of the antiviral functions of αRep4E3 and αRep9A8	108
3.8.1 Influence of αRep4E3 and αRep9A8 on HIV-1 infectivity: (i) maturation of the Pr55Gag precursor	108
3.8.2 Influence of αRep4E3 and αRep9A8 on HIV-1 infectivity: (ii) encapsidation of the viral genome	111
3.8.3 Intracellular interaction of αRep and Gag proteins in HIV-1 infected cells	113
3.9 Mapping of the αRep binding sites on the viral Gag target	115
Chapter 4 Discussion	118
Chapter 5 Conclusion	125
References	127
List of publications	138
Appendix A	139
Appendix B	144
Appendix C	145
Curriculum Vitae	152

LIST OF TABLES

	Page
Table 1 HIV-1 proviral integration in SupT1 cells harvested at day 14 pi.	103

LIST OF FIGURES

	Page
Figure 1.1 Schematic overview of the HIV- 1 replication cycle	28
Figure 1.2 Diagram of HIV-1 virus particle structure	30
Figure 1.3 Schematic representation of the HIV-1 genome	36
Figure 1.4 Design of the α Rep motif	45
Figure 1.5 Structure of filamentous phage	50
Figure 1.6 Structure of baculovirus virions	53
Figure 1.7 Baculovirus life cycle	54
Figure 1.8 Schematic representation of HIV vectors	58
Figure 2.1 The schematic figure of pQE-31 vectors construction for expression of 6xHis-tagged α Rep proteins in bacterial cells	64
Figure 2.2 Luciferase based VLP assembly assay	67
Figure 2.3 The schematic figure of CGW lentiviral transfer vectors construction for stable expression of α Rep proteins in target cells	69
Figure 2.4 Production of VSV-G pseudotyped lentiviral vector particles	71
Figure 2.5 CA ₂₁ -SP1-NC full-length bait and deletants	76
Figure 3.1 Amino acid sequences and the NMR structure of the SP1 nucleocapsid (NC)-SP2 domain of HIV-1 Gag polyprotein.	79
Figure 3.2 Screening of α Rep clones from the third round of panning	81
Figure 3.3 Target-binding activity of α Reps against GST-CA ₂₁ -SP1-NC	83
Figure 3.4 Amino acid sequence, production and purification of α Rep4E3 and α Rep9A8	85

Figure 3.5	Construction of Sf9 cells stably expressing N-myristoylated α Rep4E3-GFP and N-myristoylated α Rep9A8-GFP	87
Figure 3.6	Biological effects of α Rep4E3 and α Rep9A8 on HIV-1 VLP assembly	90
Figure 3.7	Morphological analysis of VLPs from α Rep4E3-expressing insect cells	92
Figure 3.8	Morphological analysis of VLPs from α Rep9A8-expressing insect cells	93
Figure 3.9	SDS-PAGE & Western blot analysis of gradient fractions	95
Figure 3.10	Confocal microscopy of HeLa cells expressing α Reps	97
Figure 3.11	Fluorescence microscopy and flow cytometry analysis of SupT1 cells transduced by a lentiviral vector	99
Figure 3.12	α Rep4E3 and α Rep9A8-mediated protection of SupT1 cells against HIV-1 challenge	102
Figure 3.13	Concentration of HIV-1 genome copies in cell culture supernatants	104
Figure 3.14	Extracellular viral genomes released by HIV-1 infected, α Rep-expressing SupT1 cells	105
Figure 3.15	Total cell number, cell viability and cell morphology after challenge with HIV-1 _{NL4-3}	107
Figure 3.16	Maturation cleavage of Pr55Gag in viral particles released by different cell types	110
Figure 3.17	Viral infectivity assay based on Jurkat-GFP re-infection.	112
Figure 3.18	Confocal microscopy of HIV-1 infected, α Rep-expressing SupT1 cells	114
Figure 3.19	CA ₂₁ -SP1-NC full-length bait and deletants	116
Figure 3.20	SDS-PAGE Western immunoblotting of protein pull-down assay representation the binding sites of α Rep proteins on the viral target	117
Figure 4.1	Schematic representation of the distinct antiviral effects of α Rep4E3 and α Rep9A8 in HIV-1 infected SupT1 cell	124

LIST OF ABBREVIATIONS

%	percent
5'UTR	5' untranslated region
°C	degree celsius
αRep	alpha repeat protein
AcMNPV	<i>Autographa californica</i> Multicapsid Nucleopolyhedrovirus
AIDS	acquired immune deficiency syndrome
AR	ankyrin
ARM	armadillo
ART	antiretroviral therapy
BA	betulinic acid
BSA	bovine serum albumin
BV	baculovirus
BVM	bevirimat
bp	base pair (s)
CA	capsid
CCR5	C-C chemokine receptor type 5
CD	cluster of differentiation
CMV	cytomegalovirus
CRISPR	clustered regulatory interplaced short palindromic repeat
CRM1	chromosome region maintenance 1
Ct	threshold cycle
CTD	carboxyl terminal domain
DAPI	4',6-diamidino-2-phenylindole
DARPin	designed ankyrin repeat proteins
DMEM	Dulbecco's Modified Eagle's medium
DNA	deoxyribonucleic aci

EDTA	ethylenediaminetetraacetic acid
EF3	elongation factor 3
EGFP	enhanced green fluorescent protein
ELISA	enzyme-linked immunosorbent assay
Env	envelope
ESCRT	endosomal sorting complex required for transport
FBS	fetal bovine serum
FI	fusion inhibitor
Fwd	forward
g	gram (s)
GFP	green fluorescent protein
GST	glutathione S-transferases
h	hour (s)
HAART	highly active antiretroviral therapy
HBV	hepatitis B virus
HEAT	huntingtin, elongation factor 3, protein phosphatase 2A, yeast kinase TOR1
HEK293T	human embryonic kidney cell
HER2	human epidermal growth factor receptor 2
HGF	hepatocyte growth factor
HIV	human immunodeficiency virus
HIV-1	human immunodeficiency virus type 1
HRP	horseradish peroxidase
Ig	immunoglobulin
IN	integrase
INSTI	integrase strand transfer inhibitor
IPTG	isopropyl β -D-1-thiogalactopyranoside
kb	kilobases
kDa	kiloDaltons
LB	Luria-Bertani

LEDGF	lens epithelium-derived growth factor
LLRs	leucine-rich repeats
LTR	long terminal repeat
Luc	luciferase
M	molar (s)
MA	matrix protein
MFI	mean fluorescence intensity
mg	milligram (s)
min	minute (s)
ml	milliliter (s)
mM	millimolar (s)
MOI	multiplicity of infection
mRNA	messenger RNA
MW	molecular weight
Myr	myristoylation
NaOH	sodium hydroxide
NC	nucleocapsid
Nef	negative regulatory factor
Ni-NTA	nickel (II)-nitrilotriacetic acid complex
NRTI	nucleoside reverse transcriptase inhibitor
NTD	amino terminal domain
OD	optical density (-ies)
ODV	occlusion derived virus
ORF	open reading frame
PBMC	peripheral blood mononuclear cell (s)
PBS	phosphate buffered saline
PBS	primer binding site
PCR	polymerase chain reaction
PDB	protein data bank
pi	post infection

pfu	plaque-forming unit
PI	protease inhibitor
PIC	pre-integration complex
PI(4,5)P ₂	phosphatidylinositol 4, 5-bisphosphate
PP2A	protein phosphatase 2A
PR	protease
Pr55Gag	gag polyprotein precursor
P-TEFb	positive transcription elongation factor b
RCA	rolling circle amplification
RCLs	replication competent lentiviruses
RLU	relative luminescence unit
RPMI	Roswell Park Memorial Institute medium
RNA	ribonucleic acid
RNAi	RNA interference
RNA pol II	RNA polymerase II
RSV	rouv sacroma virus
RT	reverse transcriptase
RT	reverse transcription
scFv	single chain variable fragment
SDS-PAGE	sodium dodecyl sulfate-polyacrylamide gel electrophoresis
SIN	self-inactivating
SL1	stem-loop 1
SL3	stem-loop 3
SP1	spacer peptide 1
SP2	spacer peptide 2
ssDNA	single-stranded DNA
scFv	single chain variable fragment
TALENs	transcription activator-like effector nucleases
TAR	trans-activation response
Tat	trans-activator protein

TBS	Tris buffer saline
TMB	3,3',5,5'-Tetramethylbenzidine
TOR1	yeast kinase TOR1
TPR	tetratricopeptide
U	unit (s)
VEGF-A	vascular endothelial growth factor A
VEGF-B	vascular endothelial growth factor B
VLP	viral-like particle
Vif	viral infectivity factor
Vpr	viral protein R
Vpu	viral protein U
VSV-G	vesicular stomatitis virus-G
μg	microgram (s)
μl	microliter (s)
WCL	whole cell lysate
WT	wild type
ZFN	zinc finger nuclease
ZFP	zing finger protein

STATEMENT OF ORIGINALITY

1. This thesis presents a new strategy to combat the HIV-1 infection by applying the α Rep protein, a new family of repeat protein scaffold based on HEAT-like repeat for the intracellular interfering and inhibiting the virus replication cycle at the viral genome packaging and the maturation step.
2. This thesis contains a part of the study that used the newly developed method for investigating the ratio of mature per immature virus particle in the sample. This new technique was developed based on the competitive ELISA combined with using the unique anti-MA antibody which recognizes the cleaved C-terminal of MA when processed by HIV-1 protease enzyme.

CHAPTER 1

INTRODUCTION

Long-term treatment of Human Immunodeficiency Virus 1 (HIV-1) infection can be readily achieved by combinations of antiretroviral agents, usually referred to as Highly Active Antiretroviral Therapy (HAART). The combination of antiviral drugs can result in the suppression of plasma viremia to less than the limit of quantification (< 50 copies/ml) with consequential improvement in the level of CD4⁺ T cell counts. This was which associated with the resolution of established opportunistic infections although they cannot eradicate the viruses due to latent viral reservoirs. In addition, prolonged treatment tends to result in the occurrence of multi-drug resistant mutants, drug-drug interaction and drug toxic effects. All these drawbacks justify the exploration of alternative therapeutic approaches such as gene therapy and cellular therapy in order to enhance the anti-HIV-1 response (1-8).

In the past 30 years we have witnessed the feasibility of gene and protein therapies for the treatment of diverse human diseases. These approaches apply the powerful genetic engineering which is applicable to the treatment of both genetic and acquired maladies ranging from blood diseases to the treatment of infectious diseases such as HIV infection. Antibody therapy is one of the successful strategy in which a molecule of antibody or antibody-derived protein scaffold is used as the therapeutic agents. Although it is one of the major commercial success of the biotechnology industry to date, antibody molecules have their limitations (9, 10).

In the past decade the development of protein engineering techniques had made it possible to generate novel repeat scaffold protein binders called non-immunoglobulin scaffolds. The absence of disulfide bond in these scaffold molecules is the key factor which makes them suitable for intracellular applications, particularly inside the cytosolic compartment in which the proper folding of bioactive proteins should not be influenced by the reducing conditions. In addition, unlike antibodies, scaffold proteins have less complexity in the

production processes. They can be expressed in bacterial cell systems with high production levels, high solubility and high stability. For these reasons, a number of scaffold molecules are now in the preclinical and clinical development stage. DARPins, the designed ankyrin repeat proteins which are genetically engineered antibody mimetic proteins typically exhibiting highly specific and high-affinity target protein binding. These most well-known scaffold molecules are today undergoing clinical trials for targeting various types of tumor antigens for example, DARPins targeting VEGF-A (phase II/III), VEGF-A/PDGF-B (preclinical), and VEGF/HGF (phase I) as well as another type of protein binder, affibodies which specific to HER2 is now in phase I (11).

Recently, it was established that a new type of artificial protein derived from the repeat protein family called Huntingtin, elongation factor 3 (EF3), protein phosphatase 2A (PP2A), and the yeast kinase TOR1 (HEAT repeat protein) has a potential advantage in comparison to other well-known scaffold proteins (12). The HEAT repeat is a tandem repeat protein with a structural motif composed of two alpha helices linked by a short loop. It can form alpha solenoids which are found in a number of cytoplasmic proteins, often involved in intracellular transport and protein-protein interactions (13). Various repeat protein binders can be isolated by powerful bio-panning methods such as phage display or ribosome display. Many repeat proteins have been isolated and characterized, and one good example is GFP/EGFP-binding α Reps (14). This repeat protein belonged to a new artificial repeat protein family in which their design is based on the thermostable HEAT-like repeats scaffold. They were able to colocalize with EGFP inside the different cell compartments without forming any aggregates or toxicity to the cells. Therefore, the α Rep proteins are molecules of choice for the study of intracellular processes in living cells, by their direct interactions with endogenous protein of interest. In the present study we would like to apply α Rep proteins to the development of a novel type of intracellular anti-HIV-1 treatment. The viral protein that we have targeted is a portion of the Pr55Gag polyprotein precursor overlapping the last 21 amino acids of the capsid (CA), the spacer peptide 1 (SP1), and the nucleocapsid domain (NC) which refers to CA₂₁-SP1-NC. Many evidences showed that the C-terminal domain of CA (CA_{CTD}) is critical for the formation of viral capsid core and Gag oligomerization/polymerization in the step of viral assembly.

SP1 domain has been shown to be involved in the correct particle assembly. Mutation in the key amino acid residues of SP1 especially the first four amino acids can alter the viral morphology and interfere the virus infectiveness. The NC region is essential for the viral genomic RNA packaging and promote Gag-Gag interaction. As mentioned, our target protein CA₂₁-SP1-NC is critical in the process of Pr55Gag assembly and genomic RNA packaging in HIV-1-infected cells, we therefore assumed that expressing α Rep proteins which specifically interact with this viral target CA₂₁-SP1-NC inside the cells might be possible to inhibit or interfere with the normal HIV-1 replication cycle.

1.1 Literature review

1.1.1. Human immunodeficiency virus (HIV)

The human immunodeficiency virus is a member of the genus *Lentivirus*, belonging to the *Retroviridae* family. When the viruses enter the body, they attack the immune system by specifically infecting the CD4+T cells, which help the immune system fight against infections. If improperly treated or left untreated, HIV reduces the number of CD4+T cells in the body, making the infected person susceptible to microbial infections or infection-related cancers. These opportunistic infections or cancers take advantage of the deficient immune system provoked by the viruses, called acquire immune deficiency syndrome (AIDS), the last stage of the HIV infection. There are two types of HIV, HIV-1 is the cause of the majority of HIV infections globally due to the high rate of viral production, while HIV-2, mainly present in Western Africa, is less pathogenic and shows a much lower rate of disease development (15, 16). In this study the literature review will be focused mainly on the HIV-1.

1.) HIV-1 life cycle

HIV-1 begins its life cycle when the mature viruses infect their target cells (Figure 1.1). There are many phases in the HIV-1 replication cycle. It begins with the viral entry (attachment and fusion), uncoating, reverse transcription, integration, particle assembly, budding, and maturation. During the virus entry phase, HIV-1 particle attaches to the membrane outside of a CD4+ T cells. Once attached, the virus can inject its genetic material, the viral

genomic RNA and viral enzymes into the cells. After that, one of the viral enzymes, the reverse transcriptase (RT) reverse transcribes the viral RNA into the viral DNA with a high proportion of transcription errors. This promotes a high mutation rate during the replication cycle. In the next-step, the viral DNA is integrated into the host chromosome by the action of the integrase enzyme (IN), which transforms the cells into a "factory" to produce large quantities of new HIV-1 virions. After virus integrates its genome into the host chromosome, the viral components which are produced by the infected cells move to the inner leaflet of the cell membrane, where they assemble into new virus particles called the viral progeny. The newly formed virus particles then egress from the cell membrane and the maturation phase occurs when the protease (PR) enzyme of the virus cleaves the immature viral structural proteins inside the particle to transform the particles into mature infectious virions. Since there are many crucial steps in the virus life cycle, antiviral drugs or antiviral strategies were designed to target these steps for example, fusion inhibitors, CCR5 inhibitors, nucleoside reverse transcriptase inhibitors (NRTIs), non-nucleoside reverse transcriptase inhibitors (NNRTIs), integrase strand transfer inhibitors (INSTIs), and protease inhibitors (PIs).

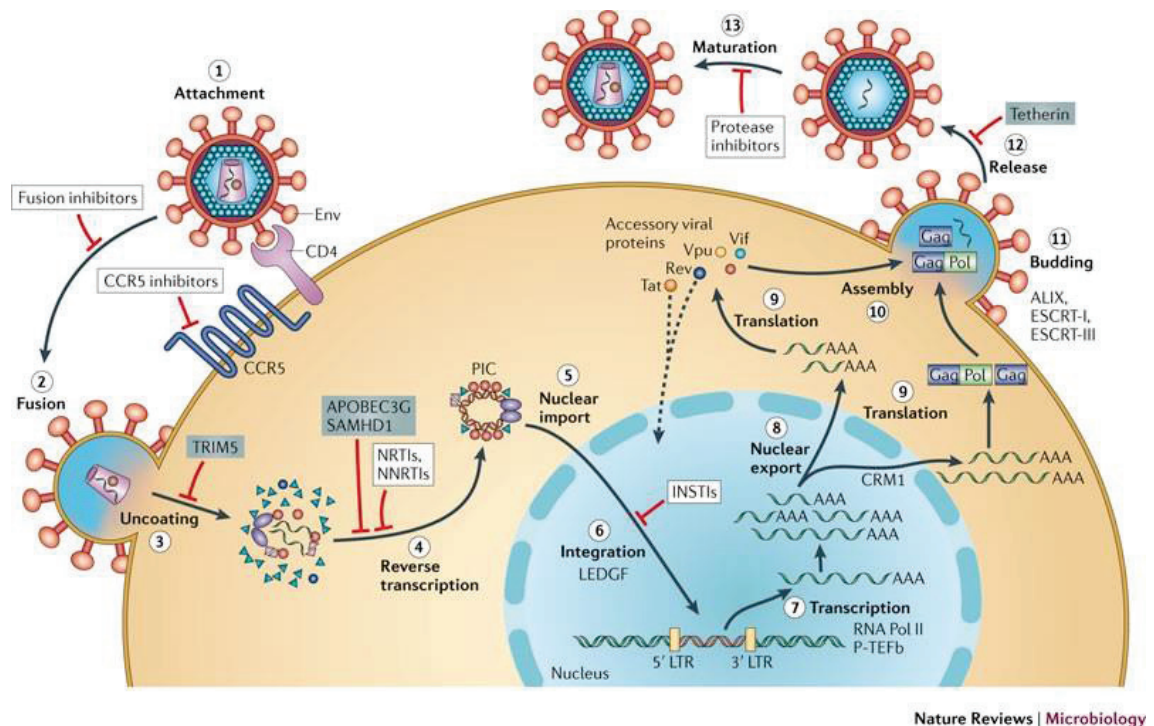


Figure 1.1 Schematic overview of the HIV-1 replication cycle. The HIV-1 infection begins when the viruses use envelope (Env) glycoprotein spikes bind to CD4 molecule and the co-receptor CC-chemokine receptor 5 (CCR5) (step 1), leading to fusion of the viral and cellular membranes and enter into the cell (step 2). The CA shell uncoating (step 3) facilitates reverse transcription (step 4), which in turn yields the pre-integration complex (PIC). Following import into the cell nucleus (step 5), PIC-associated integrase orchestrates the formation of the integrated provirus, aided by the lens epithelium-derived growth factor (LEDGF), the host chromatin-binding protein (step 6). Proviral transcription (step 7), mediated by host RNA polymerase II (RNA Pol II) and positive transcription elongation factor b (P-TEFb), generated the different sizes of viral mRNAs, the larger of which require energy-dependent export to leave the nucleus *via* host protein CRM1 (step 8). The viral protein production (step 9), and genome-length RNA is encapsidated into viral particles with other viral proteins (step 10). Viral-particle budding (step 11) and release (step 12) from the cell is mediated by ESCRT (endosomal sorting complex required for transport) complexes and ALIX and followed by protease-mediated maturation (step 13) to become an infectious viral particle. Each step in the HIV-1 life cycle is a potential target for antiviral intervention¹⁶⁵; the sites of action of clinical inhibitors (white boxes) and cellular restriction factors (blue boxes) are indicated. INSTI,

integrase strand transfer inhibitor; LTR, long terminal repeat; NNRTI, non-nucleoside reverse transcriptase inhibitor; NRTI, nucleoside reverse transcriptase inhibitor (17).

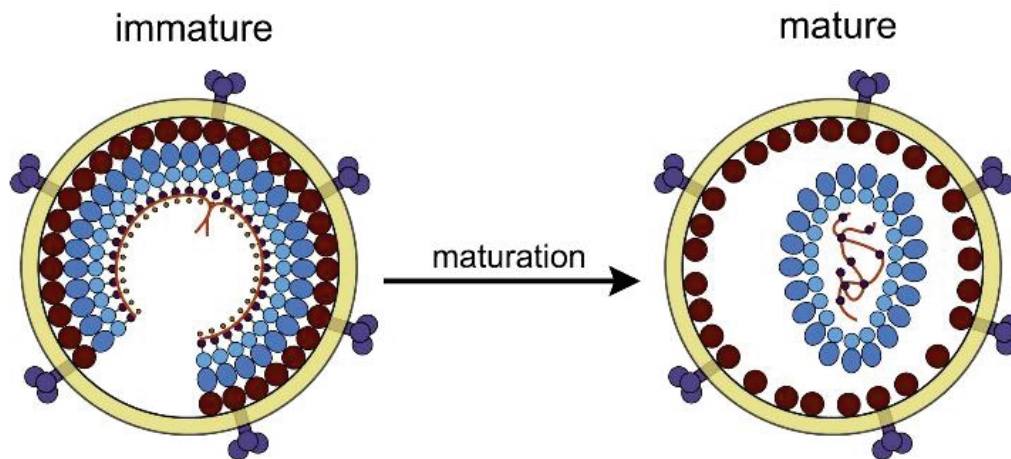
This figure has been obtained from the site:

<http://www.nature.com/nrmicro/journal/v10/n4/full/nrmicro2747.html>

2.) HIV-1 structural proteins

The proteins and gene functions of HIV-1 have been the subject of extensive research since the discovery of the virus in 1980s (18, 19). The formation of HIV-1 particles is driven by the viral structural protein, Gag polyprotein precursor (Pr55Gag) (20). The specific cleavage of Pr55Gag precursor by HIV-1 protease enzyme (PR) generates four major structural components of the mature virions including matrix (MA), capsid (CA), nucleocapsid (NC), and p6 protein and two spacer peptides (SP) which include SP1 and SP2 as shown in (Figure 1.2) (21, 22). Within the mature virions, MA domain is layered underneath membrane envelop meanwhile the shell of the core structure made of CA proteins. Inside the viral core, NC is tightly associated with the 2 copies of viral genomic RNA (23, 24). To be assemble into the new virions, the process begins at the inner leaflet of plasma membrane of the infected cells. When more than 2000 molecules of Pr55Gag and 200 Gag-Pol proteins and viral genomes are incorporated. The viral particles still in their immature form then egress from the infected cell. This form of the virus is non-infectious, and is not able to infect the new target cell as the Pr55Gag protein precursors have to be cleaved by the viral PR to generate a set of mature protein. These newly processed proteins then resemble to form mature particle morphology. MA is associated with the inner viral membrane envelope, CA assemble into conical capsid or viral cone, NC is interacted with the viral genomic RNA and packed inside the capsid core (Figure 1.2) together with viral enzymes, reverse transcriptase (RT), integrase (IN).

HIV-1 Virion:



HIV-1 gag:

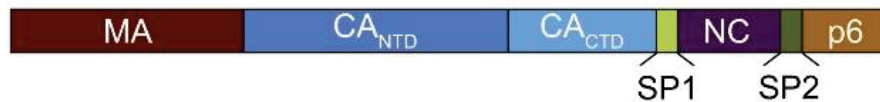


Figure 1.2 Diagram of HIV-1 virus particle structure. Top panel: Immature HIV-1 virus particle (left) and mature virus particle (right). Bottom panel: The compositions of HIV-1 Gag polyprotein, MA, CA (CA_{NTD} and CA_{CTD}), SP1, NC, SP2, and p6 respectively (25). This figure has been obtained from the site:

[http://www.cell.com/structure/pdf/S0969-2126\(10\)00355-2.pdf](http://www.cell.com/structure/pdf/S0969-2126(10)00355-2.pdf)

3.) Matrix (MA)

The MA protein is the domain of Pr55Gag which is located on the N-terminal side of the Gag precursor. The MA plays an important role in the trafficking of Pr55Gag to the plasma membrane. This process is mediated by its N-myristic signal, added to the N-terminus of Pr55Gag by cytoplasmic N-myristoyl-transferase co-acting with the Gag protein translational machinery. The membrane binding function of Gag is mediated by the insertion of myristoyl group of the myristic acid into the lipid bilayer particularly, the acidic phospholipid, PI(4,5)P2. Moreover, the highly conserved patch of basic residues of MA promotes the Gag membrane interaction. Apart from the membrane targeting function, MA is required for the incorporation of envelope (Env) glycoproteins, gp120 and gp41 into the virus particles. In addition, several studies showed that MA contains a RNA binding site which overlaps the PI(4,5)P2 binding domain. The interaction of MA with nucleic acid has been suggested to enhance the selectivity of MA for PI(4,5)P2-rich cellular membrane and prevent premature intracellular assembly (26-33).

4.) Capsid (CA)

The CA domain of Gag is critical for the viral particle assembly. In mature viral particles, CA forms the conical shape viral core observed in mature virions (23). The viral CA can be divided into two domains which have different functions in the particle morphogenesis. The N-terminal domain of CA (CA_{NTD}) comprises of two third of CA (Figure 1.2 bottom). CA_{NTD} is necessary for the mature core formation, but lacks the function necessary for the immature Gag polymerization process (34). The C-terminal domain of CA (CA_{CTD}) is critical for both core formation and Gag oligomerization/polymerization in the particle assembly process (28, 35-37). It has been reported that mutations in CA_{CTD} severely impede viral particle formation and Gag-Gag interaction (37).

5.) Nucleocapsid (NC)

The NC region of Gag, which lies downstream of the CA domain, has been shown to be important for the viral genomic RNA packaging and promoting Gag-Gag interactions (29). The NC domain contains two conserved CCHC zinc finger motifs coordinated with two zinc ions linked by a basic RAPRKKG sequence, and both N-terminal and C-terminal domain are flanked by flexible sequences (38). There is evidence suggesting that this domain is absolutely essential for the virus replication. The function of NC involves its interaction with RNA stem loops, a hundred nucleotide-long portion of the viral RNA which locates at the 5'-end of the untranslated region (UTR) of the viral RNA, and on the 5'-side of the *gag* initiation codon. This region contains the packaging signal, the so called *Psi* (ψ), which is required for the efficient encapsidation of the unspliced viral genome. Inside the mature virus particle, NC is found within the CA core where several molecules of NC coat the two copies of viral genetic material (38). Moreover, NC harbors another domain called interacting domain (I domain), which consists of basic residues mediating Gag-Gag interaction. Most of the studies review that primarily 'tethers' Gag molecules together *via* RNA bridges, then additional NC-NC interactions are underwent. Then NC-RNA tether complexes promote the increasing of Gag concentration at the assembly site, resulting in the enhancement of CA-CA interaction. (26, 29, 37-39). More interestingly recent studies show that NC also plays a key role for chaperoning nucleic acid during viral DNA synthesis by HIV-1 reverse transcriptase enzyme and prevents nonspecific self-priming that induced by TAR stem-loop structure at 3'end of minus strand ssDNA (40, 41).

6.) Spacer peptide 1 and spacer peptide 2 (SP1 and SP2)

During the viral maturation step, HIV-1 Gag precursor protein is cleaved by viral PR to obtain the major mature proteins which include MA, CA, NC, and p6 domain. Beside these major domains, there are two spacer peptides, SP1 and SP2, which act as a linker between CA-NC and NC-p6, respectively, and

are released after the PR cleavage (21, 42). The SP1 region has been shown to be essential for the assembly of viral like particles (VLP). There are two functional properties of the SP1 domain which have been characterized. Firstly, the importance of the ~6 first residues of SP1 which are involved in the particle formation. Minor changes in the first 4 residues drastically destroy the correct particle assembly in mammalian cells (42, 43). This study suggested that the proper assembly probably requires the basic residues at the N-terminus of SP1. Secondly, several reports indicate that SP1 promotes the strength of Gag-Gag interaction. In summary, SP1 is required for the immature particle assembly and in regulating the formation of the mature HIV capsid essential for virus infectivity (31, 42-45).

SP2 is the domain that separates NC from the p6 domain. Unlike SP1, the function of SP2 in virus morphogenesis and infectivity are not currently well characterized. However, there is a study reporting that the blockage of both cleavage sites between NC and p6 did not affect processing of other Gag cleavage sites upstream, but caused a severe reduction of viral infectivity, close to background levels (46-48). In addition, another study provides evidence that the release of virus particles does not require the presence or the proteolytic processing of SP2. The viral infectivity is almost abolished when both cleavage sites (the "slow" cleavage site between NC and SP2, and the "fast" cleavage site between SP2 and p6) are mutated, and severely reduced when the fast cleavage site SP2-p6 is altered. This correlates with an increased proportion of irregular core structures, although processing of CA is not affected. Mutation of the slow cleavage site NC-SP2, or deletion of most of SP2, had only minor effects on infectivity and did not induce major alterations in mature core morphology. These results suggest that the processing kinetics leading to the separation of NC and p6 is essential for successful maturation of the virions, while SP2 itself is dispensable (49).

7.) p6 protein

While MA, CA, and NC are the common proteins found in all retroviral Gag precursors, the p6 domain is a specific feature of HIV-1 and other primate lentiviruses. In the full-length Gag molecule, p6 is located at the C-terminus and separated from the NC by the short spacer peptide SP2. The p6 domain is encoded by a sequence which directs translational frameshifting into the overlapping *pol* open reading frame. Thus, p6 is the only Gag domain which is absent from the Gag-Pol polyprotein (50). It has been shown that, within the viral particle, p6 is the major phosphoprotein in the mature form, but the function of this phosphorylation remains unclear. By contrast, a major function of p6 has been well characterized: it consists of the release of assembled viruses from the cell surface and/or from each other, which is highly dependent upon p6. In the sequence of p6, the major determinant of this function is the conserved P(T/S)APP motif near the N-terminus of the p6 domain. This region is now known as the late assembly (L) domain. Moreover, the L domain can induce the recruitment of cellular factors to the site of particle assembly (51).

8.) HIV-1 genome

The full HIV-1 genome is encoded in one long strand of RNA. In the free virus particle, there are two copies of single-stranded positive-sense RNA (52) packed inside. Each RNA strand is approximately 9.7 kilobases (kb) in length. The 5' and 3' ends of the RNA genome are flanked by a long terminal repeat (LTR) promoter region (Figure 1.3). Through specific interactions *via* packaging signal Ψ , the *cis*-acting elements, the unspliced genomic RNA is packaged into virions (53). The sequences in genomic RNA that is involved in packaging include stem-loop 3 (SL3) (54) and stem-loop 1 (SL1) (55) in the 5' UTR. Viral RNA once entered into the cytoplasm of the cell, the RT converts the genomic RNA into the viral DNA which is a form ready to integrate into the host chromosome *via* the action of IN called proviral DNA. Between the two LTR regions, the viral genome contains the genes encoding

the three structural polyproteins Gag, Pol, and Env, the genes encoding four accessory proteins Vpu, Vif, Vpr, and Nef, and the genes for the two regulatory proteins Rev and Tat (56, 57).

9.) HIV-1 Antiviral Therapy

Antiretroviral therapy (ART) has proven to be highly effective in controlling HIV-1 disease progression to full blown AIDS by reducing the amount of virus in the body, preserving CD4⁺ T cells and dramatically slowing down the destruction of the immune system (58, 59). Several classes of drugs have been approved as medications and used for interrupting the viral life cycle in patients, e.g. fusion inhibitors (FIs), chemokine receptor antagonists (CCR5 antagonists), nucleoside reverse transcriptase inhibitors (NRTIs), non-nucleoside reverse transcriptase inhibitors (NNRTIs), integrase strand transfer inhibitors (INSTIs), and protease inhibitors (PIs). Each class of drugs acts at the different stages of the HIV life cycle. Typically, the therapeutic use of highly active retroviral therapy (HAART) which is a combination of at least three drugs belonging to two classes of antiretroviral agents.

10.) Entry inhibitors

HIV-1 entry inhibitors also known as fusion inhibitors are the anti-HIV-1 which interferes with the binding, fusion and entry of the virus to the host cell by blocking one of several targets. Maraviroc and enfuvirtide are the two currently available agents in this class. Maraviroc works by targeting CCR5, a chemokine receptor expressed on the surface of human helper T-cell membrane. In rare cases, individuals may have a mutation in the CCR5 delta gene which results in a nonfunctional CCR5 co-receptor and in turn, a means of slow progression of the disease or resistance to the new infection. The most famous case study is Berlin patient. He was diagnosed with HIV in 1995 and started to receive antiretroviral therapy. In 2006, Berlin patient diagnosed with acute myeloid leukemia (AML). His physician therefore, arranged for him to receive a hematopoietic stem cell transplant from a donor with the "delta 32" mutation on the CCR5 receptor results in a mutated CCR5 protein (60, 61). Those individuals who are homozygous for the CCR5 mutation are resistant to HIV and rarely progress to AIDS. The majority of HIV cannot enter a human cell without a functional CCR5 gene. An exception to this is

only a small minority of viruses that use alternate receptors, such as CXCR4 or CCR2 (62). To prevent fusion of the virus with the host membrane, enfuvirtide (INN) is one another example of inhibitor in this class. Enfuvirtide is a peptide drug that must be injected into the body and acts by interacting with the N-terminal heptad repeat of gp41 of HIV to inactivate the hetero six-helix bundle formation, therefore preventing infection of host cells (63).

11.) Nucleoside reverse transcriptase inhibitors

HIV-1 is an RNA virus, to be able to integrate its genome into the host chromosome, it must be reverse transcribed into the DNA. Since the conversion of RNA to DNA is not done in the mammalian cell, it is performed by a viral protein which makes it a selective target for inhibition. For mechanism of action, NRTIs are chain terminators such that once incorporated it will prevent other nucleosides from also being incorporated into the DNA chain because of the absence of a 3' OH group. It acts as a competitive substrate inhibitor. The examples of currently used NRTIs include zidovudine, abacavir, lamivudine, emtricitabine, and tenofovir (64).

12.) Non-nucleoside reverse transcriptase inhibitors

Non-Nucleoside reverse transcriptase inhibitor (NNRTI) is a non-competitive inhibitors of reverse transcriptase which inhibit reverse transcriptase by binding to an allosteric site of the enzyme. It can be classified into 2 classes, first generation and second generation NNRTIs. The first generation of NNRTIs are include nevirapine and efavirenz. Meanwhile, the second generation NNRTIs consists of etravirine and rilpivirine (64).

13.) Integrase strand transfer inhibitors

The integrase nuclear strand transfer inhibitors (INSTIs) also known as integrase inhibitors (INs) are the inhibitor that inhibit the function of viral enzyme integrase to prevent the integration of viral DNA into the DNA of the infected cell. There are several integrase inhibitors currently under clinical

trial. Raltegravir is the one that became the first to receive FDA approval in 2007. It contains two metal binding groups that compete for substrate with two Mg^{2+} ions at the metal binding site of integrase. Elvitegravir and dolutegravir are two other integrase inhibitors which already approved in early 2014 (65).

14.) Protease inhibitors

Protease inhibitors is a type of HIV-1 inhibitor which block the viral protease enzyme and prevent the production of mature virions upon budding from the host membrane. These drugs particulally block the cleavage of gag and gag/pol precursor proteins.[15] Virus particles produced in the presence of protease inhibitors are defective and mostly non-infectious. Examples of HIV protease inhibitors are lopinavir, indinavir, nelfinavir, amprenavir and ritonavir. Darunavir and atazanavir are currently recommended as first line therapy choices (66).

15.) Assembly and maturation inhibitors

The assembly of Gag proteins into immature viral particles followed by proteolytic disassembly of the Gag shell to mature capsids are pivotal steps for the generation of infectious HIV-1 (67). The identification of active peptides as candidates for interfering negatively with the viral assembly step is a promising strategy (27). The HIV-1 CA protein plays essential roles in viral replication and as such represents an attractive new therapeutic target. In 2005, a 12-mer peptide termed capsid assembly inhibitor (CAI), identified by phage display, was reported to disrupt both immature- and mature-like particles *in vitro* by targeting the C-terminal domain (CTD) of HIV-1 CA (68). However, the CAI peptide itself fails to inhibit HIV-1 assembly in cell culture due to its inability to penetrate cells. A structure-based rational design approach known as hydrocarbon stapling has then been developed to stabilize the alpha-helical structure of CAI and convert it to a cell penetrating peptide. The resulting molecules, named NYAD-1 and NYAD-13, efficiently disrupt HIV-1 assembly in cell cultures. However, because they have a relative low

affinity for CA, these peptides are unlikely to progress to the clinic (69). More recently, a third small-molecule binding site on CA was identified via a high-throughput screen for inhibitors of HIV replication. PF-3450074 and related compounds bind between helix 4 and helix 7 of CA_{NTD}. Molecules like the CAP-1, also termed PA-457, and most notably the peptide-based CAI are suitable leader compounds for anti-HIV drug development (67). As the proteolytic processing of Gag is conditioned by the functionality of the viral PR and by the accessibility of its recognition site in Gag, strategies aimed at interfering either with PR enzymatic activity or to reduce access to protein substrate have been considered in the development of anti-HIV-1 drugs. The later concept is represented by a new class of HIV-1 antivirals referred to as maturation inhibitors that have been developed and tested in phase IIb clinical trials. This class of compound is able to inhibit proteolytic maturation of Gag independently of an inhibition of protease activity. The lead drug of this pharmacologic class is betulinic acid (BA), a triterpene compound isolated from the clove-like plant *Zygizum cloviflorum*. This molecule has been identified as anti-cancer agent. In the last years it has been identified as an anti-HIV-1 molecule. Modification of side chains at position C3 and C28 in the BA scaffold has been used to derive a library of compounds that has been evaluated in vitro for its inhibitory properties. Among these molecules, bevirimat (BVM), potently inhibits HIV-1 replication in tissue culture and is efficacious in HIV-1 infected patients. Biochemical analyses of virus particles grown in the presence of BVM displayed the amount of processed p24 protein decreases in favor of the immature p25 protein reflecting unprocessed CA-SP1 junction. This phenotype is reminiscent of that observed for HIV-1 bearing mutation in CA or at SP1 junction that abolish CA-SP1 processing (27, 70-74).

The combinations of antiretroviral drugs result in the multiple obstacles to HIV-1 to replicate, keep the number of offspring low and reduce the possibility of a superior mutation. In the condition of mutation that conveys resistance to one of the drugs being taken arises, the other drugs will continue to suppress reproduction of that mutation. Combination of antiretroviral drugs

usually consist of three drugs from at least two different classes. This three drug combination is commonly known as a triple cocktail. However, major current issues are systemic drug toxicity and the generation of drug resistant viral mutants during prolonged therapy. In addition, viral latency remains an unsolved problem. Patients on antiretroviral therapy remain at increased risk of developing cardiovascular diseases compared to age-matched infected controls, and HIV-1 infection also significantly increases the risk of developing kidney disease, osteoporosis, and number of non-AIDS defining malignancies, even when patients are well controlled on ART (75-77). Therefore, the alternative treatments to combat HIV are required, one promising alternative approach is gene therapy, i.e. the use of therapeutic genes to treat or prevent the viral disease. This technique has gained special interest within the HIV-1 and AIDS research area. The gene therapy approaches can be classified into two types: (i) nucleic acid-based gene therapy (DNA or RNA) including RNA interference (RNAi), aptamers, and ribozymes; (ii) protein-based gene therapy (59, 77-80). In this thesis, our proposal is mainly focused on protein-based strategies. Protein-based gene therapy strategies include transdominant negative mutants, toxins, antibodies, etc. (81) To date more than 20 different antibodies have been approved in Europe and USA, providing a considerable market potential for the pharmaceutical and biotech industry (82). Antibodies can easily be generated against a wide range of target molecules. They usually possess extraordinary specificities for their targets, with affinities often in the low nanomolar to picomolar range. However, with the increasing number of their applications, several disadvantages of the antibodies have become more and more apparent. For example, they have a large size and complicated structure, comprising of four polypeptide chains, with glycosylation of the heavy chains, and at least one structurally crucial disulfide bond in each of the multiple immunoglobulin (Ig) domains (83, 84). Consequently, exploration of alternative protein reagents with the ability to specifically recognize and tightly bind antigens has been stimulated, leading to a range of different antibody fragments most prominently, Fab and single chain Fv (scFv), which

may simply be prepared by shortening the reading frame of clone Ig genes (85). Meanwhile, a new generation of receptor proteins was developed, derived from small and robust non-immunoglobulin “scaffold” that can be equipped with prescribed binding functions using the methods of combinatorial protein design. More than 50 different protein scaffolds have been described during the past 10-15 years, the most advanced approaches in this field comprise of the following protein classes; Affibodies, engineered Kunitz domains, Monobodies, Anticalins, and DARPins (83)

1.1.2 Scaffold proteins

Beside the antibody technology, the scaffold proteins are an attractive as a choice for general binding protein. They contain a variable number of modules, which stack up on each other to create a rigid protein. They have different architectures, but within one family, there are modules of almost identical structure but with individual surfaces to specifically bind to their target. These structures have special repeat at the N-terminus and C-terminus of the protein with a hydrophilic surface which function as a ‘cap’ to shield the hydrophobic core from the solvent. This modular structure introduces numerous possibilities for binding a diverse set of ligands in a specific manner. Repeat proteins follow rules derived from biophysical consideration, such as a large interaction surface necessary for tight binding. Such a binding interface should be rigid, in order not to lose conformational entropy upon binding, which would otherwise decrease the overall achievable binding free energy. The surface should be modular so that they can be individually exchangeable or modifiable by affinity maturation. These proteins do not require disulfide bonds, which allow their expression in bacterial cytoplasm (86, 87). Several well-known repeat protein families have been studied and characterized, to define the set of rules for the creation of the new artificial protein types. For examples, the successful design of full consensus leucine-rich repeats domain (LRRs), ankyrin (AR), and tetratricopeptide (TPR) repeats has been reported. More recently, the design of consensus armadillo (ARM) and HEAT repeats proteins has been reported as well (87)

1.) α Rep proteins

Recently, the new artificial repeat protein family named α Rep have been reported. Their design was based on thermostable HEAT-like repeats, in which HEAT stands for Huntingtin, Elongation factor 3 (EF3), protein phosphatase 2A (PP2A), and the yeast kinase TOR1 (HEAT). These proteins were shown to be well-expressed, well-folded, and extremely stable (13, 88). HEAT repeats firstly identified in the eukaryotes and later were found in the prokaryotes as common motifs. The biological functions of this protein are very diverse, but most of them are mainly involved in protein-protein interactions. Although HEAT repeats are very common, using them for artificial scaffold proteins library is not very widespread, maybe because of the size and irregularity of their repeats. These proteins fold as the α -helix pairs in a right-handed super-helix, giving the image of a solenoid-like structure. The juxtaposition of these α -helices resulting in the extension of the surfaces recruited by evolution as binding sites of their target. In some cases, the local flexibility and the curvature of the elongated solenoid let HEAT repeat to wrap around their targets. Each HEAT repeat protein module (one module = one α -helix pair) contains 37-47 amino acids in length, and present more variable motifs compared to other repeat protein families.

In consideration of the known structure of a thermostable HEAT repeat subfamily, their well identified consensus sequence of stable HEAT repeats, the N-cap and the C-caps, this class of HEAT-like protein derived from the phycoblylin synthase accessory protein. The library was then constructed as focus on the specific class of HEAT repeat proteins classified as PBS HEAT-like repeat by *Urvoas A. et al.*, under the name “ α Rep” (13), using the rolling circle amplification (RCA) for the generation of gene segments which code for the individual repeat modules. The RCA method is a convenient way to produce large amounts of highly polymerizable repeat sequences and usually used for genome amplification. It has been suggested that RCA can preserve the diversity of complex sequence collections and known as an efficient method to amplify the diversity in the selection experiment such as phage

display (89). In order to explore the protein sequence space around the conserve residues, protein alignment is the technique that they use to solve the problem. The sequence features of the aligned repeats ensemble is demonstrated in the Figure 1.4 (a). In the sequence, some position displays a very high conserve meanwhile some positions are hypervariable. The structure analysis demonstrated the molecular structure of the thermostable HEAT repeat protein. An example α Rep protein is made of three consecutive repeats classified as HEAT-PBS repeats. The N-terminal region of the chain is not folded (Figure 1.4 (b)). Structural superposition of an AAA-HEAT repeat and α Rep HEAT repeat is showed in Figure 1.4 (c). The structure analysis also reviews that when mapped the α Rep sequence onto the guild sequence, Mth187 repeats, the conserve position can be classified in several group. A set of apolar side chains, the highly conserve R21, the conserve G1, and the most variable positions (Figure 1.4 (d-f)).

The α Rep is a new type of repeat scaffold motif protein in which a library of α Rep contains a repertoire of artificial repeat proteins from which specific binding molecules can be selected. Isolation of α Rep protein against GFP/EGFP is one model example of using α Rep protein as a binder. The study also indicated that the α Rep-based GFP binders can be easily produced in the high level and found to be very stable protein. The isolated GFP-specific α Reps display high affinity and high specificity which are sufficient for using them as a new tool for purifying GFP-fusion proteins from the whole cell lysate in the protein pull-down assay. Interestingly, expressing α Rep inside the cells shows the accurate co-localization with their target protein without causing toxic effects to the cells or induce any protein aggregation. These suggested that α Rep protein is a very interesting scaffold protein candidates which can apply to use in many different research fields (14).

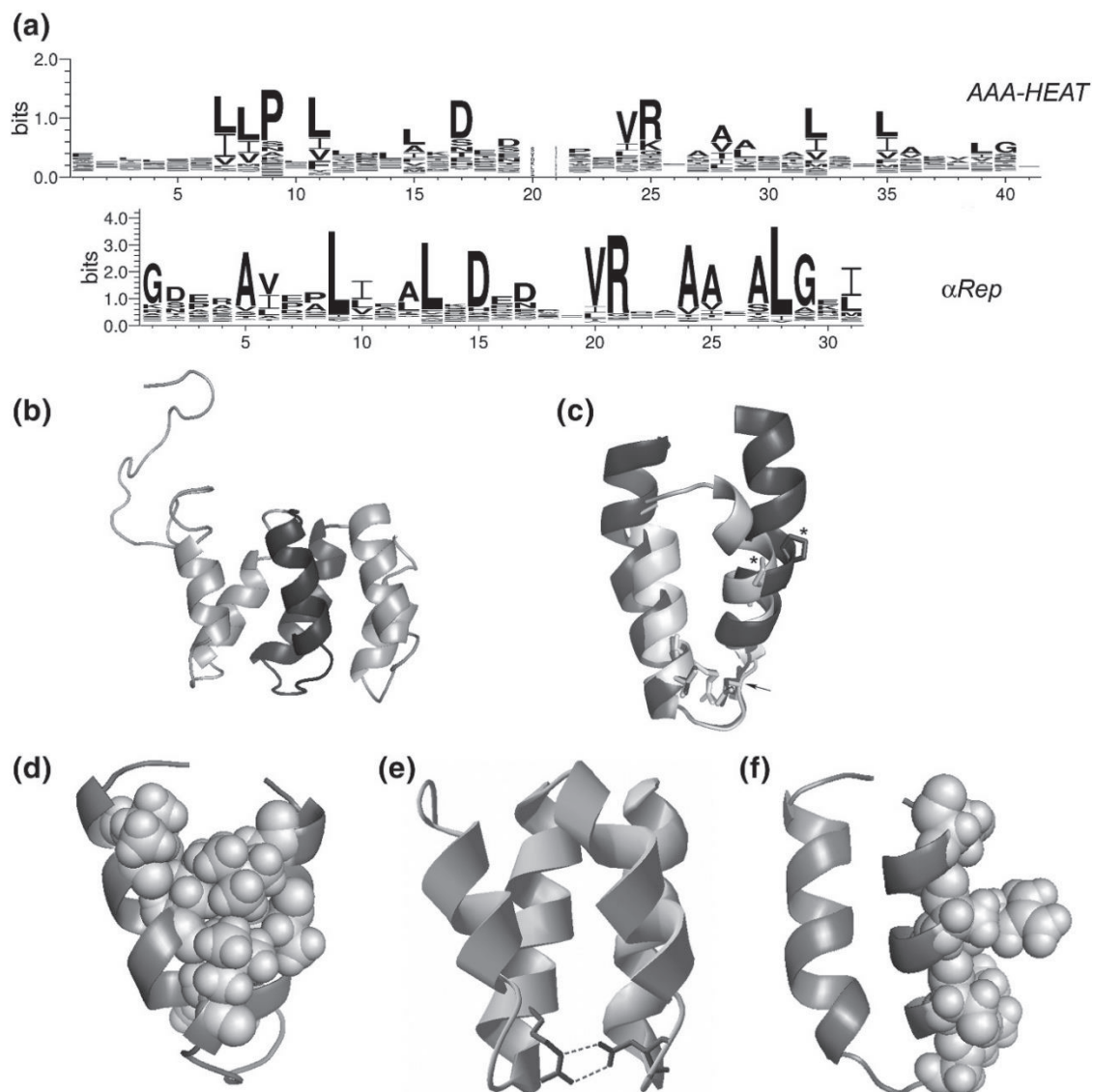


Figure 1.4 Design of the α Rep motif. (a) A Collection of amino acid protein sequences made of consecutive HEAT repeats. The alignments of each repeats are shown in the sequence logo format using the sequence numbering in each motif family as the abscissa. The conserve sequence within the HEAT-PBS repeat subgroup (α Rep) and comparison with the previously defined AAA-HEAT repeat subclass (AAA-HEAT). (b) The molecular structure of the thermostable HEAT repeat protein used as a guide (Mth187, PDB code 1TE4). This protein is made of three consecutive HEAT repeats classified as HEAT-PBS repeats. The N-terminal part of the chain is not folded. One HEAT repeat corresponds to two consecutives α -helices (dark gray). (c) Structural superposition of an AAA-HEAT repeat and an α Rep HEAT repeat. Residues 396–434 from the PR65/A subunit of human protein phosphatase 2A (dark gray, PDB code 1B3U) 26 and residues

109–139 from α Rep-n4-a protein (light gray, PDB code 3LTJ, this work) were overlaid. Positions D15, V20 and R21 in the α Rep motif are superimposable on positions D17, V24 and R25 in the AAA-HEAT motif, as indicated by the arrow. The conserved proline P9 in the AAA-HEAT motif is not structurally equivalent to P8 in the α Rep motif; these two proline side chains are shown (*). The two AAA-HEAT repeat helices are one helical turn longer than the α Rep repeat helices. (d) Residues of the central Mth187 repeat corresponding to conserved apolar residues A5, L9, L13, V20, A24, A25 and L28 are shown as spheres. These conserved residues are associated with the packing of a single repeat between the two helices and the packing with neighboring repeats. (e) Conserved H-bonds between R21 of one repeat and D15 of the next repeat in the α Rep context. (f) The highly variable positions 18, 19, 22, 23, 26 and 30 are mapped on the central repeat of Mth187 and shown as spheres. These hypervariable positions correspond to the external surface of helix 2 (13).

1.1.3 Phage-display technology

Phage-display technology was first used by *George Smith*. It has been several years before this technology became the potential biological tool as it increasing in the number and vast range of its applications show the versatility of this technique, including epitope mapping, high-affinity proteins isolation, protein engineering and drug discovery. Phage-display is based on the expression of a library of molecules of interest (the molecule on the phage can be peptides or proteins) in fusion with the amino- or carboxyl-terminus of a structural protein display on the surface of bacteriophages. After that displayed proteins/peptides on the phage particles are then selected by an affinity selection procedure, based on the ability of each individual exposed proteins/peptides to bind to a specific target, such as a purified receptor, an enzyme, a nucleic acid or another non-protein molecule. The selection process including of several cycles, each selection cycle comprising capture, washing and elution steps, to obtain the progressive enrichment and amplification of the phage population carrying molecules which can bind to the target with a higher affinity. The most widely used bacteriophages are the filamentous phages which can infect the *E.coli*, this filamentous phages can grow at extremely high titers (10^{12} - 10^{13} pfu/ml). Its DNA genome is a single-stranded DNA genome which is easy to manipulate. Therefore, it is possible to present highly diverse random peptide libraries on their surface. Bacteriophage M13, which tolerates the insertion of very long fragments of exogenous DNA into its genome, thus it is an ideal tool for phage-display, although other bacteriophages, such as fd, f1, T4 and T7, have also been used. The fd and f1 are the filamentous bacteriophage, as well as M13 bacteriophage, they were used in pioneering studies during the development of phage-display, whereas the use of T4 and T7, the icosahedral capsid bacteriophage phage, is much less common. In practice, the pVIII and pIII proteins of filamentous phages are the most effective and widely used for displaying the molecule on the surface of the phage particles. Even though, in theory the peptide of interest can be fused to any surface protein. The displayed protein or peptide is usually fused to the N-terminal region, between the signal peptide and the N-terminus of the mature protein. In antiviral research, pIII protein is the protein of choice for the exposure

of peptide libraries, because this protein presents five copies of pIII per phage. Moreover, accommodation of pIII to the large proteins and peptides cause little loss of functionality related to the ability of the phage infectivity to the bacteria. By comparison, the pVIII protein, although much more abundant (2,700 copies per phage) can display only short peptides (6-8 amino acids), due to geometric constraints during capsid assembly of the phage particle.

Phage-display techniques have two major advantages for many research field as well as the antiviral research. They can be used for the rapid and high-throughput screening of large numbers of different molecules (up to 10^{13}) in a small volume (a few microliters). For example, the privilege of selecting a phage with a frequency of $1/10^8$ in the original library has been reported. In addition, phage display defines a physical link between genotype and phenotype, because the gene encoding the protein (or peptide) displayed at the surface is directly sequenced and isolated from the phage DNA. Furthermore, directly used as expression vectors obtain from some of phagemid vector, to produce the protein or peptide of interest. Finally, using bacteriophages in a display strategy has several advantages for example (i) the genome of phage is small size, this simplifying the cloning steps; (ii) phage particles are stable, which can store at 4°C; (iii) the high efficiency of phage infection, allow the possibility to obtain the large amount of material, compatible with the screening of large libraries; (iv) phage-display libraries can be periodically regenerated, while chemical libraries consumed over time.

Nevertheless, the phage-display technology also has several drawbacks that have to be taken into account. For example, the clones can be toxic for the bacterial cells leading to the reduction of bacterial growth, or may decrease the infectivity of phage and/or phage particle secretion. Some clones are unlikely to be selected will therefore disappear rapidly from the pool library, regardless of the selection process. In addition, the expression level of certain peptide sequences in *E.coli* is variable (depending on the codon usage), introducing another potential bias into the bacteria may affect selection process. Finally, successive amplifications of the library may rapidly decrease the diversity of the library in order to the clones with a growth advantage are likely to increase significantly within the population, at the

expenses of the other clones. In another unfortunate case, the selected peptides or proteins, once synthesized as soluble form, those molecules may not retain their optimal binding activity outside of the microenvironment of the phage and/or in the complex environment such as cell or animal. The phage-display of combinatorial peptide libraries has already been used successfully several times over the last 20 years, in the discovery of inhibitory peptides active against viruses (90). The first viruses to be targeted were hepatitis B virus (HBV) and HIV, and both these two viruses remain the most frequently targeted, but other viruses from other families were also described. Diverse strategies and targets have been used, providing an incidental demonstration of the versatility of the method. Two main approaches are used: (i) targeting of the viral proteins responsible for viral entry into cells (extracellular steps); (ii) targeting of the various elements of the viral replication complex and the cellular partners of viral proteins within infected cells (intracellular steps) (73, 91).

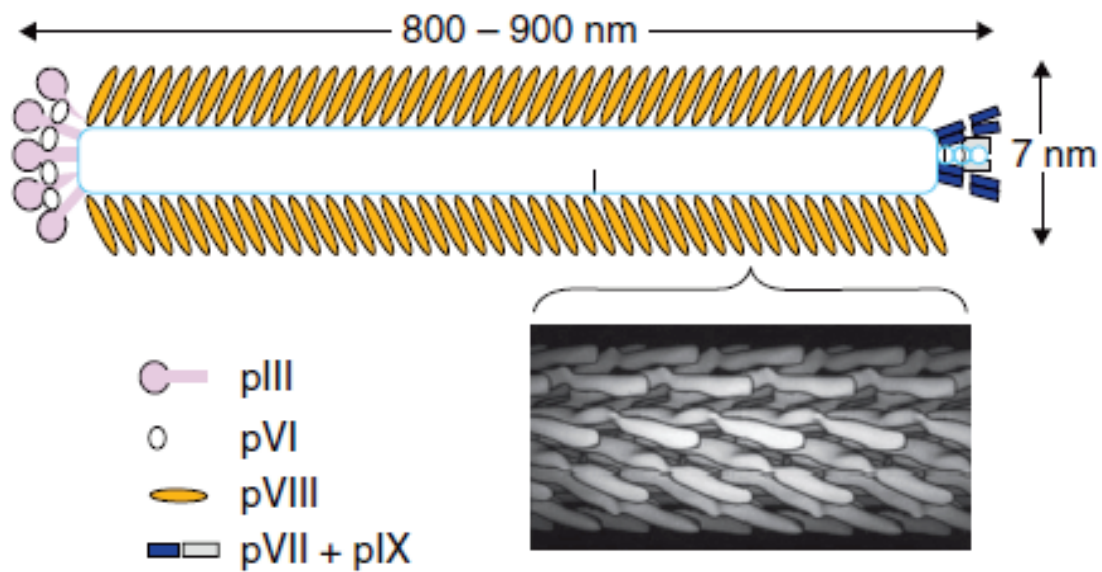


Figure 1.5 Structure of filamentous phage. Composition of phage and arrangement of major coat protein surface domains (92).

1.1.4 Baculovirus

In the early 1980s, the first-publication about the use of the baculovirus vector for the expression of a foreign gene led to a wave of great interest for recombinant protein production using baculovirus in insect cell systems. The *Baculoviridae* is a large family of viruses which harboring double stranded, circular DNA genomes. The natural hosts for these viruses are arthropods, and mainly insects. However, most of the baculoviruses have a very narrow host range, usually restricted to only one insect species. The most extensively studied and exploited member of the *baculoviridae* is the, *Autographa californica* Multicapsid Nucleopolyhedrovirus, abbreviated *AcMNPV*. It was the isolate used to develop the original recombinant baculovirus vectors (93, 94)) and its genome is still used today as a platform and backbone for the production of most baculovirus vectors today (95). The *AcMNPV* contains a 134 kb genome with 154 open reading frames (ORF). The baculovirus particle is formed of a nucleocapsid of 21 nm x 260 nm in size. The baculoviral

envelope is acquired from the cell membrane and requires a virus-coded glycoprotein called glycoprotein 64 (gp64) to be able to spread and infect new target cells. In the viral particle, the gp64 forms structures called peplomers on one end of the budded virus. Two distinct forms of baculoviruses have been characterized. The occlusion derived virus (ODV), is present in a protein matrix called polyhedrin (or granulin) and is responsible for the primary infection of the host. The other form is represented by budded virus (BV), which is released from the infected host cells later during the secondary infection. A schematic representation of the morphology and the components of the baculovirus is illustrated in Figure 1.6.

The life cycle of baculovirus is divided temporally into immediate-early, early, late, and very late phases (Figure 1.7). Viruses enter the cell by adsorptive endocytosis pathway and then move to the nucleus, where their DNA is released. DNA replication begins ~6 hours after infection. Replication is followed by viral assembly in the nucleus of the infected cell. Two different forms of viral progeny are produced during the life cycle of the virus, extracellular virus particles or non-occluded viruses (non-OCV) or budded virus (BV) during the late phase and polyhedra-derived virus particles or occluded viruses (OCV) during the very late phase of infection. The extracellular virus is released from the cell by budding, beginning at ~12 hours post infection (pi), and is produced at a logarithmic rate until 20 hours pi, after which production drops off. The OCV form, on the other hand, was found in the nucleus at ~18 hours and continues to accumulate as late as 72 hours pi, or until the cells lyse. OCV particles are embedded in proteinaceous viral occlusions called polyhedra within the nucleus of infected cells. The polyhedrin protein (29 kDa) is the major protein component of the occlusion bodies. The polyhedrin protein serves an important function for the survival and propagation of the virus in nature. Because baculoviruses are lytic, they quickly kill their insect host after infection. The polyhedrin protein serves to sequester, and thereby protect, hundreds of virus particles from proteolytic inactivation by the host. The virus is transmitted when the occlusion bodies are ingested by a new host as it feeds on a contaminated source of food. The polyhedrin protein dissolves in the alkaline environment of the new host's gut and the occluded virus is released. This virus infects the gut epithelial cells and virus replication takes place. BV is

then produced and buds from the infected gut cells. At this point, the virus spreads throughout the tissues of its new host. Although the polyhedrin protein is essential for survival of the virus in nature, it is dispensable for virus survival and propagation in tissue culture cells.

Baculovirus Multicapsid nucleopolyhedrovirus

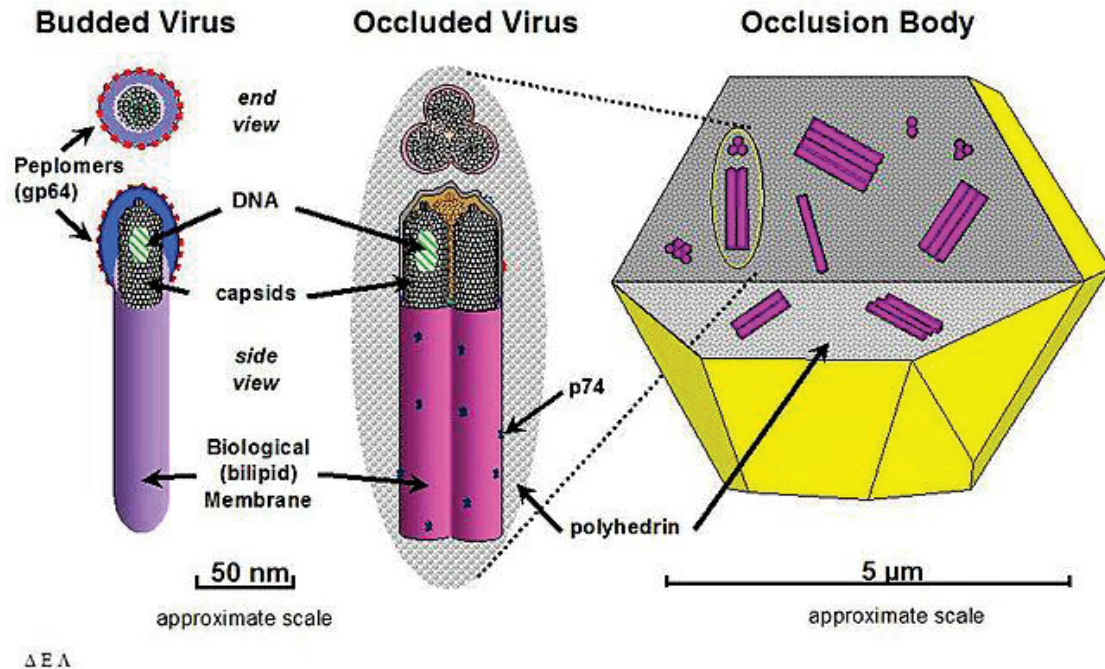


Figure 1.6 Structure of baculovirus virions. Schematic representation of the two forms of baculoviruses: (*left*) the budded virus (BV) and (*right*) the occluded virus (OCV). BV is the form that released from the cell during the secondary infection. The OCV is the form which is found in the environment, and causes the primary infection in the host. The size of the baculovirus particle is about 21 nm x 260 nm. One single particle consists of the nucleocapsid, for the viral genome coating, the gp64 forming the peplomers, and the membrane lipid bilayer issued from the infected cell.

This figure has been obtained from the site: <https://en.wikipedia.org/wiki/Baculoviridae>

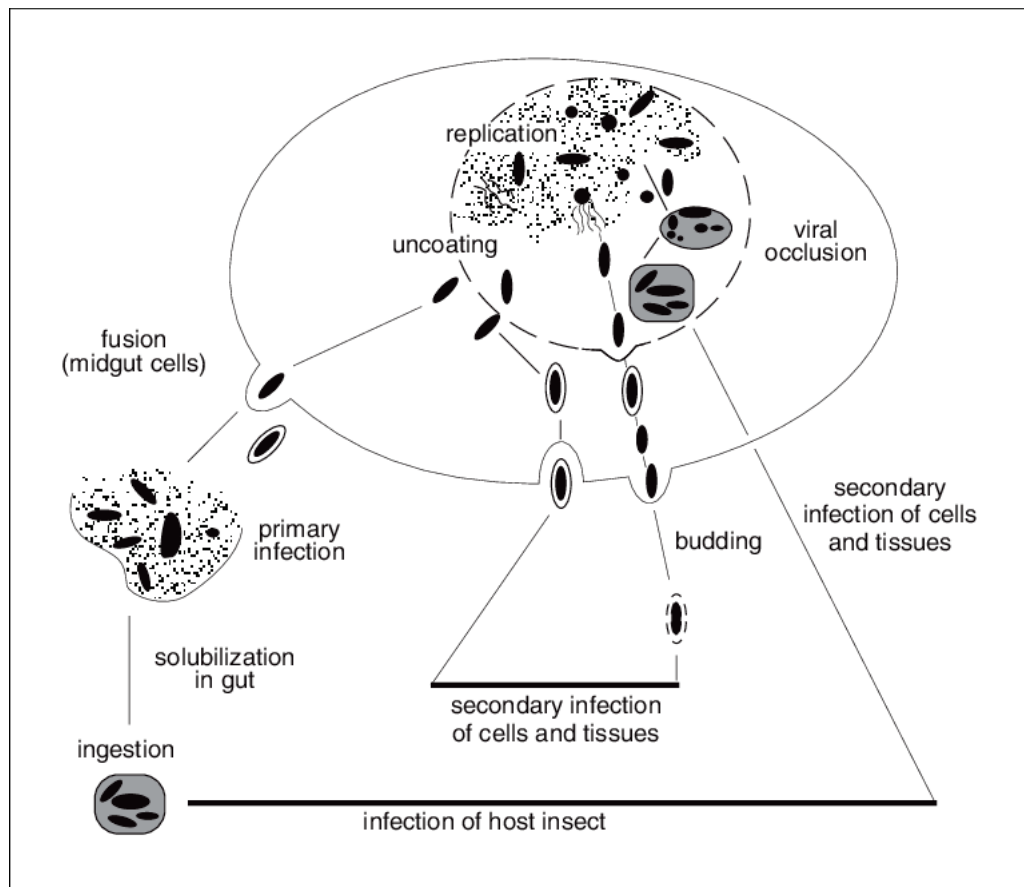


Figure 1.7 Baculovirus life cycle. Baculovirus enters their target cells by adsorptive endocytosis and then move to the nucleus, where their DNA is released. Both DNA replication and viral assembly occur in the nuclei of infected cells to generate two types of viral progeny. These include the budded virus (BV) and the occluded virus (OCV). BV is released from the cell by budding, meanwhile OCV accumulates in the nuclei of infected cells. OCV also known as Polyhedra-derived virus, it is embedded in proteinaceous viral occlusions, the major protein component of which is the viral polyhedrin protein. In the secondary infection of cells and tissues occurs by two pathways. The first one is, the BV, once budded from the site of primary infection, is free to infect neighboring cells by the pathway which has been described above. Secondly, OCV is released from occlusion bodies after an infected food source is ingested by a new host (96). The figure has been obtained from Murphy CI et al., 2001.

1.1.6 Lentivirus vectors

Lentiviral vectors are among the most popular and useful viral vectors in many research fields and clinical gene therapies. The advantages of lentivirus that make it attractive as a tool for gene-delivery vectors, are the followings: (i) it can generate a stable vector integration into the host genome; (ii) it has a large genetic capacity of transgene insertion; (iii) a broad range of tissue tropisms; (iv) and the ability to transduce both dividing and non-dividing cells (52, 97). In the early era of lentiviral vectors, genetically modified HIV was constructed as gene delivery vehicle. The first prototype was the HIV based-vector with the components of viral vector separated into two plasmids, a plasmid encoding HIV-1 proviral DNA with a deletion in the *env* gene and a second plasmid that encodes only *env* gene (98, 99). Since the *trans*-complementation of Env protein is in a separated plasmid, the viral vector is produced by a single-round infection. In this HIV viral vector the transgene was designed to be inserted into the *nef* or *env* gene and its expression is controlled by the 5'LTR. The HIV-1 based vector was also constructed to have the essential *cis*-acting elements for genome packaging, reverse transcription and integration, and expression of genome transcripts, i.e. the ψ signal, the LTRs and RRE, respectively. In addition, the foreign gene was controlled by an external promoter such as the immediate-early cytomegalovirus (CMV) promotor. Since HIV-1 Env required the CD4 molecule at the cell surface as specific receptor, the range of cell types susceptible to this gene transfer system was broadened by introducing the vesicular stomatitis virus envelope glycoprotein G (VSV-G) into the viral vector production system. VSV-G binds to the ubiquitous membrane component phosphatidylserine, and this makes these VSV-G pseudotyped vectors able to transduce a broad range of cell types, not only mammalian cell but also non-mammalian cells such as fish cell (100). The VSV-G pseudotyping offers additional advantages to the vectors: for instance, VSV-G is substantially more stable than retroviral or lentiviral envelopes; consequently the VSV-G pseudotyped vectors can be concentrated by ultracentrifugation to obtain high-titer vector stocks.

Lentiviral vectors are derived from the highly pathogenic virus HIV-1. Therefore, using this technology, the most important issue that have to be considered is the

biological safety, and more specifically the possibility of generating replication competent lentiviruses (RCLs). The first generation of lentivirus vectors was made to reduce this risk. Hence, replication-deficient recombinant HIV-1 vectors are produced from three separate elements (i) a packaging construct; (ii) a plasmid encoding the Env glycoprotein; and (iii) a transfer vector which contains the gene of interest (Figure 1.7 (A)) The packaging construct harbors the genes which code for HIV Gag, Pol and regulatory/accessory proteins, under the control of a strong mammalian promoter. The second plasmid is the *env*-encoding plasmid, the mostly used is VSV-G, to provide the advantageous broad range of host cells. These two plasmids were specifically engineered to lack any packaging signal or LTRs to avoid their transmission into vector particles and to reduce the production of RCL in vector preparations. The plasmid vector which carries the gene of interest contains all the *cis*-acting elements required for packaging, reverse transcription, integration and expression of the transgene (ψ signal, LTRs and RRE), without the expression of any HIV protein. However, since the *trans*-activator Tat is not encoded together with the transgene in the transfer vector, the activity of the 5'-LTR promoter is minimal. Therefore, for the protein production from the transgene, an internal promoter specific of the transduced cells is used to control the transgene expression.

To further increase the biosafety, second-generation vectors have been developed by modifying the accessory genes in the system (Figure 1.7 (B)). HIV-1 contains four accessory protein which are Vif, Vpu, Vpr, and Nef, which are necessary for the propagation of the virus and its virulence in primary cell infection. Although these accessory genes are important for HIV as a pathogen, they were deleted in second-generation lentiviral vectors (101). Therefore, these second-generation vectors include only four of the nine HIV genes: *gag*, *pol*, *rev* and *tat*.

To be able to integrate into the host chromosome by functional integrase, the cassette of the transfer vector must be flanked with LTRs on both 5'- and 3'-ends. If a wildtype HIV-1 infect the transduced cells, it would act as a helper virus and rescue the integrated transgene into new viral particles which would spread the transduction beyond the original target cells. The LTRs usually contain three

regions: U3, R, and U5. U3 is a viral enhancer/promoter and R in the 3'-LTR is the polyadenylation signal. The mRNA translated from the proviral DNA, does not contain the 5' U3 and 3' U5 elements, but it has the R region caps at both ends of the RNA strand. The duplication of LTR elements occurs during reverse transcription and prior to the integration phase, when U3 in the 3'-LTR is copied and transferred to the 5'-LTR. The first report of this mechanism has been shown for the MLV vector: when part of U3 in the 3'-LTR was deleted, the same deletion was transferred to the 5'-LTR's promoter/enhancer region. This deletion therefore results in transcriptional inactivation of potentially package-able viral genomes in the transduced cell (102). Thanks to this knowledge, the self-inactivating (SIN) mechanism was generated and introduced into HIV vectors (SIN vectors) by deleting the 3'-LTR elements. This SIN modification can reduce the propagation of spontaneously produced replication-competent recombinant HIV-like viruses.

The HIV vector has been continuing to improve, and third-generation vectors were later constructed. To increase safety, the Tat protein has been removed and Rev provided from a separate plasmid as shown in Figure 1.7 (C). The Tat-independent plasmid is obtained by replacing the U3 promoter region of the 5'-LTR in the transfer vector with the heterologous strong viral promoters from CMV or Rous sarcoma virus (RSV) (103, 104). Four plasmids are used in this version of lentivirus vectors: (i) a packaging construct which carried only *gag* and *pol* genes; (ii) a plasmid coding for Rev; an Env (VSV-G) plasmid; and a transfer plasmid with the heterologous promoter. In summary, this third-generation lentiviral vector contains only three genes out of nine genes of HIV. Since the viral genetic material is split into four separate plasmids, there is less possibility for the generating of replication-competent HIV-1-like virus.

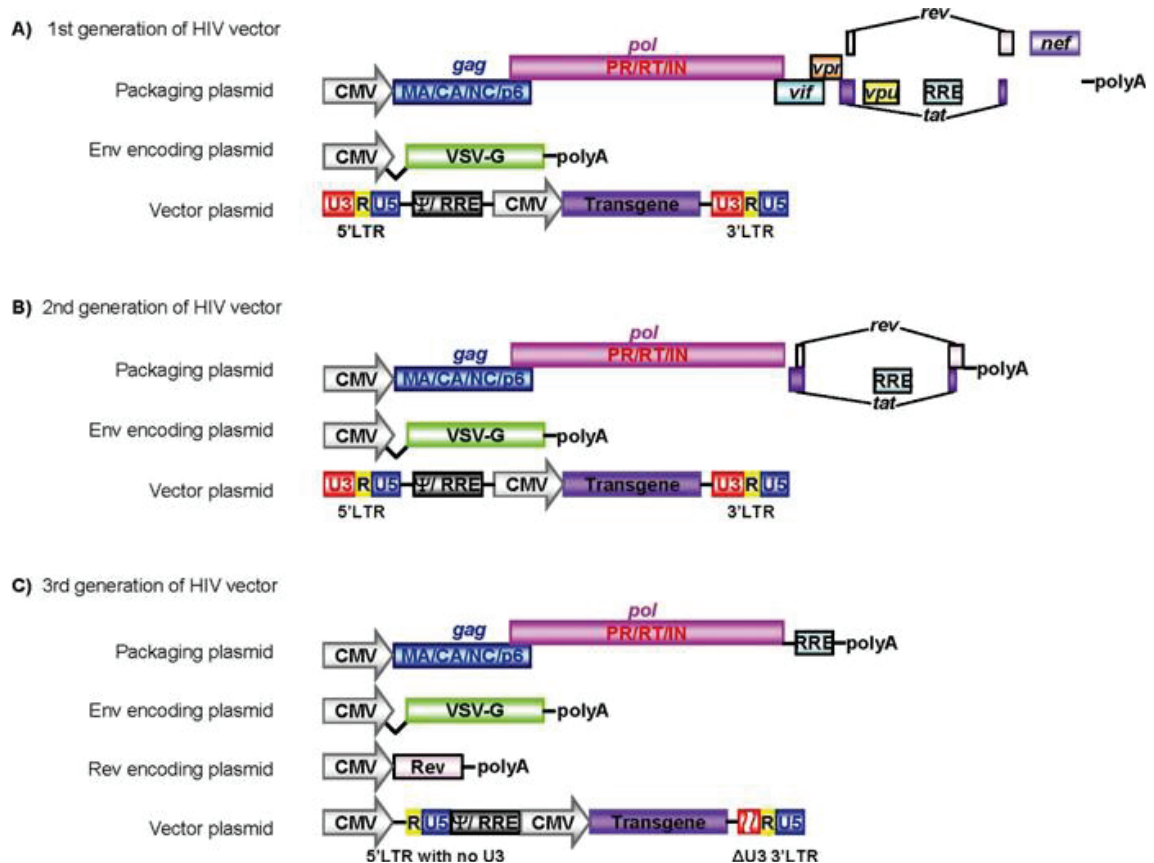


Figure 1.8 Schematic representation of HIV vectors (A) The first generation of HIV vectors includes all of the viral proteins, except the envelope glycoprotein, in a packaging plasmid. VSV-G is provided by a different plasmid. HIV vector plasmid contains LTRs and the transgene is expressed under a strong viral promoter such as the CMV promoter. (B) The second generation of HIV vectors, all of the accessory proteins are removed from the packaging plasmid. Similar to the first generation of HIV vectors, expression of glycoprotein and transgene are provided by different plasmids. (C) The third generation of HIV vectors requires four different plasmids. In addition, to the three plasmids (i.e. the packaging plasmid, Env-encoding plasmid and vector plasmid), Rev protein is provided by a different plasmid. The vector plasmid is also modified by deleting the U3 region from 5'-LTR and partially deleting 3'-LTR to reduce the possible production of replication-competent viruses, and a strong viral promoter such as CMV or RSV is inserted for expression of the vector (52).

1.2 Objectives

- 1.2.1 To isolate and characterize α Rep with high affinity and high specificity for GST- CA₂₁-SP1-NC using phage display strategy
- 1.2.2 To generate the biological and cellular tools necessary to assess the intracellular antiviral effects of GST- CA₂₁-SP1-NC binders
- 1.2.3 To evaluate the intracellular antiviral effects of GST- CA₂₁-SP1-NC binders on viral like particle production using baculovirus system
- 1.2.4 To evaluate the intracellular antiviral effects of GST- CA₂₁-SP1-NC binders on HIV-1_{NL4-3} production using SupT1 human T cell lines

CHAPTER 2

MATERIALS AND METHODS

2.1 Chemicals and equipments

Chemical agents and equipments used in this study are listed in Appendix A. Cell lines and microorganisms are indicated in Appendix B. Antibodies are listed in Appendix C and restriction enzymes are detailed in Appendix D. The recipes for reagent preparations are shown in Appendix E.

2.2 *E. coli* strains

XL-1 Blue (Stratagene, La Jolla, CA) was used as a host for the α Rep phage library generation and amplification. M15[pREP4] bacterial cells (Qiagen, Hilden, Germany) were used for production of soluble 6xHis-tagged α Rep proteins. BL-21 was used as a host for the preparation of GST-tagged recombinant truncated Gag domains.

2.3 Plasmids and vectors

The pQE-31 expression vector (Qiagen, Hilden, Germany) was used for the production of 6xHis-tagged recombinant α Rep proteins in M15[pREP4] bacterial cells. pIB/V5-His (Invitrogen, Carlsbad, CA) was used for the construction of insect Sf9 cell lines stably expressing α Rep scaffold molecules under the control of *OpIE2* promoter for their constitutive expression. Blasticidin (Gibco, Grand Island, NY) was used as a selection agent to obtain a stable polyclonal population or stable clonally cell lines. The pCEP4 vector (Invitrogen, Carlsbad, CA) was used as an episomal mammalian expression vector of α Rep proteins, with the cytomegalovirus (CMV) immediate early enhancer/promoter for high level expression of transgene. pCEP4 vector carries the hygromycin B resistance gene for stable selection in transfected cells. CGW, a third-generation of lentiviral vector, was used as the backbone vector to transfer genes encoding for α Rep proteins into Human embryonic kidney (HEK) 293T cells and SupT1 cells. The pGEX-4T-1 vector

(Stratagene, La Jolla, CA) was used in this study to produce the high level expression of GST-tagged recombinant truncated Gag domains. pNL4-3 was used to produce the HIV-1 virus.

2.4 Cells

The Sf9 cell line was derived from pupal ovarian tissue of the fall armyworm *Spodoptera frugiperda* (Invitrogen, Calsbad, CA). This cell line is highly susceptible for the infection of *Autographa californica* nuclear polyhedrosis virus (AcNPV) and can be used with the baculovirus expression vectors. Sf9 cells were used to generate the stable cell lines expressing α Rep proteins fused to GFP protein. Cells were propagated and maintained in non-humidified environment at 27 °C in Grace's insect medium (Gibco, Grand Island, NY) supplemented with 10 mM L-glutamine, (Gibco, Grand Island, NY), 10% fetal bovine serum (FBS) (Gibco, Grand Island, NY), penicillin (100 Units/ml), and streptomycin (100 μ g/ml).

Human embryonic kidney (HEK293T) cell obtained from the American Type Culture Collection (Manassas, VA) and human cervical cancer cell line (HeLa), a generous gift from Prof. Dr. Andre Lieber (University of Washington, Seattle, WA, USA) were maintained in Dulbecco's Modified Eagle's medium (DMEM) (Gibco, Grand Island, NY) supplemented with 10% FBS (HyClone, Cramlington, UK), 2 mM L-glutamine, penicillin (100 Units/ml) and streptomycin (100 μ g/ml).

Human T cells lymphoblastic lymphoma (SupT1) cell were obtained from the ATCC (Manassas, VA) were grown in RPMI-1640 medium containing penicillin (100 U/ml), streptomycin (100 μ g/ml), 2 mM L-glutamine, and 10% FBS (all cell lines were maintained in a humidified 37°C incubator containing 5% CO₂).

2.5 Construction of α Rep library

The α Rep library was previously constructed by the polymerization of synthetic microgenes which correspond to the repeats in the phage display or periplasmic expression vector. The intermediate vector construct called acceptor vector (pHDIEx-acc) was constructed. This vector was used for low level expression of α Rep proteins fused to the M13 g3p truncated protein in phage display experiments. Since this construction had also a T7 promoter and a suppressible stop codon between the α Rep protein and g3p

coding sequences, it could also be used for periplasmic expression of non-fused α Rep protein in non supE strains of *E. coli* expressing T7 polymerase. For cytoplasmic expression, the sequence encoding soluble α Rep proteins were inserted into the pQE-31 expression vector, using M15[pREP4] strain for protein expression. Bacterial cells, XL-1 Blue were used as a host cells for generation of the library and propagation of phages displaying the artificial α Rep proteins. The α Rep library was kindly provided by Professor Philippe Minard, University Paris-Sud, Orsay.

2.6 Screening of α Rep phage library on the viral targets

The viral target used, was the GST-CA₂₁-SP1-NC polyprotein derived from HIV-1 GagPr55 including the 21 amino acids of C-terminal domain of CA fused to SP1 and NC. This protein was used for the screening of phage-displayed α Rep library. The α Rep clones that bind to immobilized target GST-CA₂₁-SP1-NC were isolated. Phage clones were amplified and three rounds of selection/elution step were repeated. The elution of GST-CA₂₁-SP1-NC bound phages were performed using acidic buffer for first two rounds, followed by specific ligands elution using excess of GST-CA₂₁-SP1-NC as competitors in the third round. Individual phage particles were then prepared in small scale using the 96-wells format. Briefly, random colonies from each round of selection were picked and cultured in 2X YT broth containing ampicillin 100 μ g/ml and 1% (w/v) glucose in 96 well plate, 37°C overnight. Then 10 μ l of overnight culture were transferred to new plate containing 150 μ l of 2X YT broth containing ampicillin 100 μ g/ml, tetracycline 10 μ g/ml, and 1% (w/v) glucose and cultured at 37°C with shaking for 4 hours. Bacterial cells were infected with 20 MOI of helper phage and incubated at 37°C without shaking for 30 minutes at 37°C and with shaking for 30 minutes. Two hundred microliters of infected cells was transferred to 96-well storage plate containing 1.5 ml of 2X YT broth containing ampicillin 100 μ g/ml and kanamycin 70 μ g/ml. The plate was covered with gas permeable adhesive seals and cultured at 30°C with shaking for 16-18 hours. Phages in the culture supernatant were collected after the centrifugation and used for phage ELISA to determine their binding activity. Purified GST-CA₂₁-SP1-NC were diluted in coating buffer, then added into a microtiter plate and left for overnight at 4°C in the moisture chamber. The coated wells were washed four times with 0.05% Tween 20 in Tris buffered saline (TBST). The wells were then blocked the non-specific binding

with blocking solution (2% BSA in TBST; 200 µl/well) at room temperature for 1 hour with shaking. After the washing step, 100 µl of the culture supernatant of each clone containing phage particles were added and incubated at room temperature for 1 hour. Hundred microliters of mouse anti-M13 conjugated HRP (GE Healthcare Life Sciences) at dilution 1:5,000 in blocking solution were added after the washing step. The wells were then washed again prior adding 100 µl SureBlue™ TMB MicrowellSubstrate (KPL, Gaithersburg, MD) and the optical densities at 450 nm (OD_{450nm}) were measured after adding 1 N HCl.

2.7 Production of αRep proteins

2.7.1 Construction of pQE-31 expression vectors for soluble αRep proteins production

pQE-31 acceptor vector was used for the production of 6xHis-tagged αRep proteins in M15[pREP4] bacterial cells. The DNA fragments encoding for the αRep proteins were amplified from pHDiExDsbA phagemid vector using a pair of primers; pQE-31_Fw_αRep*Bam*HI (5'-GAG GAG AGG AGA AAT TAA CTA TGA GAG-3') and pQE-31_Rv_αRep*Hind*III (5'- GAG GAG CTA TCC AGA TGG AGT TCT GAG G-3') followed by digestions with *Bam*HI and *Hind*III. The insert fragments were then ligated into linearized pQE-31 vector pretreated with the same cut sites. Subsequently, the recombinant plasmids as shown in the Figure 2.1 were transformed into the XL-1 Blue competent cells. The isolated colonies were picked for colony PCR. The clones which give the PCR product band at correct size were then selected for restriction enzyme analysis using *Bam*HI and *Hind*III and confirmed by DNA sequencing. The correct plasmid clones were further transformed into M15[pREP4] competent cells for protein expression.

2.7.2 Expression and purification of αRep proteins

M15[pREP4] bacterial cells harboring pQE-31-αRep recombinant plasmids were grown in 500 ml Luria-Bertani (LB) broth supplemented with ampicillin 100 µg/ml, kanamycin 25 µg/ml, and 1% (w/v) glucose, at 37°C with shaking up to OD₆₀₀ of 0.8 was reached. Protein expression was induced by addition of 0.1 mM Isopropyl β-D-1-thiogalactopyranoside (IPTG), and maintained in culture for 4 hours at 30°C

with shaking. Bacterial cells were then pelleted by centrifugation at 1,200 x *g* for 30 minutes at 4°C. Pellets were resuspended in phosphate buffered saline (PBS) containing a cocktail of protease inhibitors (Roche Diagnostics GmbH) then physically lysed bacterial cells by sonication. Bacterial cells lysates were next clarified by centrifugation at 15,000 x *g* for 30 minutes at 4°C. The soluble form of α Rep proteins was purified by HisTrap affinity columns (GE Healthcare Life Sciences, Piscataway, NJ). Purified proteins were analyzed by 12% SDS-PAGE and PageBlue™ protein staining solution (Thermo Fisher Scientific, Waltham, MA), or SDS-PAGE and western blotting.

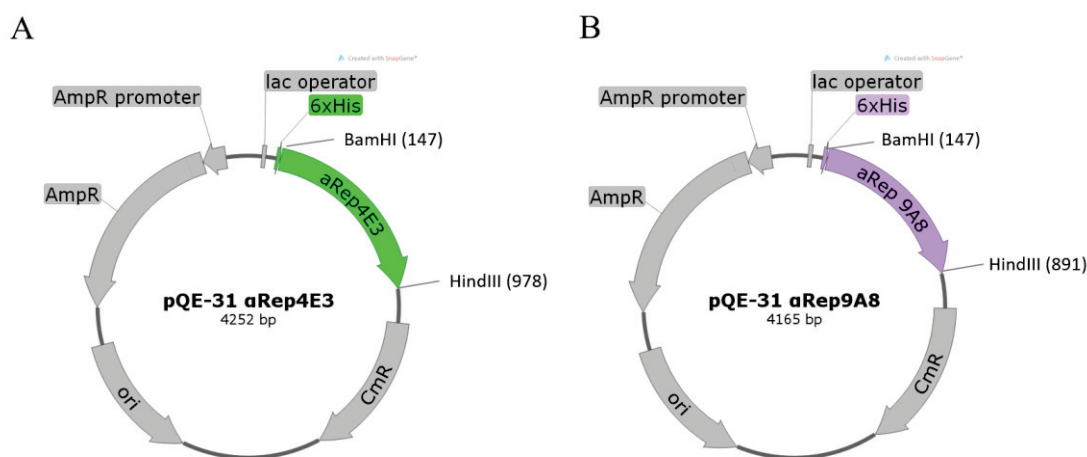


Figure 2.1 The schematic figure of pQE-31 vectors construction for expression of 6xHis-tagged α Rep proteins in bacterial cells. The DNA sequences encoding for α Rep proteins were inserted into pQE-31 vector using *Bam*HI and *Hind*III cloning sites. (A) pQE-31- α Rep4E3 and (B) pQE-31- α Rep9A8

2.8 Western immunoblotting

To determine the α Rep proteins expression, bacterial cells were pelleted, and washed once with PBS then resuspended in PBS containing a cocktail of protease inhibitor (Roche Diagnostics, Germany). The bacterial cells were physically lysed by sonication. After clarifying the cell lysate by centrifugation, the concentration of protein was measured using Pierce™ BCA Protein Assay Kit (Thermo Fisher Scientific, Waltham, MA). Equal amounts of total protein were separated by 12% SDS-PAGE and transferred to PVDF membrane (GE healthcare, UK). After blocking with 5% skim milk in PBS, the PVDF membrane was incubated with mouse monoclonal anti-6xHis (Applied Biological Materials (ABM) Inc, Richmond, Canada), and probed with HRP-conjugated goat anti-mouse antibody (KPL, Gaithersburg, MD). The immunoreactive proteins were visualized by color development.

2.9 Construction of Sf9 stable cell lines stably expressing α Rep proteins fused to GFP

2.9.1 Construction of pIB vectors expressing (Myr+) α Rep4E3-GFP and pIB_(Myr+) α Rep9A8-GFP

To construct the pIB vector for the expression of the two α Rep proteins, (Myr+) α Rep4E3-GFP and (Myr+) α Rep9A8-GFP, the pIB backbone vector was treated with *Bam*HI and *Hind*III restriction enzymes. The insert fragments of these two genes were obtained from pQE-31- α Rep4E3 and pQE-31- α Rep9A8 by PCR technique using a pair of specific primers, pIB_Fw_(Myr+) α Rep (5'-GAG AAG CTT ATG GGA TCC AGA AAA-3') and pIB_Rv_ α Rep (5'-GAG GAG AAG CTT TTA TGG GCT-3') then treated the PCR products with the same cut sites as backbone vector. The ligation was performed using T4 DNA ligase and the ligation products were transformed into XL-1 Blue competent cells followed by plating the cells on the LB agar containing 100 μ g/ml of ampicillin. Isolated colonies were picked for colony PCR and restriction enzymes analysis. The positive clones were confirmed by DNA sequencing.

2.9.2 Establishment of Sf9 cells stable expressing (Myr+) α Rep4E3-GFP and pIB_(Myr+) α Rep9A8-GFP

Aliquots of Sf9 cells were transfected with 2.5 μ g pIB-based vectors (Thermo Fisher Scientific, Waltham, MA) encoding the myristoylated α Rep protein fused to green fluorescence protein, pIB_(Myr+) α Rep4E3-GFP and pIB_(Myr+) α Rep9A8-GFP, using the DOTAP Liposomal Transfection Reagent (Roche Diagnostics GmbH, Mannheim, Germany) as protocol directed. The transfected cells were maintained in complete Grace's insect medium containing 100 μ g/ml blasticidin (Thermo Fisher Scientific, Waltham, MA) to isolate the blasticidin resistant cell lines. Two cell lines were generated, Sf/(Myr+) α Rep4E3-GFP and Sf/(Myr+) α Rep9A8-GFP. The (Myr+) α Rep4E3-GFP and (Myr+) α Rep9A8-GFP protein expression was monitored under fluorescence microscope and western blotting analysis using rabbit polyclonal anti- α Rep protein followed by phosphatase-labeled anti-rabbit monoclonal antibody.

2.10 Luciferase-based quantitative assay of α Reps on HIV-1 VLP assembly

Sf9-derived cell lines, Sf/(Myr+) α Rep4E3-GFP and Sf/(Myr+) α Rep9A8-GFP were seeded on 6-well plate to have 70-80% confluent then infected with the recombinant baculovirus carrying gene encoded HIV-1 Gag polyprotein (AcMNPV^{gag}), or coinfecting with AcMNPV^{gag} and HIV-1 auxiliary protein Vpr fused to the luciferase reporter gene (AcMNPV^{lucvpr}) at multiplicity of infection (MOI) 10 PFU/cell. At 48 hours post-infection the viral-like particles (VLPs) produced from the cells in culture supernatant as shown in Figure 2.2 were collected isolated by 30%-50% sucrose gradient ultracentrifugation. After ultracentrifugation in an SW41 Ti Swinging-Bucket Rotor at 28,000 rpm, the membrane-enveloped VLP pellet were resuspended in lysis KDT buffer (0.1 M potassium phosphate buffer, pH 7.8, 1 mM DTT, containing 0.2% Triton X-100) for 30 minutes at 37°C with vortexing every 10 minutes. Enzymatic assay of VLP-associated luciferase activity were then measured after adding luciferase substrate solution (0.1 M Tris acetate pH 7.8, 1 M DTT, 0.5 M EDTA, 1 M MgSO₄,) to quantify the level of VLP production using a Lumat LB-9501 luminometer (Berthold Technologies, Bad Wildbad, Germany).

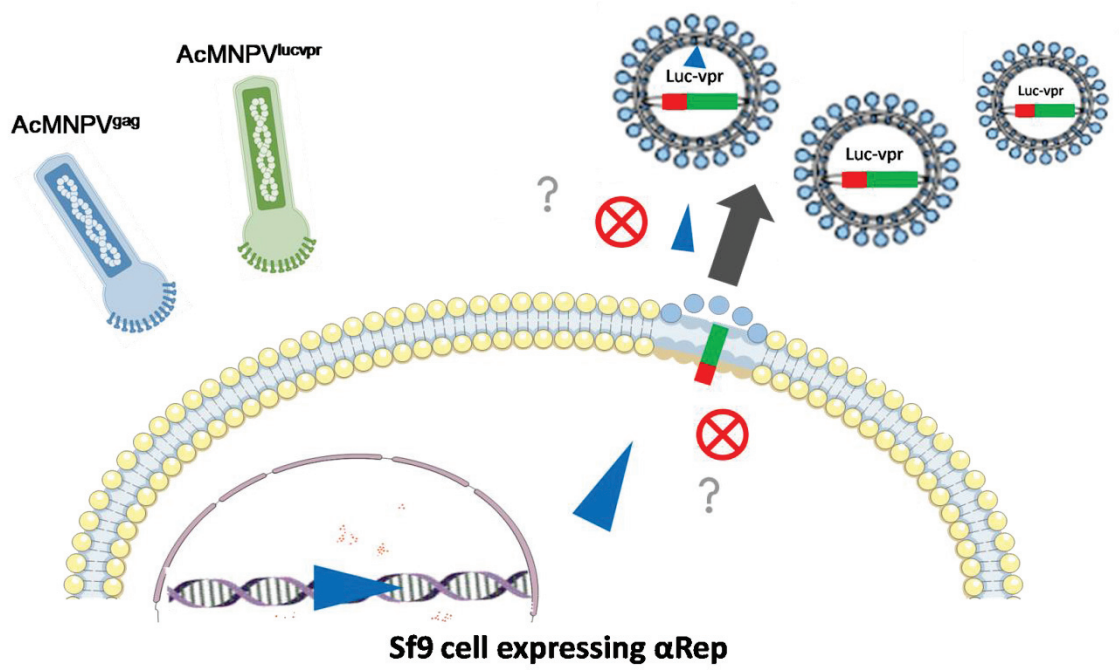


Figure 2.2 Luciferase based VLP assembly assay. After double infection α Rep expressing cells with two recombinant baculoviruses, AcMNPV^{gag} and AcMNPV^{lucvpr}, VLPs carrying the Luc-Vpr fusion protein are released in the culture supernatant and can be isolated by conventional centrifugation methods or by isopicnic ultracentrifugation in 30%-50% sucrose-D₂O density gradient at 48 hours post-infection and assayed for luciferase activity.

2.11 Electron microscopy analysis of HIV-1 Gag assembly into VLPs in Sf/(Myr+)αRep4E3GFP or Sf/(Myr+)αRep9A8GFP

Recombinant baculovirus AcMNPV^{gag} infected Sf9 cell control, Sf/(Myr+)αRep4E3-GFP and Sf/(Myr+)αRep9A8-GFP were harvested at 48 hours post-infection. Infected cells were pelleted and fixed with 2.5% glutaraldehyde in 0.1 M phosphate buffer, pH 7.5, post fixed with osmium tetroxide (2% in H₂O) and treated with 0.5% tannic acid solution in H₂O. The samples were dehydrated and embedded in Epon (Epon-812, Fulham, Latham, NY). Ultrathin sections were stained with 2.6% alkaline lead citrate and 0.5% uranyl acetate in 50% ethanol, then post stained with 0.5% uranyl acetate solution in H₂O. Grids were examined under a Jeol JEM-1400 electron microscope, equipped with an ORIUSTM digitalized camera (Gatan France, 78113-Grandchamp).

2.12 Construction of lentiviral vectors

The third generation of self-inactivating (SIN) CGW lentiviral vector (kindly provided by Dr. Bruce E. Torbett, The Scripps Research Institute, CA, USA) was used to prepare a backbone vector for transferring of the αRep protein coding genes; αRep4E3-EGFP and αRep9A8-EGFP into target cells. The vector contains MND promoter (a synthetic promoter containing the U3 region of a modified MoMuLV LTR with the myeloproliferative sarcoma virus enhancer) to ensure the high level expression of transgenes. All constructs were generated by polymerase chain reaction (PCR) using pCEP4 which harboring each of αRep genes as a template. The PCR products were purified using GeneJET PCR Purification kit (Thermo Fisher Scientific, Waltham, MA) followed by treated with *EcoRI* (Thermo Fisher Scientific, Waltham, MA) and *BstXI* (New England Biolabs, Ipswich, MA). The insert genes were ligated into CGW lentiviral vector pretreated with the same restriction enzymes as shown in Figure 2.3 using T4 DNA ligase, then transformed the ligation products into the competent *E. coli* XL-1 Blue cells. Transformation reactions were plated on LB agar containing 100 µg/ml of ampicillin. The single colonies were picked and preliminary identified by colony PCR and restriction enzymes analysis. The positive clones were then confirmed by DNA sequencing.

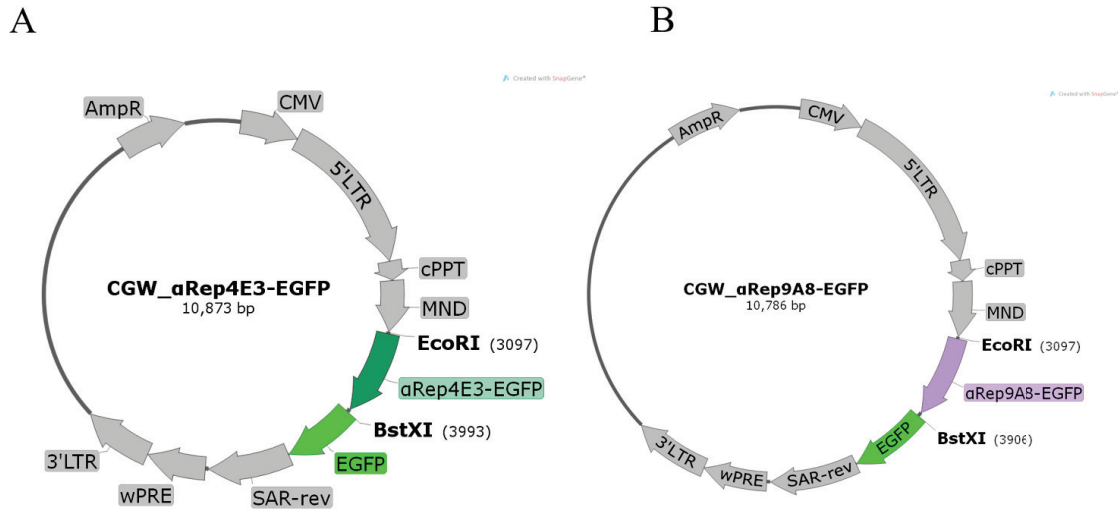


Figure 2.3 The schematic figure of CGW lentiviral transfer vectors construction for stable expression of α Rep proteins in target cells. The DNA sequences coded for α Rep proteins were inserted into CGW lentiviral vector using *EcoRI* and *BstXI* cloning sites. **A**, α Rep4E3-EGFP and **B**, α Rep9A8-EGFP.

2.13 Production of VSV-G-pseudotyped lentiviral vectors

VSV-G-pseudotyped lentiviral vector particles were produced in HEK293T cells, using four separate plasmids and transfected into the cells by calcium phosphate co-transfection method as the schematic showed in Figure 2.4. Briefly, co-transfection of CGW transfer vector 10 μ g/dish with the packaging construct pRSV-Rev 2.5 μ g/dish, pMDLg/pRRE 6.5 μ g/dish, and pMD.2G 3.5 μ g/dish into 70-80% confluent HEK293T cells in 10-cm dish was performed. At 16 hours post-transfection fresh C-DMEM containing 5% FBS was replaced and cells were further incubated. The particles of lentiviral vector were harvested from the culture supernatant at 24 and 48 hours post-transfection. They were filtered through sterile syringe filters with a 0.45 μ m pore size (Millex-HA filter unit; Merck Millipore, Hessen, Germany). The higher-titer of viral vector stocks was prepared by 20% sucrose cushion ultracentrifugation at 100,000 \times g, in 4°C, for 2 hours and 20 minutes. Viral vector pellets were resuspended in sterile PBS (EMD Millipore Corp., Billerica, MA) containing 0.1% Bovine Serum Albumin (BSA) (EMD Millipore Corp., Billerica, MA), split into 50 μ l aliquots, and kept at -80°C. The viral titer were determined

by the percentage of EGFP positive cells by infection of HEK293T cells with serial dilution of the samples at 48 hours post-transduction. The equation for calculation the titer is described below.

$$\text{Viral vector titer (TU/ml)} = (\text{Number of cells per well at the time of viral vector addition}) \times (\text{average \% fluorescence positive cells}/100) \times (\text{dilution factor}) \times (1 \text{ ml}/0.4 \text{ ml})$$

Note: the titer must be calculated from a sample corresponding to a vector dilution when fluorescence positivity of cells ranges between 5%-25%, in order not to underestimate the titer when multiple transduction events per cell have occurred.

2.14 Construction of the stable SupT1 cell lines stably expressing α Rep proteins

Aliquots of SupT1 cells were transduced with 1 MOI of the VSV-G-pseudotyped CGW_ α Rep-EGFP vectors by spinoculation at 2,500 x g, 32 °C for 2 hours in growth medium containing 8 μ g/ml of Polybrene (Sigma–Aldrich, St. Louis, MO). At 16 hours post-transduction cells were washed three times using serum free medium then maintained at 37°C and 5% CO₂ in fresh C-RPMI supplemented with 10% FBS, penicillin 100 U/ml, and streptomycin 100 μ g/ml. The cells were further maintained in fresh C-RPMI medium and divided every 3 days. The transduction efficiency and stability were monitored by fluorescence microscopy and flow cytometry.

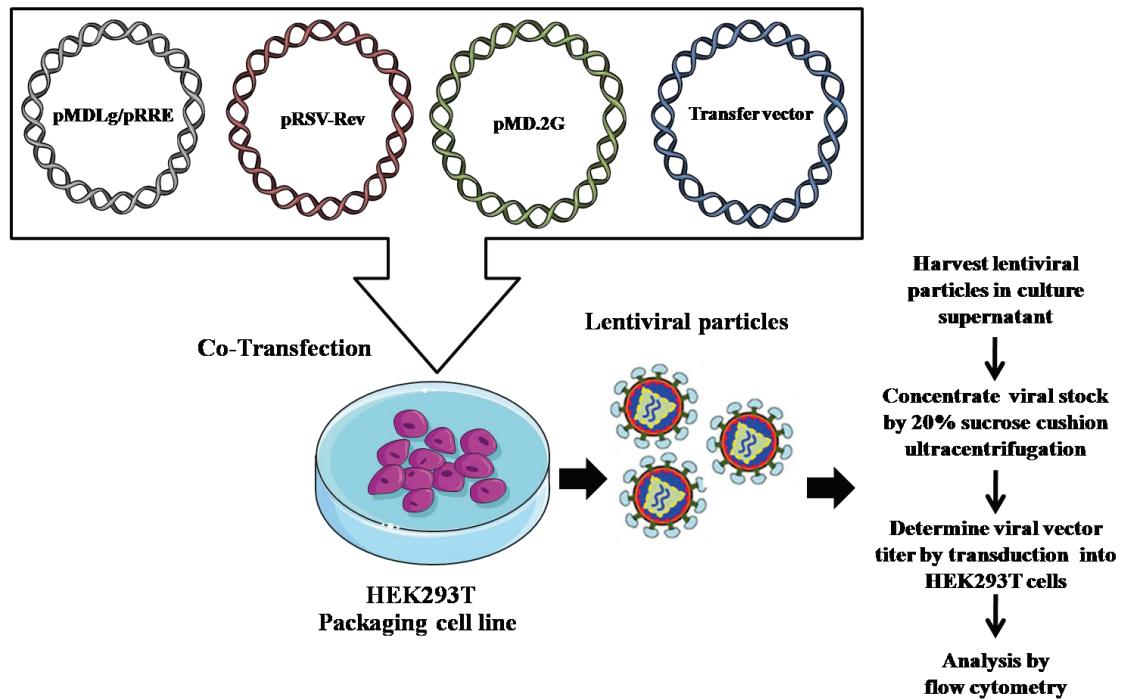


Figure 2.4 Production of VSV-G pseudotyped lentiviral vector particles. VSV-G pseudotyped lentiviral vector particles carrying α Rep gene was produced from HEK293T cells through transient co-transfection of vectors which encode genes for the viral components of including (1.) packaging vector (pMDLgag/polRRE), (2.) Rev expressing vector (pRSV-Rev), (3.) Envelope vector (pMD.2G) VSV-G, and (4.) CGW transfer vector. Pseudotype lentiviral vector particles were then harvested from the culture medium and concentrated by 20% sucrose cushion ultracentrifugation. The viral vector titer was determined by transduction into HEK293T cells following analysis by flow cytometry.

2.15 Flow cytometry

Flow cytometry was used to measure the efficacy of transfection or lentiviral vectors and HIV-1 virus transduction. Cell samples were harvested at 48 hours post-transfection or transduction. Cells were washed with PBS for the first round follow by 1% FBS-0.02% NaN₃ in PBS. After washing step, the cells were resuspended in 1% paraformaldehyde in PBS and analyzed by flow cytometry. The samples were analyzed by flow cytometry (BD Accuri™ C6, BD Biosciences).

2.16 Confocal microscopy

To investigate the sub-cellular localization of α RepEGFP proteins, the confocal microscopy was used in this experiment. HeLa cells were transfected with pCEP4 vectors encoding for each of α RepEGFP proteins. At 48 hours post transfection, cells were seed in an 8-chamber slide (Nunc, Denmark), and left overnight culture before imaging. The nucleus of the cell was stained with Hoechst 33342 nuclear stain (Thermo Scientific, Waltham, MA) at dilution 1:3,000. Non-fixed cell imaging was performed using Nikon C2 Plus confocal fluorescence microscopy (Nikon, Japan).

Colocalization of EGFP-fused α Rep proteins and Pr55Gag in HIV-1-infected SupT1 cells was examined by confocal microscopy. Cells were collected at D10 pi, fixed, permeabilized and immunolabeled with Qdot705 (Thermo Scientific, Waltham, MA) conjugated anti-CAP24 G18 mAb. Nuclei were counterstained with 4',6-diamidino-2-phenylindole (DAPI; Thermo Scientific, Waltham, MA) at dilution 1:5,000. Cell imaging was performed using Nikon C2 Plus confocal fluorescence microscope (Nikon, Japan). Excitation wavelengths were 405 nm for DAPI, 488 nm for EGFP and 561 nm for Qdot705. All renderings were processed using the Nikon NIS-elements of the AR 4.20.00 software.

2.17 HIV-1 stock

Replication-competent X4 tropic virus HIV-1_{NL4-3} virus was produced by transiently transfect the pNL4-3 plasmid into the HEK293T cells. Briefly, monolayers of HEK293T cells were seeded into the 10-cm dish at 4×10^6 cells to obtain the monolayer of the producer cells follow by transfected with 5 μ g of the pNL4-3 plasmid using transIT-X2 transfection reagent (Mirus Bio, Madison, WI) according to the manufacturer's protocol. The cells were allowed to grow in the culture medium for 48 hours. HIV-1 virus particles in culture supernatant were then harvested and filtrated through the sterile syringe filters with a 0.45 μ m pore size. HIV-1 stock was aliquoted and stocked at -80°C . The virus titer was determined using conventional p24 antigen ELISA, using the Genscreen ULTRA HIV Ag-Ab assay (Bio-Rad, Marnes-la-Coquette, France). The viral load was determined using the COBAS AMPLICOR HIV-1 Monitor test (Roche Molecular Systems, Branchburg, NJ).

2.18 Evaluation of antiviral activity of α Rep proteins in SupT1 stable cell lines

The level of intracellular antiviral protection conferred by myristoylated α Rep4E3EGFP, non-myristoylated α Rep4E3EGFP, myristoylated α Rep9A8EGFP, and non-myristoylated α Rep9A8EGFP were determined by challenging these cell lines with the X4-tropic virus, HIV-1_{NL4-3}. Control SupT1 cells and SupT1 cells stably expressing α Rep proteins, were cultured in the fresh growth medium for at least 4 weeks before HIV-1 challenging. To perform the infection assay, spinoculation of target cells were performed with 1 MOI of HIV-1 for 16 hours. The cells were next washed three times using serum-free medium, and resuspended in fresh growth medium. At 3-day intervals, cells were split (1:2) to maintain the density of the cells. The yields of HIV-1 replication was monitored in the culture supernatants using p24 antigen ELISA (Bio-Rad, Marnes-la-Coquette, France) and viral load assay (COBAS AMPLICOR HIV-1 Monitor test, version 1.5; Roche Molecular Systems, Branchburg, NJ). The cell pellets were kept for the determination of the proviral integration level. The cell viability was performed in parallel by the trypan blue dye exclusion staining assay.

2.18.1 Determination of p24 level by p24 antigen ELISA

The p24 level in culture supernatant collected from infected SupT1 cell control and SupT1 cell lines were quantified by p24 antigen ELISA (Bio-Rad, Marnes-la-Coquette, France) following the manufacturer's recommended protocol. The concentration of p24 from were calculated from the standard HIV-1 p24 antigen which was diluted to prepare a series of varying concentrations. A standard curve was constructed from which optical density values of culture supernatant samples are interpolated to determine their concentration.

2.18.2 Quantitation of integrated proviral DNA by SYBR RT-PCR-based integration assay

The integration of HIV-1 DNA in SupT1 stable cell lines and SupT1 control were quantified by using SYBR RT-PCR-based integration assay. The genomic DNA of infected SupT1 cell control and SupT1 stable cell lines were extracted by using the High Pure PCR template kit (Roche, Mannheim, Germany). The PCR reaction was performed by SensiFAST™ SYBR No-ROX Kit (Bioline, Luckenwalde, Germany) in total volume 20 µl as the standard protocol directed. The genomic DNA template used in the PCR was adjusted to 5 ng/µl and 1 µl was used per reaction. The reactions were performed using the CFX96 real-time PCR system with the following program: 20 second of hot start at 95°C, followed by 40 cycles of denaturation at 95°C for 30 second, annealing and extension at 68°C for 30 second.

2.19 Infectivity Assay of HIV-NL4-3 derived from SupT1 cells lines stably expressing αRep proteins

After quantification of the level of p24, the culture supernatant samples were adjusted to have equal amount of p24 at 15 µg/ml in fresh C-RPMI. Jurkat-GFP cells (105, 106) were prepared at 2.5×10^5 cells/well in 96 wells culture plate containing 8 µg/ml of Polybrene (Sigma–Aldrich, St. Louis, MO). Hundred microliter of diluted culture supernatant were added into each well, then incubated at 37°C and 5% CO₂. At 16 hours post-infection, C-RPMI 100 µl were added into the wells. Jurkat-GFP cells were then harvested at D14 post-reinfection and assayed for GFP positive cells by flow cytometry.

2.20 ELISA based HIV-1 Pr55Gag maturation assay

Microtiter plates were coated with 100 μ l of 5 μ g/ml of mouse anti-MA HB-8975 monoclonal antibody diluted in coating buffer 1M NaHCO₃ pH 8.6 and incubated overnight at 4°C in a moisture chamber. The anti-MA antibody, hybridoma clone MHSVM33C9/ATCC HB-8975, was obtained from the American Type Culture Collection (ATCC, Manassas, VA). It is known to recognize the epitope (DTGHSSQVSQNY) located at the C terminal MA of Gag polyprotein (107, 108). The coated wells were washed 3 times with PBST and blocked with 200 μ l of blocking solution (2% BSA PBS) at room temperature for 1 hour. After the washing step, 60 μ l culture supernatant from each infected SupT1 expressing Rep-EGFP was normalized the p24CA titers to final concentration 80 μ g/ml. The samples were then pre-incubated with 1% Triton X-100 at room temperature for 10 minutes and 10 ng/ml of biotinylated synthetic p17MA C-terminal peptide were added to the well and incubated for 1 hour. There is competition when the culture supernatant contains the mature form (free cleaved MA) of Gag protein or if HIV PR is able to specifically cleave at MA-CA junction and free C-terminal of MA is exposed. The same epitope present as a biotinylated synthetic p17MA C-terminal peptide, is recognized by an anti-MA HB-8975 monoclonal antibody. The reaction were then reviewed by streptavidin conjugated HRP. The TMB micro well peroxidase substrate 100 μ l were added after 1 hour incubation time followed by stopped reaction with 1 N HCl and measured the optical density OD at 450 nm.

2.21 Generation of HIV-1 target proteins

Our viral targets consisted of various GST-fused polyproteins derived from the HIV-1 GagPr55 precursor (LAI isolate). GST-CA₂₁SP1-NC included the 21 amino acids of the C-terminal domain of the capsid protein (CA), fused to the SP1 linker and the whole nucleocapsid (NC) domain, encompassing its two zinc fingers (ZF) until residue F433. A series of C-truncated mutants of GST-CA₂₁SP1-NC were also constructed (Figure 2.5). The DNA fragments coding for each construct were rescued by PCR amplification from pGEX-GST-CA₂₁SP1-NC, using specific oligonucleotide primers. The amplification products were purified by GeneJET PCR Purification kit, and a first step gene cloning was performed using InsTAclone PCR cloning kit (ThermoFisher Scientific, Waltham, MA). XL-1 Blue competent cells were transformed by the ligation products, and plated

on LB agar containing ampicillin (100 µg/ml). Colonies were picked for PCR amplification, restriction enzyme analysis using *Bam*HI and *Xho*I, and DNA sequencing. The DNA fragments of each construct were isolated from the pTZ57R/T vector and transferred to pGEX-GST expressing vector using the same restriction sites, *Bam*HI and *Xho*I. Three pGEX-GST-gag plasmids were thus obtained: (i) pGEX-GST-CA₂₁SP1-NC; (ii) pGEX-GST-CA₂₁SP1-NCΔZF2; and (iii) pGEX-GST-CA₂₁SP1. BL21 cells were used for recombinant Gag protein production. BL-21 harboring each of the recombinant pGEX-GST-gag plasmids were cultured in 200 ml LB broth containing 100 µg/ml ampicillin and 1% (w/v) glucose, at 37°C with shaking. When OD₆₀₀ reached 0.8, protein expression was induced by addition of 0.1 mM IPTG, and maintained in culture at 30°C overnight with shaking. Cells were pelleted by centrifugation at 1,200 x g for 30 min at 4°C. Cell pellets were resuspended in PBS containing a cocktail of protease inhibitors (Roche Diagnostics GmbH), then lysed by sonication. Soluble proteins were purified by affinity chromatography on glutathione-agarose gel (ThermoFisher Scientific), following the protocol of the manufacturer, and analyzed by SDS-PAGE and Western blotting.

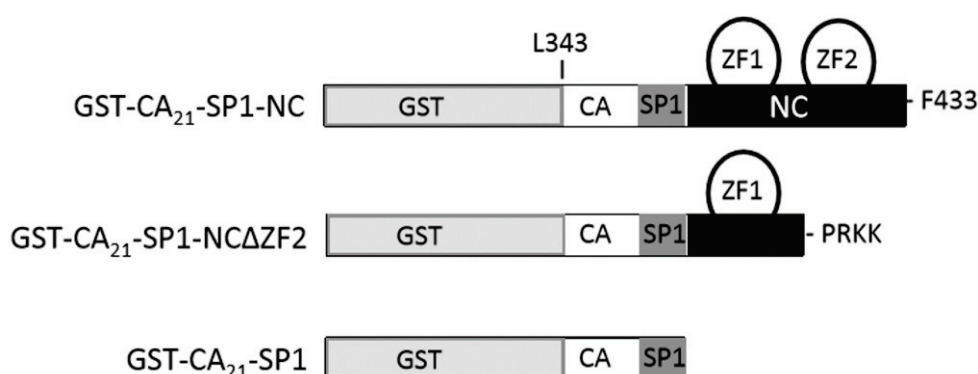


Figure 2.5 CA₂₁-SP1-NC full-length bait and deletants. From top to bottom: full-length target CA₂₁-SP1-NC; deletion of the C-terminal Zinc finger (ΔZF2); deletion of the two Zinc fingers ZF1 and ZF2.

2.22 Protein pull-down assays

The *E. coli* BL21 cells were transformed with plasmids pGEX-4T1 harboring the genes encoding the GST-CA₂₁-SP1-NC, GST-CA₂₁-SP1-NCΔZf2, and GST-CA₂₁-SP1 proteins, and bacterial cells cultured in Terrific broth (TR) medium supplemented with ampicillin (100 µg/mL), and glucose (1%; w/v) at 37°C with shaking. When the OD₆₀₀ of the cultures reached 0.8, protein expression was induced by addition of 0.1 mM isopropyl β-D-1-thiogalactopyranoside, and the culture was further maintained at 30°C for 16 hours with shaking. Bacterial cells were then pelleted by centrifugation at 1,200 x g at 4°C for 30 min, resuspended in PBS containing a cocktail of protease inhibitors (Roche Diagnostics GmbH), and sonicated. After clarification by centrifugation (15,000 x g at 4°C, for 30 min), aliquots of supernatants containing GST-CA₂₁-SP1-NC, GST-CA₂₁-SP1-NCΔZf2, or GST-CA₂₁-SP1 protein were incubated with purified αRep4E3 or αRep9A8 protein (300 µg) in PBS-0.01% Tween-20 (1 ml total volume), for 2 hours at RT with shaking. Aliquots (20 µl) of glutathione (GSH)-coated agarose beads (Pierce Glutathione Agarose; Thermo Scientific, Waltham, MA) were then added to the reaction mixture, and further incubated for 1 hour at RT with shaking. Beads were centrifuged at low speed, washed 4 times with 0.05% Tween-20 in PBS, and resuspended and heat-denatured in SDS-PAGE loading buffer.

CHAPTER 3

RESULTS

3.1. A new scaffold protein library and the CA₂₁-SP1-NC domain of the Gag polyprotein precursor as target

In this PhD project, we used a new repeat-protein library called alpha-Repeat (α Rep) which was constructed and provided by the lab of Prof. Philippe Minard (CNRS Paris-Orsay). In brief, the structures and sequences of a new type of artificial repeat protein, HEAT-like repeat was described. From the known structure of a thermostable HEAT repeat subfamily, the consensus sequences of the HEAT repeat protein were identified and devised to become N-Cap and C-Cap. The protein library was then assayed the biophysical properties. The results obtained suggested that in this library, the proteins differ by the number of internal repeat motifs and the local amino acid residues of each repeat in the variable positions. The α Rep proteins have advantages over the ankyrin repeat proteins in particular, their thermostability ($T_m > 70^\circ\text{C}$) and other properties discussed in Chapter 1. Since the aim of our study was to isolate molecules which would negatively interfere with the morphogenetic process of the virus particle, we screened the α Rep library for binders against the CA₂₁-SP1-NC domain of the Gag precursor. The SP1 linker is a short, 14-residue peptide acting as a hinge between the capsid (CA) and the nucleocapsid (NC) domains of the Pr55Gag polyprotein precursor and has been shown to be essential for the correct oligomerization of Pr55Gag and the assembly of membrane-envelope virus particles but mainly involved in the virus maturation and infectiveness. The NC domain is essential for assembly, encapsidation of the viral genome, and acts as nucleic acid chaperone (27, 38).

The SP1 domain is framed by two crucial protease cleavage sites, and this region is essential for the immature particle assembly and in regulating the formation of the mature HIV-1 capsid essential for virus infectivity (43, 45). For all the reasons mentioned above, SP1-NC is our privileged target for screening the α Rep library to obtain a new family of

HIV-1 assembly inhibitors. The protein interactors of SP1-NC could have several effects: (i) on the Pr55Gag structure and oligomerization process; (ii) on the viral protease activity and the blockage of the maturation cleavage of CAp25 into CAp24-SP1, viral genome packaging and the infectivity of the virus. We have chosen the polyprotein domain of Pr55Gag between L343 and F433 (91 residues) overlapping the C-terminal 21 residues of the CA protein, the SP1 linker and the region of the NC protein encompassing its two zinc fingers (abbreviated CA₂₁-SP1-NC) as the bait for our selection of α Rep molecules. The NMR structure of SP1-NC-SP2 was shown in the Figure 3.1 to elucidate the folded structure of this protein domain.

The SP1-nucleocapsid(NC)-SP2 domains of HIV-1

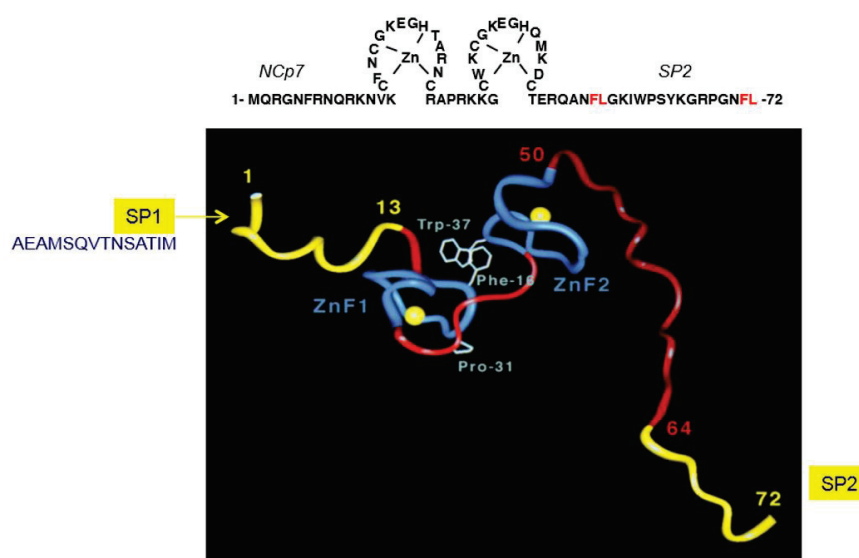


Figure 3.1 Amino acid sequences and the NMR structure of the SP1-NC-SP2 domain of HIV-1 Gag polyprotein. Top panel shows the sequence of amino acids of NC containing the two zinc finger motive CCHC and SP2. Bottom panel is the 3D structure of NC-SP1 as determined by NMR. The position of individual amino acid are indicated in the number, zinc ions are showed in the yellow round symbol.

3.2. Selection of CA₂₁-SP1-NC binders from a library of phage-displayed α Rep proteins

The phage display is the method to express binder peptides or proteins of interest at the surface of phage particles. The peptides or proteins which are interactors of a given target can be identified by affinity selection, a technique called "*bio-panning*" (109). The phage display system allows production of protein or peptide libraries with a high diversity of randomized ligands, making it a very versatile and high-throughput screening method for the identification of potential binding molecules specific for different types of target molecules of interest. In this study, the α Rep scaffold phage library used for our screening against the CA₂₁-SP1-NC domain of Pr55Gag has been constructed and described in Guellouz A. *et al.*, *PLoS One*. 2013 (88). To obtain the α Rep binders against the viral target CA₂₁-SP1-NC, three rounds of phage-display selection were performed on microtiter plate-immobilized GST-CA₂₁-SP1-NC. The CA₂₁-SP1-NC-binding clones were then identified using a phage-ELISA method. By this method, phages produced from individual α Rep clones were incubated with the immobilized target and detected by using an anti-bacteriophage antibody (HRP-conjugated anti-M13). This bio-panning method provided us with 30 individual clones from the library, which were then randomly picked and analyzed. Eighteen α Rep clones positively reacted towards immobilized GST-CA₂₁-SP1-NC with varying intensities of their binding signal, and among them, six showed a significantly higher signal ($OD \geq 0.3$): 4D4, 4E3, 4F2, 5A12, and 5F1 (Figure 3.2) and 9A8 (not shown). This indicated that certain phage-displayed α Reps clones were able to bind to our viral target with different affinities. Glutathione S-transferase (GST; *light grey bars*) served in this experiment as the background control for non-specific binding, and the GST signal was subtracted from the GST-CA₂₁-SP1-NC signal for guiding the clone selection. The six strong binding α Rep clones 4D4, 4E3, 4F2, 5A12, 5F1 and 9A8 as shown in Figure 3.2 were isolated for further characterization

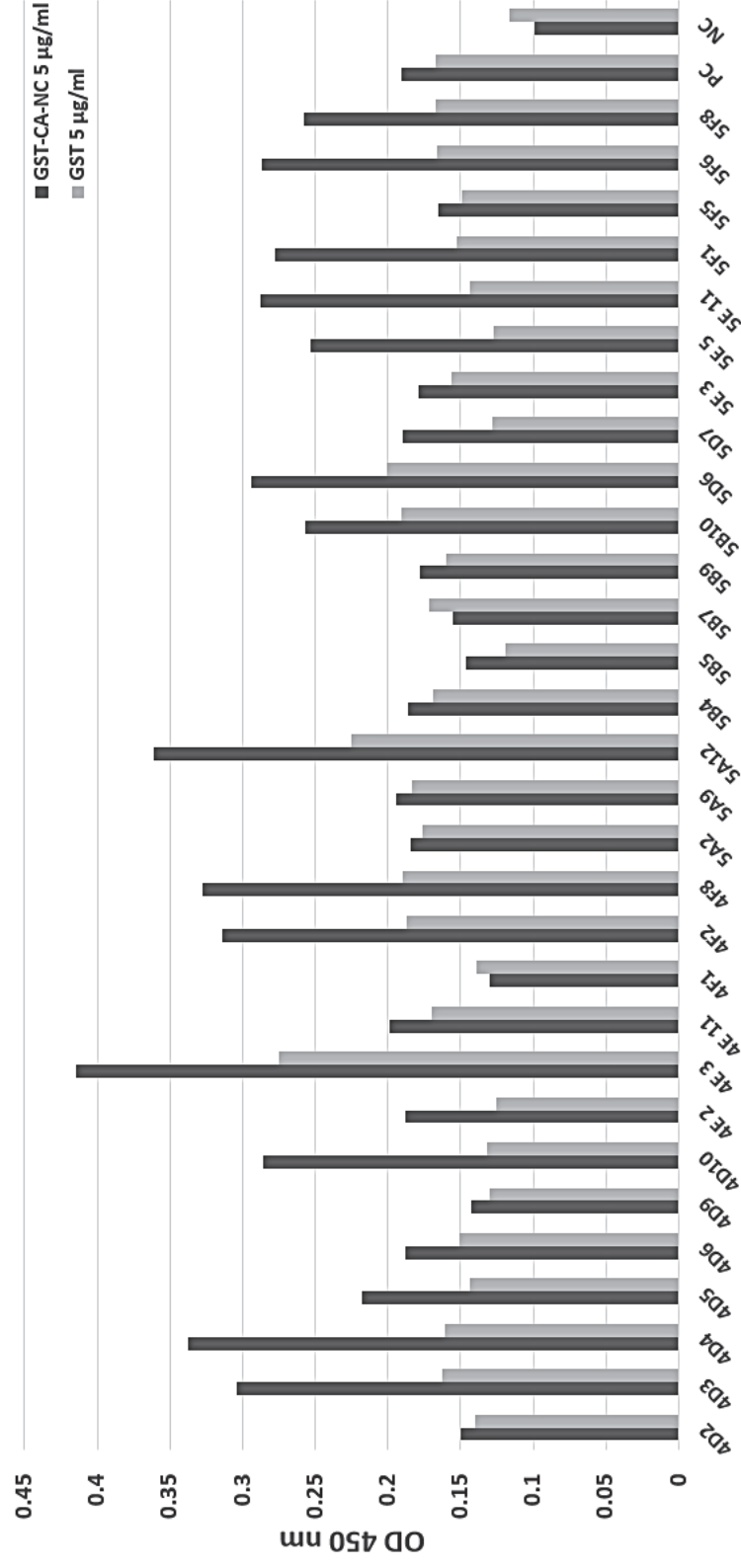


Figure 3.2 Screening of 30 α Rep clones from the third round of panning. Phages obtained from single individual clones were used to determine the high affinity binders against the GST-CA₂₁-SP1-NC target protein. GST served as a negative control for non-specific binding.

3.3 Biochemical and biophysical characterization of CA₂₁-SP1-NC binders

To characterize the six α Rep protein clones obtained from phage-ELISA, the α Rep genes were sub-cloned into the plasmid expression vector pQE-31, and verified by DNA sequencing. The α Rep proteins were then expressed in *E. coli* M15 [pREP4]) and purified by affinity chromatography using HisTrap columns. The soluble form of the six selected α Reps were analyzed for their binding activity to the viral target *in vitro*, using indirect ELISA technique. Microtiter ELISA plates were coated with GST-CA₂₁-SP1-NC, the α Rep proteins were added individually to the well, and their binding activity was detected by using a rabbit polyclonal anti- α Rep antibody followed by peroxidase-conjugated goat anti-rabbit antibody. The results were shown in Figure 3.3 A. Anti-GST antibody was used to confirm that target GST-CA₂₁-SP1-NC and control GST were successfully immobilized onto the micro-well plates (Figure 3.3 B). Distinct binding activities between the α Reps clones were revealed when the wells were coated at 5 μ g/ml GST-CA₂₁-SP1-NC, compared to wells coated with GST proteins. The α Rep 4E3 clone showed the highest binding activity, and 9A8 the second highest. The other four clones showed a lower binding activity to the target protein (Figure 3.3 A). This has already been observed for certain phage-displayed proteins, whose binding properties change with their environment. Within the gp3 fusion structure, their binding interfaces can be significantly altered, positively or negatively. This seemed be the case for α Rep clones 4D4, 4F2, 5A12, and 5F1 which behaved differently in fusion with phage gp3 protein (strong binders), and in soluble form (moderate binders). Thus, only the two α Reps, α Rep4E3 and α Rep9A8, were selected for further characterization in the next experiments.

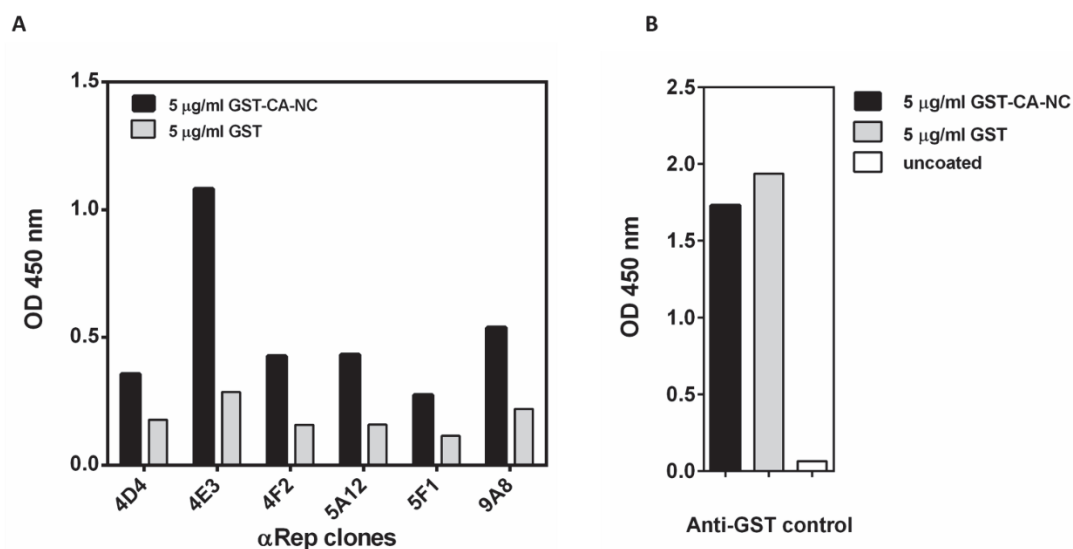


Figure 3.3 Target-binding activity of α Reps against GST-CA₂₁-SP1-NC. Binding activity of soluble α Rep clones were measured by ELISA. **A**, Binding of α Reps to the viral target GST-CA₂₁-SP1-NC (*black bars*), with GST used as a background control (*grey bars*). Target protein and control GST protein at 5 μ g/ml were immobilized on the plate. Soluble purified α Rep clones were used at 10 μ g/ml, and the level of α Rep binding was assayed using specific anti- α Rep antibody. **B**, Anti-GST antibody was used to perform the quality control of the coated plates in terms of target protein immobilization.

The histidine tagged α Rep4E3 and α Rep9A8 proteins were expressed in bacterial cells and consequently purified by affinity chromatography. In parallel, their apparent molecular weight (MW) and the degree of purity of the purified α Rep samples were evaluated by SDS-PAGE. Their DNA sequences and the number of their repeats were determined. The results of the DNA sequencing was translated into amino acids sequences, and allowed us to determine the conserved and variable regions of α Rep4E3 and α Rep9A8. As shown in Figure 3.4 **A & C**, the two binders shared a few common features, including His-tag at the N-terminal region, N-terminal cap (N-cap), C-terminal cap (C-cap), and constant regions (indicated in black letters, using the one single-letter code for the amino acids alphabet). However, they differed both in the number of their repeats (7 and 6 repeat motifs were found for α Rep4E3 and α Rep9A8, respectively) and in the nature of residues found at the variable positions (presented in red alphabet).

Therefore, each internal repeat of α Rep contains five random variable amino acids which serves as the keys binding residues. In summary, the difference in repeat numbers and in amino acids occupying the variable positions in α Rep4E3 and α Rep9A8 explained their difference in binding activity towards the viral target.

After protein production and purification, a single band of α Rep protein was observed in SDS-PAGE analysis, migrating at 32 kDa for α Rep4E3 and at 28 kDa for α Rep9A8 (Figure 3.4 **B & D**). The high intensity of both α Rep protein bands over the background of bacterial proteins suggested that α Rep4E3 and α Rep9A8 were expressed at high yields, and in a highly soluble form, in the bacterial expression system. Moreover, our results indicated that α Rep4E3 and α Rep9A8 were able to retain their target binding function *in vitro*. In the next step, these two α Rep candidates were further tested for their function inside the cell, using the insect cell expression system.

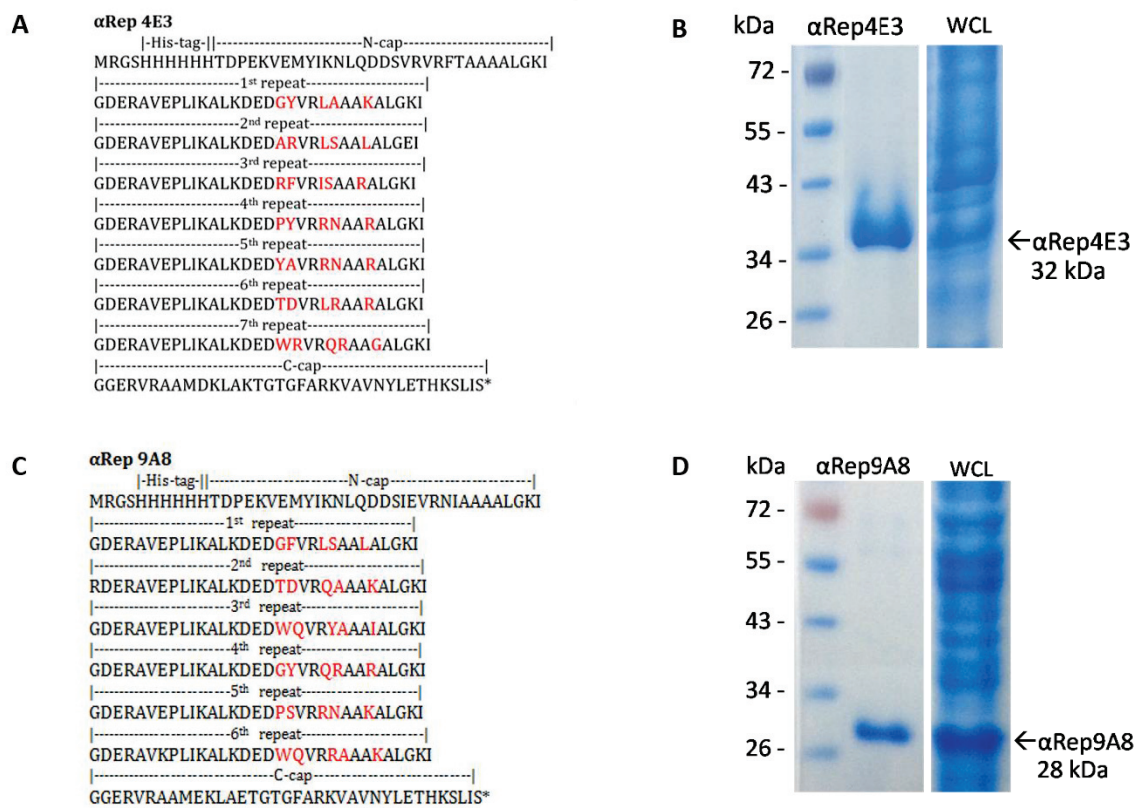


Figure 3.4 Amino acid sequence, production and purification of α Rep4E3 and α Rep9A8. **A & C**, Amino acid sequences of α Rep4E3 and α Rep9A8, with each of amino acid indicated in one single-letter code. Constant regions of the proteins are in black letters, whereas variable residues are shown in red. An oligo-His tag is fused to the N-terminus of each protein. The multiple repeat motifs are stacked between N-cap and C-cap. **B & D**, SDS-PAGE analysis of α Rep4E3 and α Rep9A8 purified by affinity chromatography on Ni-NTA agarose resin. WCL, whole cell lysate before α Rep purification, containing all soluble proteins.

3.4 Effects of α Rep4E3 and α Rep9A8 on HIV-1 virus-like particle assembly

Since α Rep4E3 and α Rep9A8 showed a significant binding activity towards the CA₂₁-SP1-NC domain of HIV-1 Pr55Gag *in vitro*, we next explored their effect on the assembly of HIV-1 virus-like particle (VLP) *in vivo*, in a heterogenous cell expression system. The first experiment was performed using the recombinant baculovirus-infected insect cells system.

3.4.1 Construction of Sf9-derived cell lines stably expressing α Rep proteins

The genes of the α Rep4E3 and α Rep9A8 were designed and fused to the green fluorescent protein (GFP) encoded gene and to the coding sequence of the oligo-Histidine tag at their C-terminus. In parallel, the N-terminus of both proteins was modified to become a substrate for cytoplasmic N-myristoyl-transferase. This design resulting in the co-translational amidification of the alpha-amino group of the N-terminal glycine residue by the myristic acid, and the attachment of a myristoyl group to the N-terminus of α Rep4E3 and α Rep9A8 *via* a covalent amide bond (110). The aim of adding the N-myristoylation to the α Rep proteins was to address them to the inner leaflet of the cell plasma membrane, where the VLP assembly occurs.

The schematic diagram of the construction of these modified α Rep-GFP genes is shown in Figure 3.5 (A). The gene constructs were cloned into the pIB/V5-His vector which contained a blasticidin resistance gene. The recombinant plasmids were then performed the DNA sequencing analysis. The correct DNA sequence of the constructs were transferred to Sf9 cells by liposome-mediated transfection, to generate the Sf/(Myr+)4E3-GFP and Sf/(Myr+)9A8-GFP cell lines. Cells were treated with blasticidin, a potent translational inhibitor, to eliminate the parental Sf9 cells and only maintain in culture those cells which have received the recombinant plasmid carrying the blasticidin-resistant gene, and which stably expressed the α Rep-GFP molecules. In these two cell lines, the α Rep4E3-GFP and α Rep9A8-GFP genes were integrated into the cellular genome resulting in cells stably expressing the α Rep-GFP proteins under the control of the baculovirus immediate-early promoter, *OpIE2* promoter. The expression of (Myr+) α Rep4E3-GFP and

(Myr+)αRep9A8-GFP proteins was successfully produced intracellularly as monitored by fluorescence microscopy as shown in the Figure 3.5 B. The top panel represented the Sf9 cells expressing the (Myr+)αRep4E3-GFP and the bottom panel shows the protein expression of (Myr+)αRep9A8-GFP. Each panel displays the phase contrast and GFP signal on the left and right hand side respectively.

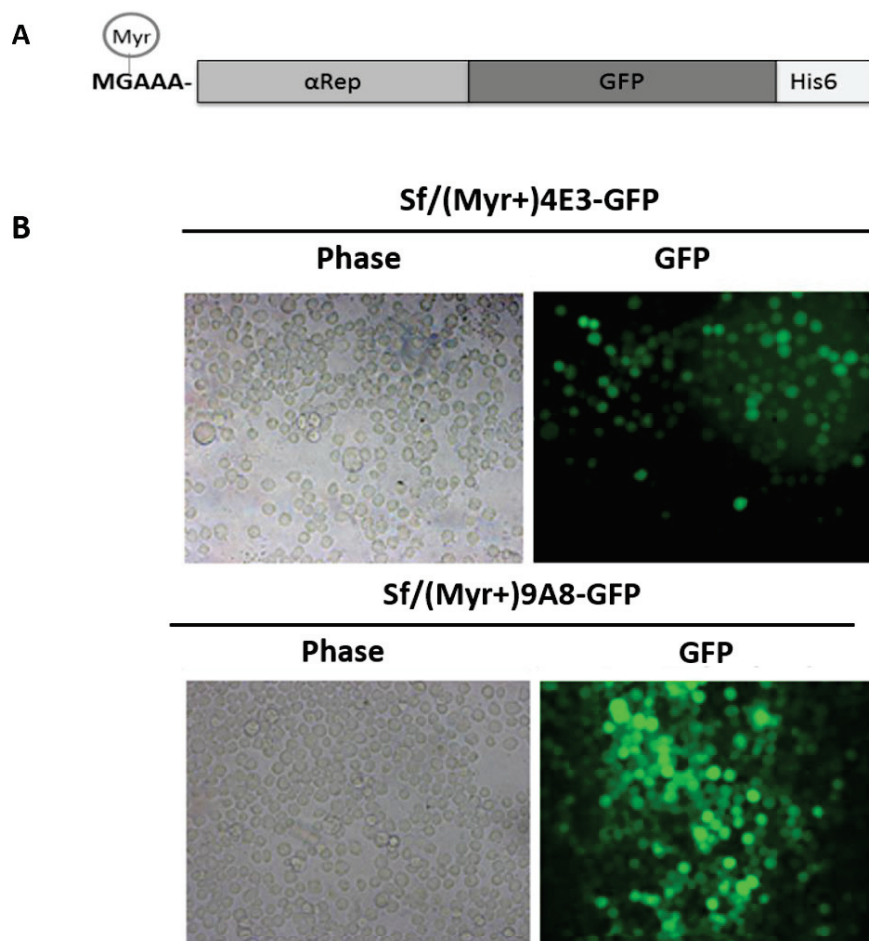


Figure 3.5 Construction of Sf9 cells stably expressing N-myristoylated αRep4E3-GFP and N-myristoylated αRep9A8-GFP. A, Schematic diagram of the αRep genes designed for stable expression of the N-myristoylated αRep4E3 and αRep9A8 proteins in Sf9-derived cells [Sf/(Myr+)4E3-GFP and Sf(Myr+)9A8-GFP]. The genes coding for the αRep proteins were modified to carry the sequence MG₂AAA at their N-terminus, and GFP and His6-tag at their C-terminus respectively. The peptide MG₂AAA is a substrate for N-myristoyl-transferases. In this enzymatic process, methionine-1 is removed and the new N-terminus of glycine at position 2 is the receiver of the N-myristoyl group.

B, Intracellular expression of the GFP-fused α Rep proteins monitored by the GFP signal under the inverted fluorescence microscope. Top panel and bottom panel are Sf/(Myr+)4E3-GFP and Sf/(Myr+)9A8-GFP respectively (left: phase contrast and right: GFP).

3.4.2 Biological effects of (Myr+) α Rep4E3 and (Myr+) α Rep9A8 on HIV-1 virus-like particle production in baculovirus infected Sf9 cells: quantitative aspects

Sf9-derived cell lines stably expressing N-myristoylated α Rep proteins, (Myr+) α Rep4E3 and (Myr+) α Rep9A8, were infected with baculovirus AcMNPV^{gag} alone (negative control of luciferase activity in VLPs), or co-infected with AcMNPV^{gag} and AcMNPV^{lucvpr}. This assay is based on the observation that the HIV-1 auxiliary protein Vpr and Vpr-fusion proteins can be co-packaged with Gag precursor protein into HIV-1 virions or membrane-enveloped virus like particle (VLP). In the case of a Luciferase-Vpr fusion, the activity of the enzyme luciferase co-incorporated with Vpr into the VLPs directly correlate with the amounts of VLPs in the extracellular medium (73). The yields of extracellular VLPs released by Sf/(Myr+)4E3-GFP and Sf/(Myr+)9A8-GFP were compared with those released by control, parental Sf9 cells. The scheme of the principle of this experiment is illustrated in Figure 3.6 A. VLPs were isolated from AcMNPV^{gag} + AcMNPV^{lucvpr}-co-infected Sf/(Myr+)4E3-GFP and Sf/(Myr+)9A8-GFP cells by ultracentrifugation in sucrose-D₂O density gradient. The VLP production was evaluated semi-quantitatively by immunoassays of extracellular, pelletable Gag polyprotein, and quantitatively evaluated by enzymatic assays of VLP-associated luciferase activity (73).

As presented in in Figure 3.6 B, Western blot analysis of concentrated total VLPs from culture supernatants of control Sf9 cells and Sf/(Myr+)4E3-GFP and Sf/(Myr+)9A8-GFP cells showed that all samples contained equivalent amounts of Gag precursor band at 55 kDa. This suggested that similar yields of VLPs were released in all cellular media. This result was corroborated by the luciferase activity assays performed on gradient fractions containing VLPs. In cells co-infected with recombinant baculoviruses AcMNPV^{gag} and AcMNPV^{lucvpr} a luciferase signal was

observed in fractions 9 to 13, whereas no signal was detected in the same gradient fractions from cells infected with AcMNPV^{lucvpr} alone (Figure 3.6 C). This result confirmed that VLPs produced by Sf9 cells efficiently incorporated functional luciferase enzyme *via* the co-encapsidation of Vpr and Gag into of HIV-1 particles during their formation. In the culture medium of AcMNPV^{gag} + AcMNPV^{lucvpr}-infected Sf/(Myr+)4E3-GFP and Sf/(Myr+)9A8-GFP cells, a peak of luciferase activity was found at fraction 9 to 13, as in the culture medium of control Sf9 cells (Figure 3.6 D). Comparison of the VLP yields indicated that there was no significant difference between the two α Rep-expressing cells. The results of Western blot analysis and luciferase assays therefore suggested that α Rep4E3 and α Rep9A8 exerted no significant quantitative effect on the production and extracellular release of VLPs by AcMNPV^{gag}-infected insect cells co-expressing the HIV-1 GagPr55 and the α Reps 4E3 or 9A8.

3.4.3 Biological effects of α Rep4E3 and α Rep9A8 on HIV-1 VLP production in heterologous system: qualitative aspects

Although the VLP production by AcMNPV^{gag}-infected insect cells was not influenced by the co-expression of α Rep4E3 or α Rep9A8, it was important to verify their quality in terms of size, morphology and internal structure. Ultrathin sections of AcMNPV^{gag}-infected Sf/(Myr+)4E3-GFP and Sf/(Myr+)9A8-GFP cells were analyzed under the electron microscope (EM) at 48 hours post-infection, in comparison with control AcMNPV^{gag}-infected Sf9 cells, with a special focus on the plasma membrane and VLPs budding into the extracellular milieu. Both α Rep4E3 and α Rep9A8 altered the morphogenetic pathway of VLPs, resulting in the assembly and extracellular release of aberrant forms, but with significant differences between α Rep4E3 and α Rep9A8.

The electron microscopic analysis showed that these VLPs could adopt different shapes such as oval or irregular particles, the latter consisting of twin-, triple-, or multi- particles budding inside the same membrane envelope. These "multiparticle buds" were more particularly visible in sections of Sf/(Myr+) α Rep4E3 cells (Figure 3.7 **B-F**), although irregular particles were also frequently observed in sections of Sf/(Myr+) α Rep9A8 cells (Figure 3.8 **(B-D)**). However, the aberrant assembly of VLPs in Sf/(Myr+) α Rep9A8-GFP cells showed an additional and specific pattern, consisting of the accumulation of Gag protein at the inner leaflet of the plasma membrane, an effect which was not observed with α Rep4E3 (Figure 3.8 **E-G**). The results of this EM observation showed that both α Rep4E3 and α Rep9A8 negatively interfered with the HIV-1 Gag assembly process, but in two different ways, and thus that α Rep4E3 and α Rep9A8 exhibited two distinct phenotypes.

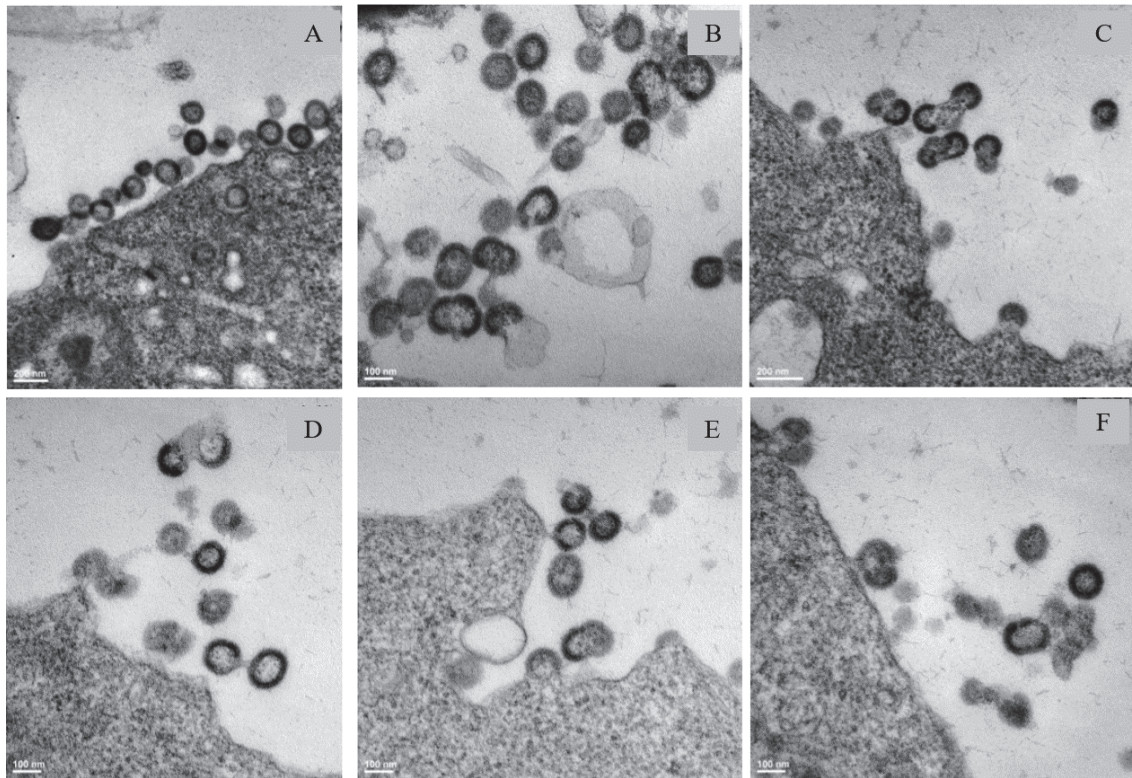


Figure 3.7 Morphological analysis of VLPs from α Rep4E3-expressing insect cells. Electron micrographs of ultrathin sections of AcMNPV^{gag}-infected cells, showing VLPs budding from their plasma membrane. **A**, control Sf9 cells; **B-F**, Sf/(Myr⁺) α Rep4E3-GFP cells. Cells were infected with recombinant baculovirus AcMNPV^{gag}, harvested at 48 hours pi, and samples processed for EM observation. Note the number of aberrant VLPs in panels **B-F**, contrasting with the regular shape of VLPs from control Sf9 cells, shown in panel **A**.

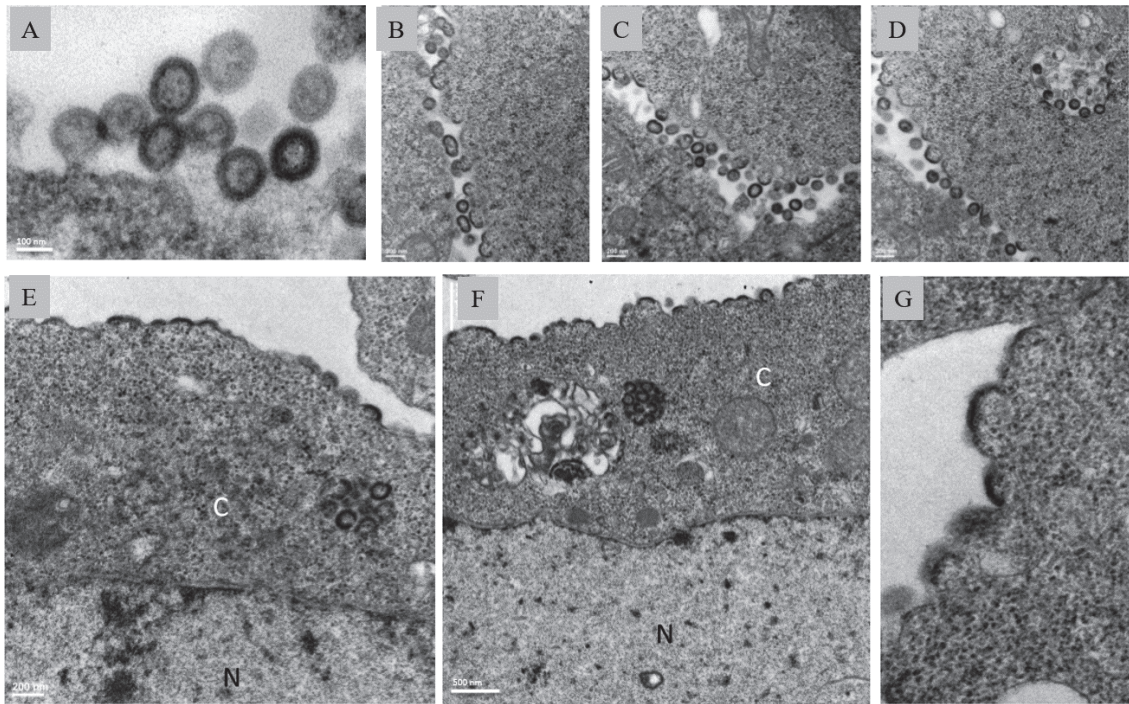


Figure 3.8 Morphological analysis of VLPs from α Rep9A8-expressing insect cells. Electron micrographs of ultrathin sections of AcMNPV^{gag}-infected cells, showing VLPs budding from their plasma membrane. **A**, Control Sf9 cells; **B-G**, Sf/(Myr+)αRep9A8-GFP cells. Cells were infected with recombinant baculovirus AcMNPVgag, harvested at 48 hours pi, and samples processed for EM observation. **A**, VLPs from control Sf9 cells showed a regular spherical shape. Aberrant VLPs are presented in panels **B-D**. Note the abnormal accumulation of Pr55Gag polyprotein at the plasma membrane, visible in panels **E-G**.

3.4.4 Co-encapsidation of (Myr+)αRep4E3-GFP and (Myr+)αRep9A8-GFP into VLPs

Since αRep4E3 and αRep9A8 were binders of a domain of GagPr55, the only viral protein component of VLPs released by AcMNPV^{gag}-infected insect cells, and were responsible for their defective assembly, we hypothesized that they could be co-packaged with Gag into aberrant VLPs budding at the cell surface. To test this hypothesis, VLPs released from AcMNPV^{gag}-infected Sf/(Myr+)αRep4E3-GFP and Sf/(Myr+)αRep9A8-GFP cells were purified by ultracentrifugation through a sucrose-D₂O density gradient, as described above. VLPs present in each gradient fraction were concentrated by pelleting, and analyzed by SDS-PAGE and immunoblotting. Anti-histidine tag antibody was used to detect αRep-GFP, and anti-Gag antibody to detect the Gag polyprotein. The immunoblots showed protein bands at 59 kDa in the αRep4E3-GFP samples, and at 55 kDa in the αRep9A8-GFP samples (Figure 3.9). Importantly, the intensity of the signal of the 59 and 55 kDa proteins in the gradient fractions followed the same pattern as that of the Pr55Gag band, suggesting that the αRep-GFP proteins did not behave like free protein molecules, but sedimented like particles of $\rho = 1.18$ in density. This implied that aberrant VLPs produced by cells stably expressing αRep(My⁺)4E3-GFP or αRep(My⁺)9A8-GFP were able to encapsidate αRep(My⁺)4E3 and αRep(My⁺)9A8, two Gag-binder αRep proteins.

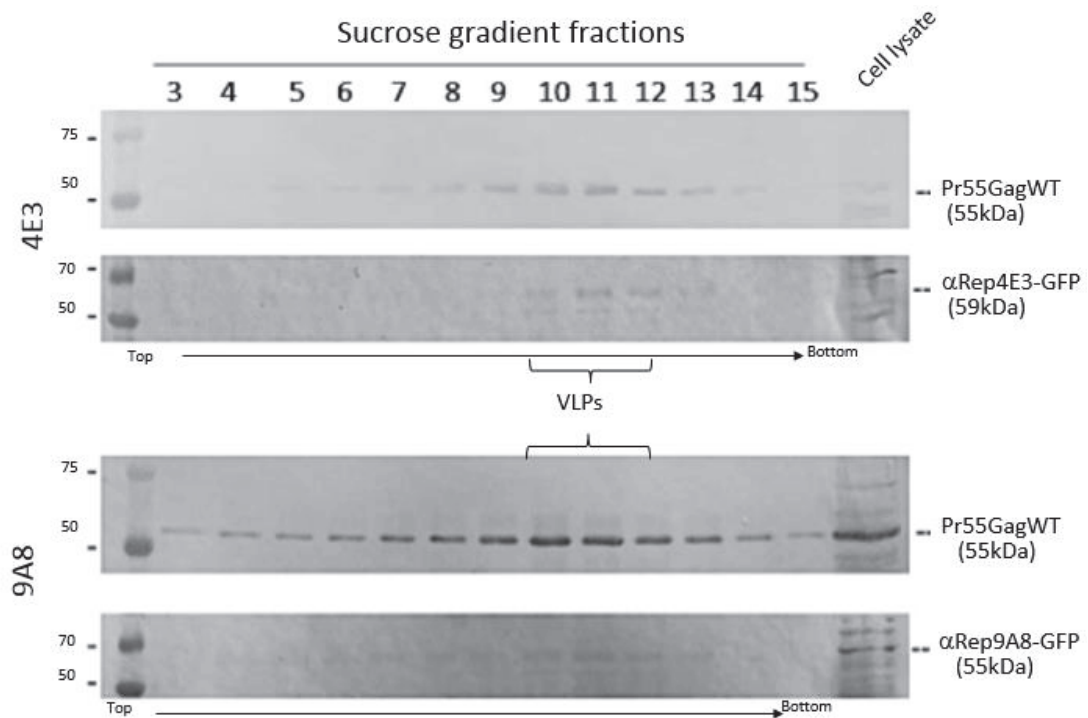


Figure 3.9 SDS-PAGE & Western blot analysis of gradient fractions. Sf/(Myr+) α Rep4E3 and Sf/(Myr+) α Rep9A8 cells were infected with AcMNPV^{gag}. At 48 hours pi, culture media were analyzed by ultracentrifugation through a sucrose-D₂O density gradient, and gradient fractions probed with anti-Gag and anti-His tag antibodies. The fractions containing VLPs and corresponding to the relative density $\rho = 1.18$ are indicated by an accolade.

3.5 Expression of α Rep4E3-GFP and α Rep9A8-GFP proteins in HeLa cells using a lentiviral vector

SIN CGW vector, the third-generation lentiviral vector harboring each of the α Rep-GFP genes was introduced into HeLa cells. At 48 hours post-transfection, the expression of α Rep4E3-GFP and α Rep9A8-GFP was monitored by confocal microscopy. The results showed that we are able to observe the EGFP reporter protein in HeLa cells which transfected with our two α Reps (Figure 3.10). Suggesting that α Reps were produced by HeLa cell due to the construction of vector which were designed to fuse α Rep genes to the EGFP gene at the upstream position.

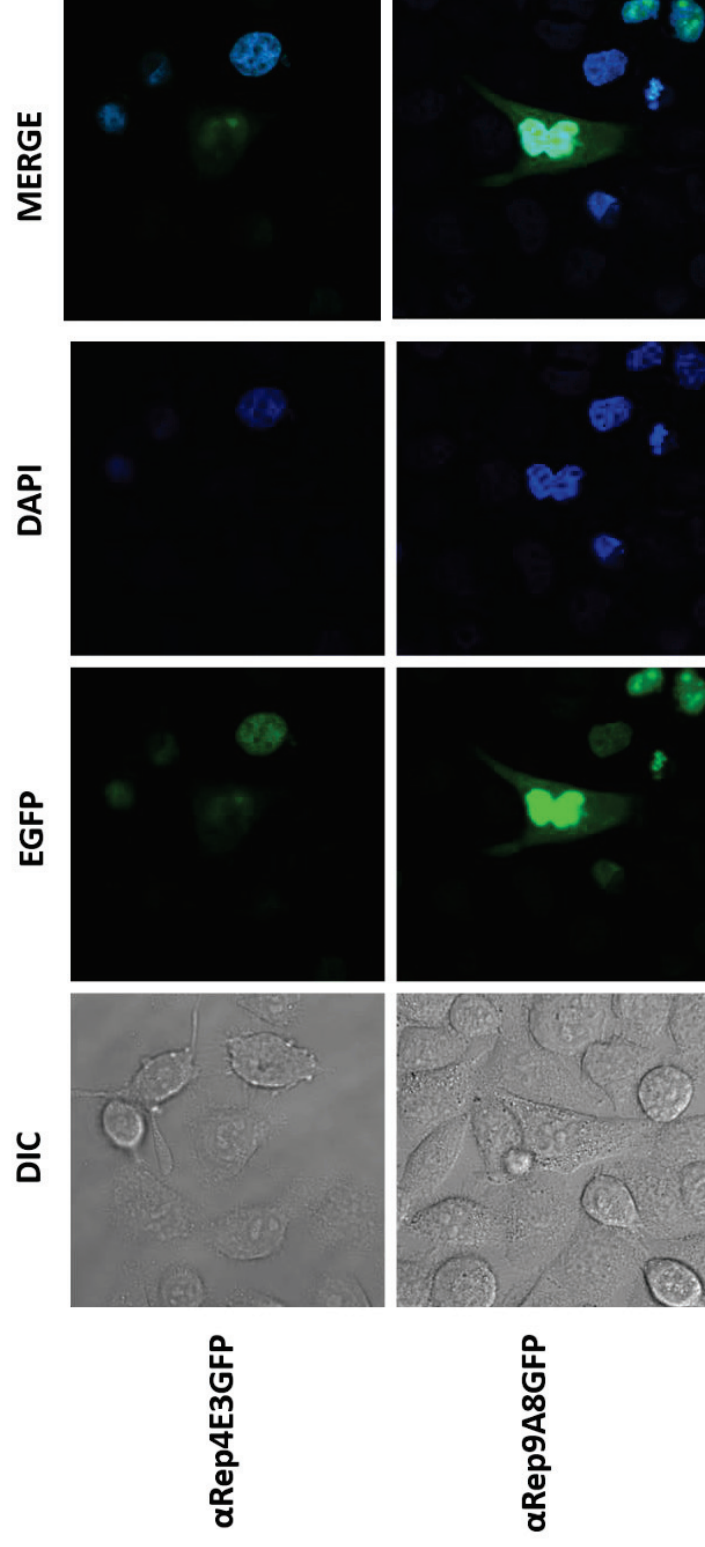


Figure 3.10 Confocal microscopy of HeLa cells expressing α Reps. The top and bottom rows of panels show HeLa cells transfected with CGW_ α Rep4E3-GFP and CGW_ α Rep9A8-GFP vectors, respectively. The columns (*starting from left to right*) show cell samples in phase contrast (DIC), the EGFP signal, the 4,6-diamidino-2-phenylindole (DAPI) signal, and the merging of the fluorescent DAPI and EGFP images, respectively

3.6 Construction of SupT1 cell lines stably expressing α Rep proteins

After verification that α Rep4E3-EGFP and α Rep9A8-EGFP were correctly expressed in HeLa cells, our next step consisted of producing VSV-G-pseudotyped lentiviral vector SIN CGW in HEK293T cells. The culture supernatants containing lentivirus harboring the α Rep4E3-EGFP gene or the α Rep9A8-EGFP gene were collected, concentrated, and assayed for their transduction efficiency. To this aim, aliquots of SupT1 cells were transduced with the CGW_ α Rep-EGFP vectors at 2 MOI by spinoculation. The efficiency of transduction and percentage of SupT1 cells that expressed α Reps-EGFP were determined by fluorescence microscopy and flow cytometry (Figure 3.11). A strong EGFP signal was observed in all SupT1 cells which received each individual CGW_ α Rep-EGFP vector: this included CGW_ α Rep4E3-EGFP and CGW_ α Rep9A8-EGFP, expressing the two α Reps of interest, but also CGW_ α Rep9C2-EGFP, expressing an irrelevant α Rep used as negative control. The percentage of α Rep-EGFP-positive cells were 0.7%, 96.8%, 96.2%, and 99.0% for non-transduced SupT1, SupT1/ α Rep9C2-EGFP, SupT1/ α Rep4E3-EGFP, and SupT1/ α Rep9A8-EGFP cells, respectively. This result suggested that the SIN CGW lentiviral vector is a tool of choice for the efficient delivery of α Rep-EGFP genes into target SupT1 cells.

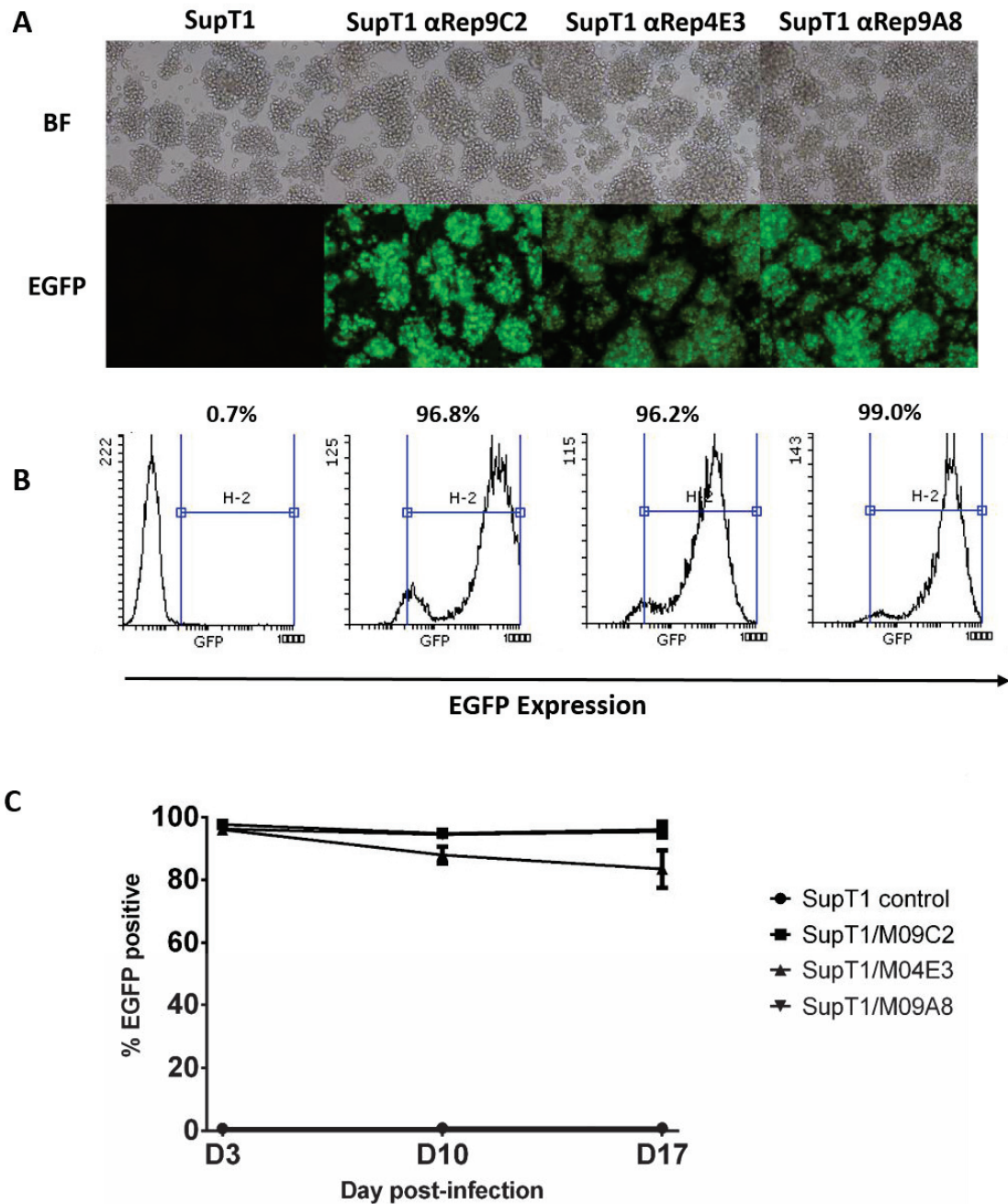


Figure 3.11 Fluorescence microscopy and flow cytometry analysis of SupT1 cells transduced by a lentiviral vector. **A**, The cell morphology and expression of EGFP expression were monitored by light and fluorescence microscopy, using an inverted fluorescence microscope at 100X magnification. **B**, Flow cytometry analysis of

transduced SupT1 cells. **C**, Kinetics of expression of EGFP in control SupT1 and α Rep-EGFP-expressing SupT1 cells infected with HIV-1 at MOI 1. Data presented are the average of triplicate experiments (mean \pm SD; n=3).

3.7 α Rep4E3- and α Rep9A8-mediated protection of SupT1 cells against HIV-1 infection

3.7.1 Determination of HIV-1 production by CAp24-ELISA

The antiviral effects of the α Reps were investigated by challenging SupT1 cells expressing α Rep4E3-EGFP or α Rep9A8-EGFP with infectious HIV-1 (laboratory strain HIV-1_{NL4-3}) at 1 MOI, in comparison with non-transduced SupT1 cells and with SupT1 cells expressing an irrelevant α Rep9C2-EGFP used as negative control. The level of HIV-1 CAp24 antigen was determined in the culture supernatants collected at different days (D) after challenge (D3, D7, D14, and D21 pi), and the cell morphology monitored by phase-contrast microscopy (Figure 3.12). The results showed that the CAp24 antigen could only be detected at D14 pi in samples from SupT1/ α Rep4E3-EGFP and SupT1/ α Rep9A8-EGFP cells, with an increased level at D21. By contrast, in control, non-transduced SupT1 cells and SupT1/ α Rep9C2-EGFP cells, the CAp24 antigen was observed earlier, at D7 pi, with a decrease at D21. The CAp24 level in both SupT1/ α Rep4E3-EGFP and SupT1/ α Rep9A8-EGFP samples was therefore \sim 10-fold lower at D14 pi, compared to its level in samples from control, non-transduced SupT1 cells and SupT1/ α Rep9C2-EGFP cells. However, this negative effect was partial and apparently transient, and the maximum virus particle production delayed, from D14 pi (as in the control samples) to D21 pi (Figure 3.12 **B**). This suggested that the two α Rep proteins exerted some inhibitory function against HIV-1, by altering the kinetics of viral progeny production.

The morphology of HIV-1-infected cells, as observed under the light microscope, revealed that HIV-1 infection induced syncytium formation and cell lysis at earlier times in both types of control cells, non-transduced SupT1 cells and SupT1/ α Rep9C2-EGFP cells, compared to SupT1/ α Rep4E3 and SupT1/ α Rep9A8. Of note, the observed decrease of CAp24 levels in control samples at D21 pi compared to their augmentation in SupT1/ α Rep4E3 and SupT1/ α Rep9A8 samples,

was likely due to the cell death, which drastically reduced the number of HIV-1-infected, CAp24-producer cells, as shown in Figure 3.12 C. The addition of new fresh culture medium to the wells every 3 day to maintain the culture alive diluted the extracellular CAp24 antigen.

To ensure that our lentiviral vector-modified SupT1 cell lines were able to maintain the expression of antiviral α Rep molecules throughout the time of the HIV-1 challenging experiment, the percentage of EGFP-positive cells was controlled by flow cytometry at each time pi. As presented in Figure 3.11 C, our stable SupT1 cell lines stably expressed α Rep proteins at a level close to 100%.

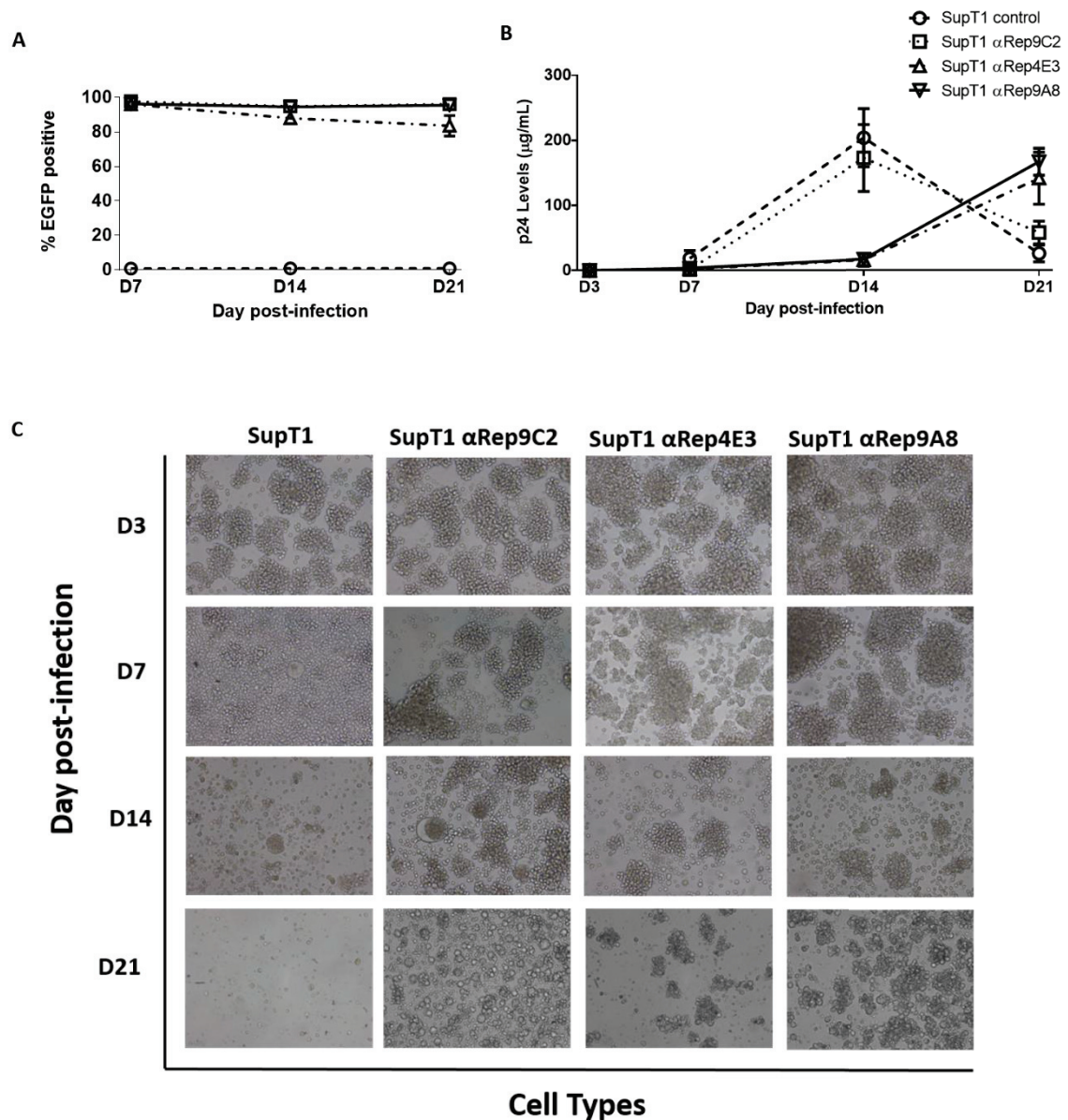


Figure 3.12 α Rep4E3 and α Rep9A8-mediated protection of SupT1 cells against HIV-1 challenge. **A**, Expression of EGFP in HIV-1 infected SupT1 cells and SupT1 expressing α Rep-EGFP over time. The data presented were the average from triplicate experiments. Bars represent mean \pm SD ($n=3$). **B**, SupT1 cells stably expressing α Rep-EGFP proteins were infected with HIV-1 at a multiplicity of infection of 1 (MOI 1). Culture supernatants were collected at day 7, 14, and 21 pi, and the levels of CAP24 antigen determined by enzyme-linked immunosorbent assay. **C**, The morphology of the infected cells was monitored the same day as the assays for extracellular CAP24.

3.7.2 HIV-1 proviral DNA detection

The level of viral genome integration in HIV-1-infected SupT1 cells and in SupT1 expressing α Rep proteins was evaluated at day 14 pi by SYBR based-quantitative PCR amplification of host cell DNA extracts, using primers specific to the *pol* gene. As shown in Table 1, there was no significant difference between α Rep-expressing SupT1 cells and control cells, indicating that the α Rep-mediated antiviral effect occurred at the post-integration phase of the virus life cycle.

Table 1. HIV-1 proviral integration in SupT1 cells harvested at day 14 pi.

Figures in the Table represent the Cts values, mean \pm SD ($n=3$).

Sequence amplified	SupT1 control	SupT1 α Rep9C2	SupT1 α Rep4E3	SupT1 α Rep9A8
Pol (PR)	22.8 \pm 0.2	21.4 \pm 0.2	22.7 \pm 0.4	23.6 \pm 0.6

3.7.3 Status of the extracellular HIV-1 genomic RNA molecules

CAP24-ELISA is routinely used to evaluate the quantities of HIV-1 particles released in the external milieu, since the amounts of non-particulate, free soluble CAP24 protein is negligible in the case of massive infection and lysis of infected cells. In order to confirm the negative effects of α Rep proteins on HIV-1 particle formation and release, viral loads were assayed in the culture supernatants of α Rep4E3-EGFP- and α Rep9A8-EGFP-expressing SupT1 cells. As shown in Figure 3.13 A, the concentration of viral genome copies at D14 pi was significantly inferior in the culture media of SupT1/ α Rep4E3-EGFP and SupT1/ α Rep9A8-EGFP, compared to control samples, a result which correlated with the CAP24 levels. The results indicated that in SupT1/ α Rep4E3-EGFP, the concentration of genomic RNA copies was 8.7-fold lower than the control SupT1 cells, and 7.4-fold lower than the irrelevant α Rep-expressing SupT1/ α Rep9C2-EGFP cells. With SupT1/ α Rep9A8 cells, the concentration of genomic RNA copies was only 2.6-fold lower than the control SupT1 cells, and 2.2-fold lower than the SupT1/ α Rep9C2-EGFP cells (Figure 3.13 B). These results indicated that α Rep4E3 had a more pronounced negative effect on genome packaging, compared to α Rep9A8. Of note, D14 pi was therefore the point at which the inhibitory effect of α Rep4E3 and α Rep9A8 on the HIV-1 yields was

the most pronounced, whereas at D21 the virus production resumed at D21 for the reasons of cell viability evoked above.

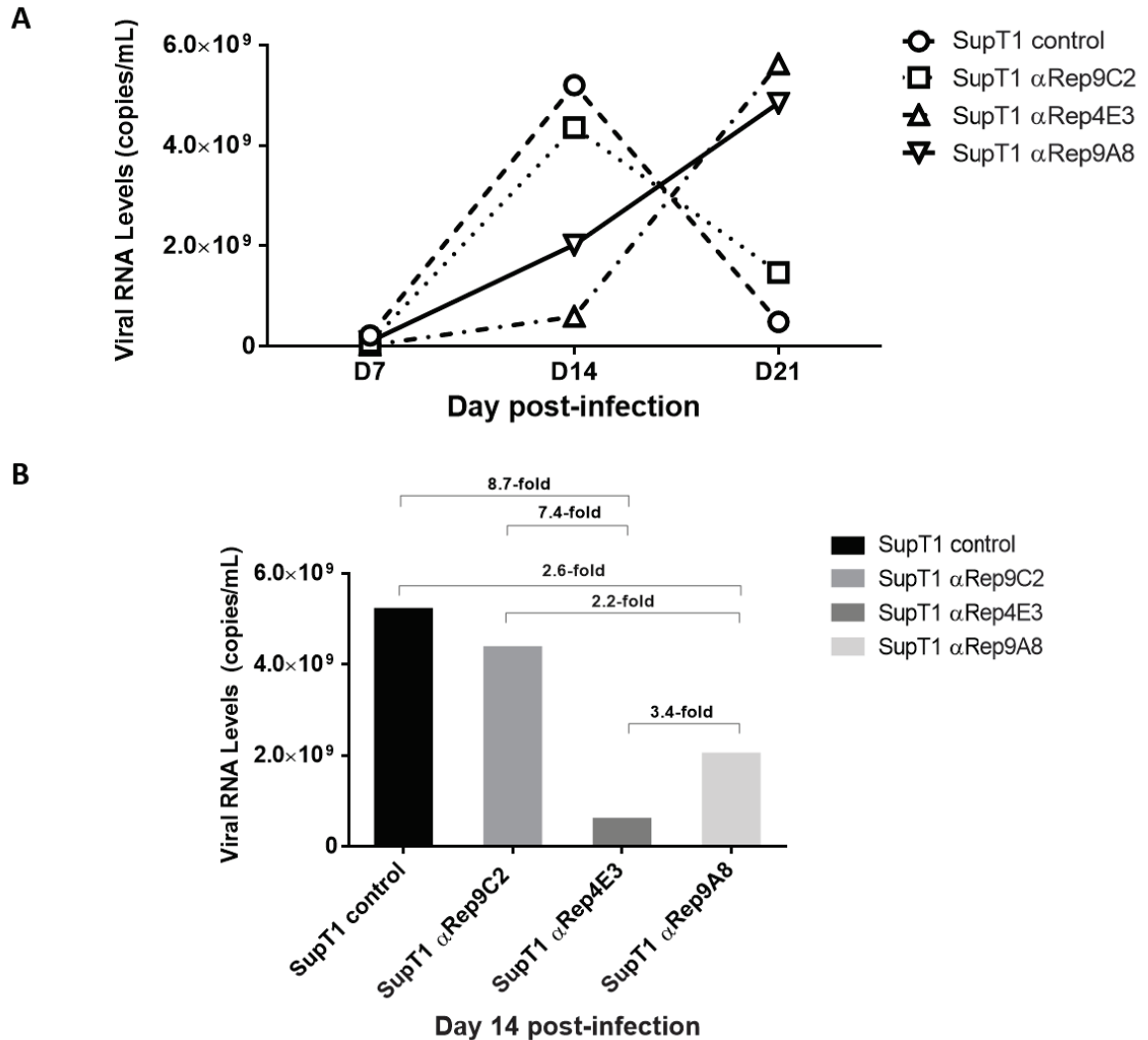


Figure 3.13 Concentration of HIV-1 genome copies in cell culture supernatants. A, Evolution of the number of viral genome copies per mL, as determined on days 7, 14 and 21 pi. **B,** Bar graph representing the concentrations of viral genomes (copy number/mL) on D14 pi in culture media, and the fold change in SupT1/ α Rep4E3-EGFP and SupT1/ α Rep9A8-EGFP in comparison with control SupT1 cells and irrelevant α Rep-expressing SupT1/ α Rep9C2-EGFP cells.

To further confirm the negative effect on viral genome packaging of α Rep proteins, the genome encapsidation was evaluated again by calculating the ratio of the concentration of extracellular viral genome copies to that of CAp24 antigen. Viral load assay were performed after normalized the CAp24 levels from all samples to be equal 25 μ g and its efficiency was compared in the different SupT1 cell lines. The result confirmed that this inhibitory function was altered in both cell lines SupT1/ α Rep4E3-EGFP and SupT1/ α Rep9A8-EGFP, but to significantly different levels as showed in Figure 3.14. The stronger negative effect observed in α Rep4E3-expressing cells is 10- to 13-fold lower compared with SupT1 control cells and α Rep9C2-expressing cells respectively, and 3-fold compared to α Rep9A8-expressing cells. This implied that the antiviral activity associated with α Rep4E3 was predominantly directed against viral genome packaging.

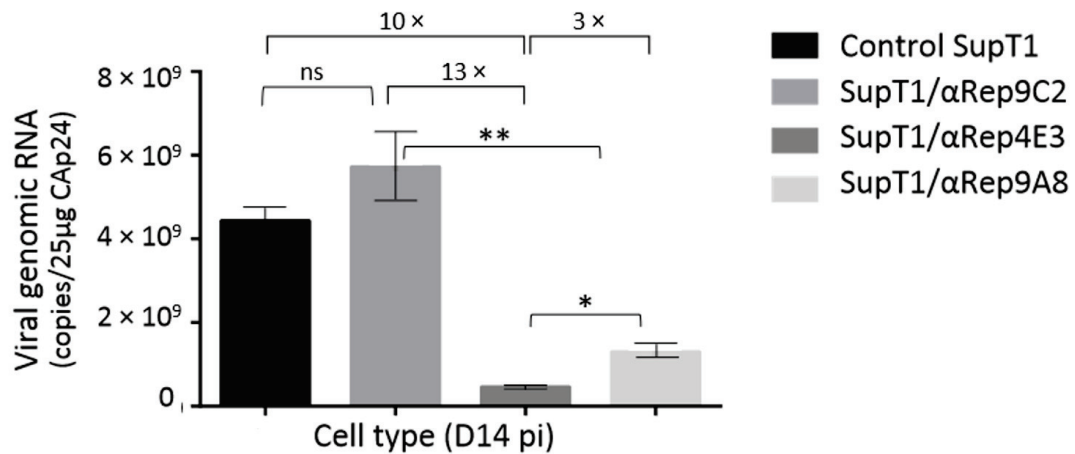


Figure 3.14 Extracellular viral genomes released by HIV-1 infected, α Rep-expressing SupT1 cells. Bar graph representing the concentrations of viral genomes in culture supernatant fluids per 25 μ g of Cap24 antigen and the fold-changes in SupT1/ α Rep4E3-EGFP and SupT1/ α Rep9A8-EGFP cell culture media, compared to control cell lines SupT1 and SupT1/ α Rep9C2-EGFP.

3.7.4 Cell viability and α Rep protein expression in HIV-1 infection SupT1 cells

HIV-1 infection generally induces a marked cytopathic effect characterized by the occurrence of giant cells or syncytia. The change in cell morphology and viability is a reliable indicator of the level of cellular infection. Taking this point into consideration for our HIV-1 challenge assay, our different types of modified or non-modified SupT1 cells, with or without α Rep protein expression, were infected with HIV-1 at the same MOI, and the cell cultures maintained for one month. Every three days, the cells were collected and controlled for morphology, viability and numeration. The results showed that both cell count and viability decreased with time during HIV-1 infection (Figure 3.15 A & B), except for the early phase (D3-D7 pi). During this phase, the cell concentration increased (Figure 3.15 A), because the virus does not cause much effect on cellular homeostasis early in infection. Unexpectedly however, there was a rebound of cell growth for the SupT1/ α Rep9A8-EGFP cells on D28-D38 pi, shown by both cell count and cell viability assays. In addition, these cells looked perfectly healthy under the light and fluorescence microscope. The extracellular medium of SupT1/ α Rep9A8-EGFP cells at D38 was also investigated for the Cap24 level and viral genomes. The result showed that culture supernatant contained viral particles and viral genomes (Figure 3.15 D & E), at the level similar to those measured at D14 pi. Of note, these concentrations were respectively 10-fold lower for CAp24 (Figure 3.12 B) and lower for viral genome copies (Figure 3.13), compared to those of control cell media at the same time point. More interestingly, the viral infectivity assays showed that the extracellular HIV-1 particles released by SupT1/ α Rep9A8-EGFP at D38 pi were noninfectious (Figure 3.15 F).

Our results indicated that the antiviral effects mediated by α Rep4E3 and α Rep9A8 took place at a late step of the HIV-1 replication cycle, after the integration step. Both α Rep proteins were able to significantly, but transiently, reduce the viral production by SupT1 cells, as assessed by the CAp24 assay and genome copy titration. However, significant differences were observed in the biological properties of the two α Reps: (i) α Rep4E3 seemed to be more efficient than α Rep9A8 in the reduction of extracellular viral genomes, and thus more detrimental

to genome encapsidation; (ii) whereas no living cells were detectable in cultures of control SupT1 cells or SupT1/ α Rep4E3-EGFP cells infected with HIV-1 at D21-D28 pi, while α Rep9A8-expressing SupT1 cells regained viability at later times pi (D38).

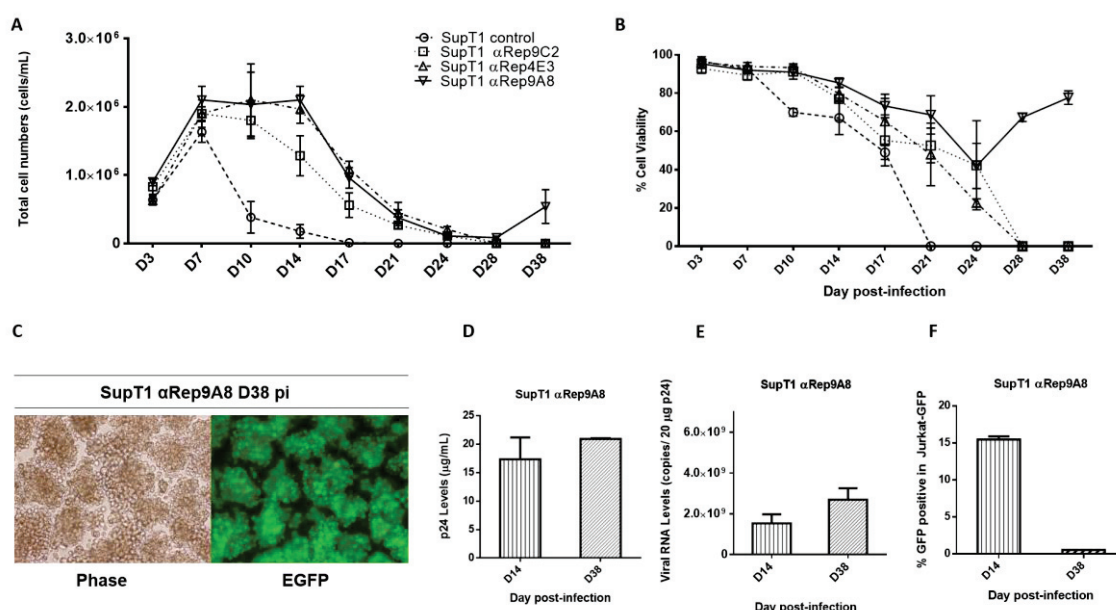


Figure 3.15 Total cell number, cell viability and cell morphology after challenge with HIV-1_{NL4.3}. (A) Total cell number per mL; (B) percentage of cell viability at different days pi. Bars represent the mean \pm SD ($n=3$). (C) Light and fluorescence microscopy analysis of SupT1 α Rep9A8 cells at D38 pi, using an inverted fluorescence microscope at 100 \times magnification. (D) Comparison of the CAp24 levels in the cell culture medium of HIV-1 infected SupT1/ α Rep9A8-EGFP cells at D14 and D38 pi. (E) Concentrations of viral genomes in the cell culture medium of HIV-1 infected SupT1/ α Rep9A8-EGFP cells at D14 and D38 pi. (F) Infectivity titers of viral particles present in the cell culture medium of HIV-1 infected SupT1/ α Rep9A8-EGFP cells at D14 and D38 pi, expressed as the percentage of GFP-positive Jurkat-GFP reporter cells.

3.8 Molecular mechanisms of the antiviral functions of α Rep4E3 and α Rep9A8

Two major parameters control the HIV-1 infectivity: (i) the degree of protease-mediated maturation of Pr55Gag, and more particularly the cleavage of CAp25 into CAp24 + SP1; (ii) the genome content of the virus particles, and thus the ability of the viral particle to pack its genomic RNA during its morphogenesis process. Retroviruses in general produce large numbers of defective, genome-lacking particles, and their infectivity index (infectivity index = the ratio of infectious to noninfectious particles) is usually over 1:1,000. These two parameters were investigated in HIV-1-infected SupT1 cells expressing our different types of α Rep proteins.

3.8.1 Influence of α Rep4E3 and α Rep9A8 on HIV-1 infectivity:

(i) maturation of the Pr55Gag precursor

Maturation of the Gag polyprotein of HIV-1 can be observed by using the ELISA based maturation assay. This technique was developed in our laboratory by taking advantage of the unique anti-MA monoclonal antibody clone HB-8975 which is known to recognize the epitope (DTGHSSQVSQNY) located in the C terminal MA of Gag polyprotein when processed by HIV-1 PR. The competitive ELISA was set up by immobilizing anti-MA HB-8975 on the microtiter plate. Culture supernatant fluids containing p24CA samples, pre-treated with 1% triton X-100 for particles lysis were added into the wells at the same time as biotinylated synthetic p17MA C-terminal peptide carrying the same epitope of cleaved MA, which act as a bait or competitor. After that the reaction was developed by adding the streptavidin conjugated HRP. A decrease in optical density (OD) signal would indicate a high amount of free cleaved p17MA which can compete against biotinylated synthetic p17MA C-terminal peptide to bind to anti-MA monoclonal antibody clone HB-8975 on the ELISA plate. An increase in OD can presume the level of mature virus particles in the culture supernatant fluids.

With regards to the viral load assay, even after normalization of the CAp24 levels in the culture supernatant of SupT1 α Rep4E3 and SupT1 α Rep9A8 (Figure 3.10 (B); D14 pi), there was a 3.4-fold difference in the viral genome copy numbers (Figure 3.13 B). This suggested that the molecular mechanism of the biological activity of

these two α Rep proteins were not the same. We therefore hypothesized that the binding of one of these α Rep proteins to the target CA₂₁-SP1-NC, which contains two HIV-1 PR cleavage sites (CA-SP1 junction and SP1-NC junction), could interfere with the PR-target interaction or the accessibility of the enzyme to its target, and affect the viral maturation. ELISA-based maturation assay was thus performed to test this hypothesis. Culture supernatants of all samples were normalized to equal amount of CAp24 (80 μ g) before the determination of the mature form of the Pr55Gag polyprotein. The bar graph shown in Figure 3.16 represents the percentage of α Rep-mediated inhibition obtained from the ELISA-based maturation assays, and these values directly correlate with the degree of maturation of the HIV-1 virions. The results indicated that only 35% viral particles budding from the SupT1 α Rep9A8 were mature particles, versus nearly 80% for SupT1 α Rep4E3, and 85% for control SupT1 cells. This suggested that α Rep9A8 negatively interfered with the virus maturation, which in turn would reduce the infectiveness of the virus.

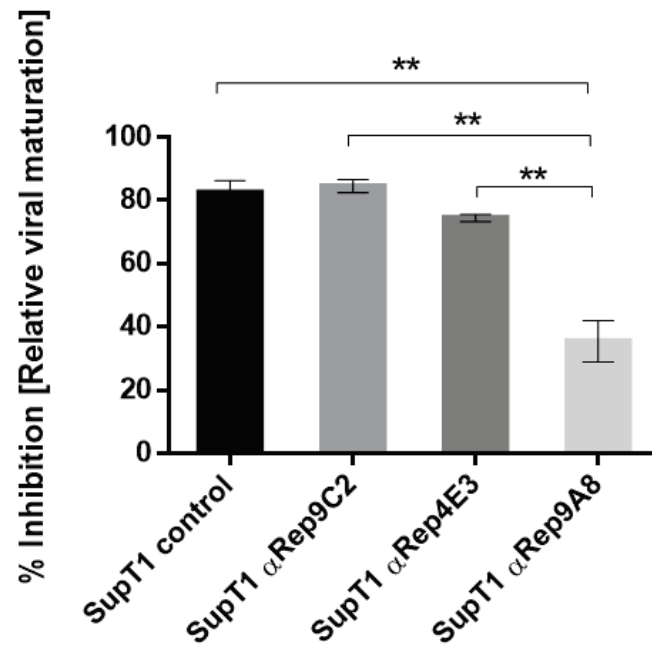


Figure 3.16 Maturation cleavage of Pr55Gag in viral particles released by different cell types. Control SupT1 cells, SupT1αRep9C2, SupT1αRep4E3 and SupT1αRep9A8 were infected with HIV-1, and extracellular media were collected. After normalization of the CAp24 level (80μg in all samples), the degree of PR-mediated cleavage of Pr55Gag was determined using our ELISA-based maturation assay (Refer to Materials & Methods). The percentage of %inhibition or %relative viral maturation obtained in this assay is directly related to the percentage of maturation of extracellular viral particles, and therefore their degree of infectivity. Results presented are from triplicate experiments (mean ± SD; $n=3$). Note the lower degree of maturation of viral particles issued from SupT1αRep9A8 cells, compared to SupT1αRep4E3 and to control cells, SupT1 and SupT1αRep9C2, which all three show similar levels of particle maturation.

3.8.2 Influence of α Rep4E3 and α Rep9A8 on HIV-1 infectivity:

(ii) encapsidation of the viral genome

The results of our experiments reported above have showed that α Rep4E3 and α Rep9A8 act differently against the HIV-1, and this suggested that they possessed two distinct antiviral functions (or two distinct "phenotypes"): α Rep4E3 would mainly interfere with the genome packaging [*pkg*(-)], whereas α Rep9A8 would mainly interfere with the Pr55Gag maturation [*mat*(-)]. We next determined the infectivity of the virus particles released from our different SupT1 cell lines, control SupT1 cells, SupT1 α Rep9C2, SupT1 α Rep4E3[*pkg*(-)], and SupT1 α Rep9A8[*mat*(-)] cells. This was performed using Jurkat-GFP cells, a reporter cell line designed for HIV-1 infection (105, 106). They are Tat-dependent indicator T-cells which will express GFP only upon infection with HIV-1. The culture supernatants of these HIV-1-infected SupT1 cells were collected at D14 pi, normalized to the same amount of CAp24 (15 μ g per sample) to obtain the same viral input, and inoculated to Jurkat-GFP cells. At D10 and D14 post-reinfection, Jurkat-GFP were collected and analyzed by flow cytometry for GFP-positive cells.

The results obtained on D10 post-reinfection (Figure 3.17) indicated that the amounts of HIV-1 which egressed from SupT1/ α Rep4E3 (1.4%) and SupT1/ α Rep9A8 (1.25%) were significantly lower (15 to 17-fold) than those from control cells, SupT1 (24%) and SupT1/ α Rep9C2 cells (19.5%). At D10 post-reinfection however, no difference was detectable in the infectious titers of the cell culture supernatants between SupT1/ α Rep4E3 and SupT1/ α Rep9A8. The Jurkat-GFP cultures were therefore further maintained, and cells analyzed by flow cytometry at D14 post-reinfection (Figure 3.17; rightmost bars). A significant difference (almost 2-fold) was then visible between SupT1/ α Rep4E3 (27.8%) and SupT1/ α Rep9A8 (15.4%). Of note, the possible difference between the cells of the control set could not be assessed at D14 post-reinfection, due to their massive infection by mature infectious viruses produced by SupT1 cells which do not express any antiviral molecule.

Considering the normalization of virus particles in the viral inocula (based on the CAp24 titers), this result would imply that a negative interference with Gag maturation, such as the one provoked by α Rep9A8[*mat*(-)], would be more detrimental to HIV-1 infectivity, compared to the negative interference with genome packaging, such as the one provoked by α Rep4E3[*pkg*(-)]. In terms of probabilities, viral loads and antiviral therapy, this would mean that if a given antiviral drug (A) provokes a 50% decrease in mature virions in a viral inoculum, and another drug (B) provokes a 50% decrease in virions with a full-genome content, the resulting infectivity will be lower in the first inoculum, compared to the other. As a practical consequence, although both drugs would result in the extracellular release of 50% defective particles, drug A will be more efficient as antiviral against HIV-1, compared to B.

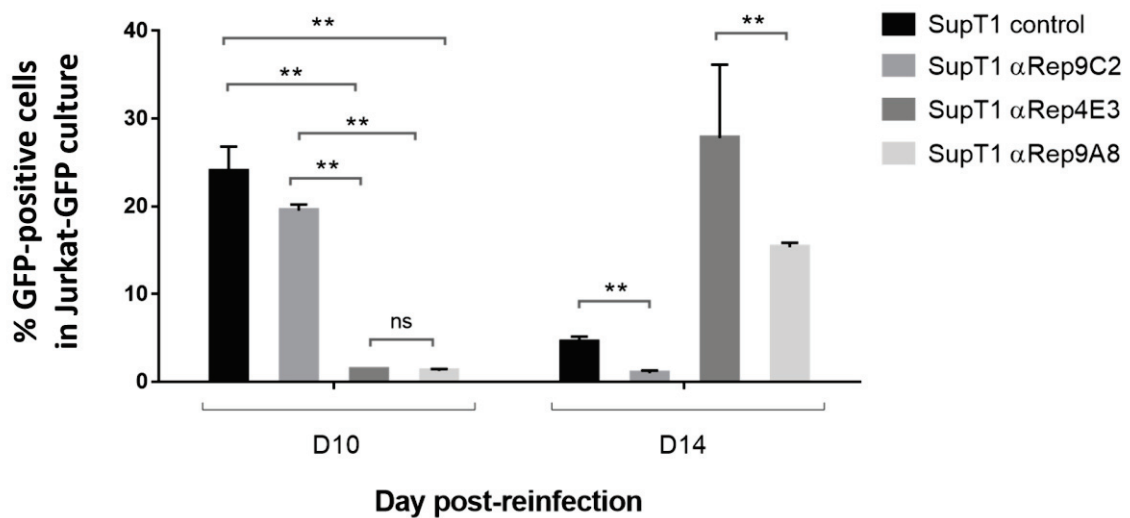


Figure 3.17 Viral infectivity assay based on Jurkat-GFP re-infection. Percentage of GFP-positive Jurkat cells after reinfection by the culture supernatants of HIV-1-infected SupT1 cells (control, no α Rep), SupT1/ α Rep9C2 (control, irrelevant α Rep), SupT1/ α Rep4E3 and SupT1/ α Rep9A8. The results presented are mean \pm SD ($n=3$). The two groups of bars correspond to D10 and D14 post-reinfection, respectively. At D10 (leftmost bars), the percentages of GFP positive cells infected with virus released from SupT1/ α Rep4E3 and SupT1/ α Rep9A8 cells were compared with the percentage obtained in the set of control cells. At D14 (rightmost bars), the difference is only evaluated between the percentages of GFP positive cells infected with virus from SupT1/ α Rep4E3 and SupT1/ α Rep9A8.

3.8.3 Intracellular interaction of α Rep and Gag proteins in HIV-1 infected cells.

Control SupT1 and SupT1/ α Rep9C2-EGFP cells, and antiviral α Rep-expressing SupT1/ α Rep4E3-EGFP and SupT1/ α Rep9A8-EGFP cells were infected with HIV-1_{NL4-3} at 10 MOI for 16 hrs at 37 °C. Cells were harvested at D10 pi, fixed, permeabilized and reacted with Qdot705-conjugated anti-CAP24 antibody. Confocal microscopy showed that all three EGFP-tagged, non-N-myristoylated α Rep protein 9C2, 4E3 and 9A8 accumulated mainly within the nucleus of SupT1 cells, whereas, the red signal of Gag proteins was confined to the cell membrane. No colocalization of Gag and irrelevant α Rep9C2-EGFP was detected in any of the cells examined. However, in cells expressing α Rep4E3-EGFP and α Rep9A8-EGFP, certain areas of cytoplasm close to membrane showed the superimposition of the red and green fluorescent signals of Gag and α Rep-EGFP, suggesting a direct interaction between α Rep4E3 and α Rep9A8 proteins and their viral target, the HIV-1 Gag polyprotein (Figure 3.18).

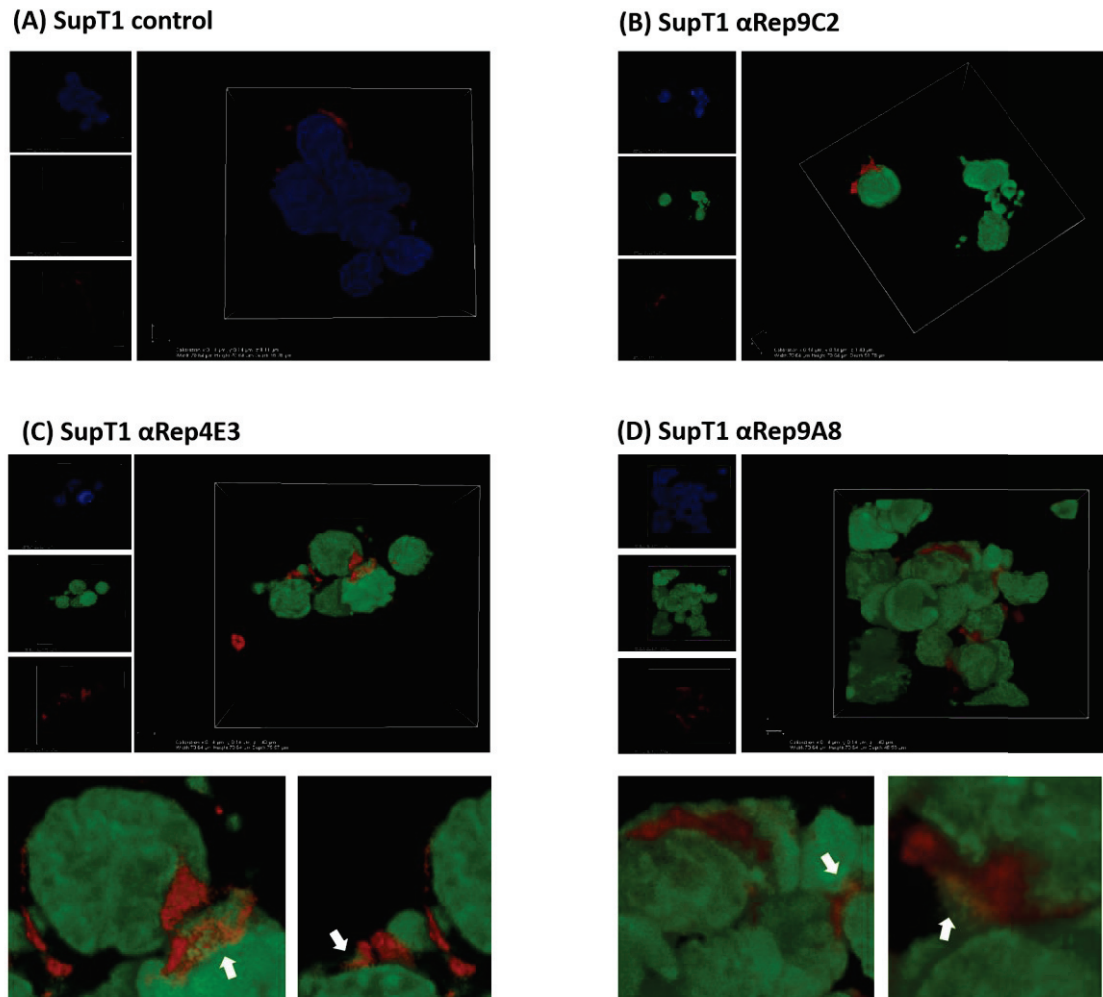


Figure 3.18 Confocal microscopy of HIV-1 infected, α Rep-expressing SupT1 cells. A, HIV-1-infected control SupT1 cells and B, α Rep-expressing SupT1/ α Rep9C2-EGFP, C, SupT1/ α Rep4E3-EGFP, and D, SupT1/ α Rep9A8-EGFP cells, were collected at D10 pi, fixed, permeabilized, and reacted with Qdot705-conjugated anti-Cap24 monoclonal antibody. Nuclei were counterstained with DAPI. A-D, Individual images obtained with the excitation wavelength 405 nm (DAPI), 488 nm (EGFP), and 561 nm (Qdot705), respectively, are presented as vignettes on the left side of each panel; merged images of EGFP and Qdot705 signals are shown on the right side. Enlargement of C and D showing the colocalization of α Rep and Gag proteins (white arrows).

3.9 Mapping of the α Rep binding sites on the viral Gag target

The respective position of the α Rep4E3 and α Rep9A8 binding sites on the CA₂₁-SP1-NC target was first investigated by ELISA, using glutathione-coated microplates and surface-immobilized GST-fused full-length target and carboxy-terminal deletion mutants of CA₂₁-SP1-NC. In this experiment protein pull-down assays were then carried out to identify the binding domain of each individual α Rep on their target protein. The glutathione-coated beads were added to the mixture of α Rep4E3 or α Rep9A8 pre-incubated with the viral target protein, GST-CA₂₁-SP1-NC or its different C-terminal deletants (Figure 3.19 A-B). The results showed that both α Rep4E3 and α Rep9A8 bound equally well to the full-length target CA₂₁-SP1-NC, but that the deletion of the two zinc fingers, as in GST-CA₂₁-SP1, completely abolished their binding. However, deletion of the second zinc finger (Δ ZF2), as in GST-CA₂₁-SP1-NC Δ ZF2, did not modify the binding pattern of α Rep9A8, whereas it decreased the α Rep4E3 binding (Figure 3.20 A). This result suggested that the binding site of α Rep9A8 was restricted to the ZF1 domain, since α Rep9A8 binding to the viral target was not influenced by ZF2. By contrast, the α Rep9A8 binding site apparently overlapped both ZF1 and ZF2, since after deletion of ZF2, attachment of α Rep4E3 to the viral target still persisted, implying the occurrence of another binding site on ZF1 (Figure 3.20 B). Of note, no essential binding determinant for α Rep4E3 and α Rep9A8 could be detected on the SP1 linker domain, using these pull-down assays.

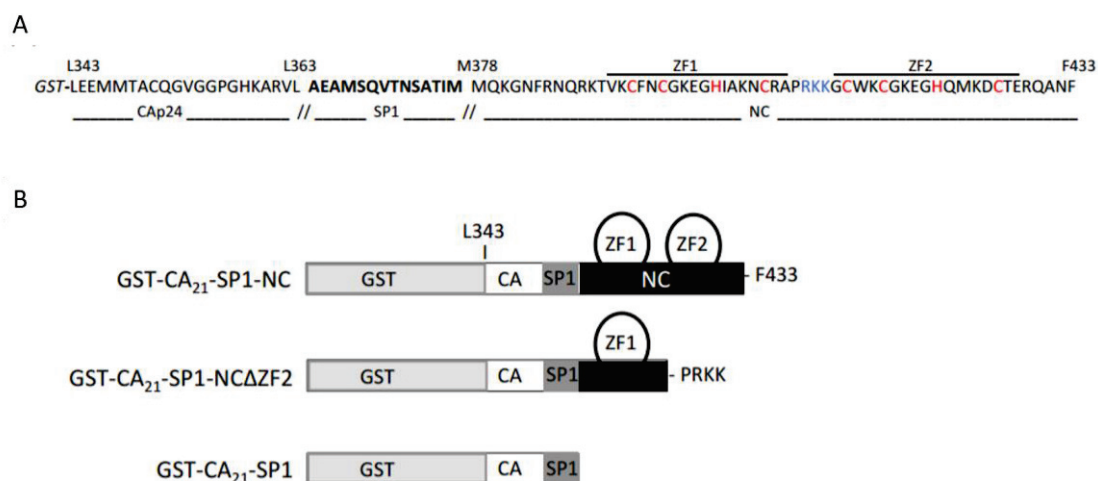


Figure 3.19 CA₂₁-SP1-NC full-length bait and deletants. **A**, Amino acid sequences of the domains of HIV-1 Gag precursor (L343-F433; HIV-1 LAI isolate) used as the viral bait of the α Rep screen. The residue of the SP1 domain are in bold; the cysteine and histidine residues of the zinc finger (ZF1 and ZF2) responsible for the Zn coordinates are in red; the residues of the basic motif separating ZF1 and ZF2 are in blue. **B**, Schematic representation of GST-fused viral construct. From top to bottom: full-length target CA₂₁-SP1-NC; deletion of the C-terminal Zinc finger (Δ ZF2); deletion of the two Zinc fingers ZF1 and ZF2.

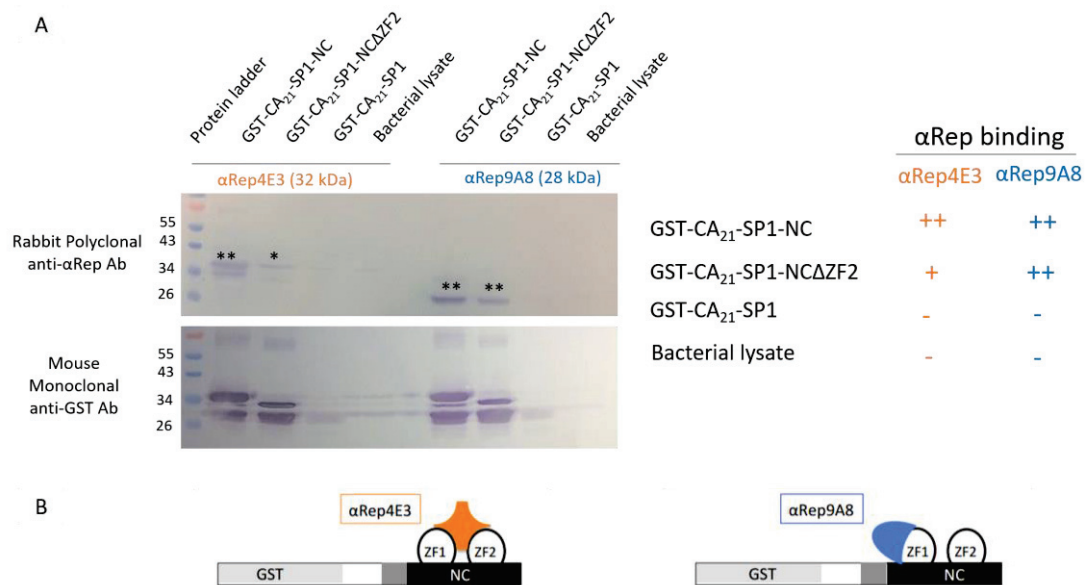


Figure 3.20 SDS-PAGE Western immunoblotting of protein pull-down assay representation the binding sites of α Rep proteins on the viral target. A, Left panel: The glutathione-coated beads were added to the mixture of α Rep4E3 or α Rep9A8 pre-incubated with the viral target protein, GST-CA₂₁-SP1-NC or its different C-terminal deletants. The pull-down phases were analyzed by SDS-PAGE and immunoblotting, using polyclonal anti- α Rep and anti-GST monoclonal antibody respectively. Right panel: summary of the binding site of the α Rep4E3 and α Rep9A8 on their viral target. **B**, The schematic represented the hypothesis of the binding site of α Rep4E3 and α Rep9A8.

CHAPTER 4

DISCUSSION

HIV-1 infection is a long-term disease which requires a long-term treatment. Although HAART is an effective strategy for the treatment of HIV-1 infected patients and the control of plasma viremia under detectable level. Nevertheless, there are limitations that emerged over time when it becomes a long-life treatment. For example, prolonged treatment can result in the occurrence of multi-drug resistant mutants, drug-drug interaction and drug toxicity (1-8, 111). For these reasons, alternative treatments have been proposed. HIV-1 gene therapy was introduced as a promising alternative treatment for infected patients (59, 77, 80, 112). These include the identification or design of genes coding for intracellular factors or interactors with antiviral activity, the genetic manipulation of hematopoietic progenitor stem cells, and the inactivation of proviral DNA *in situ* by using zinc-finger nucleases (ZFNs)(113), transcription activator-like effector nucleases (TALENs) (114), or the CRISPR (clustered regularly interspaced short palindromic repeat)/Cas9 system (115, 116). Protein therapeutics is also another promising alternative which has become an integral and significant part of current medical treatments (117). The well-known examples of this next generation medicine include engineered antibodies, bi- or multi-specific proteins, antibody mimic novel scaffold molecules, single chain variable fragment (9, 83, 118, 119). Nevertheless, antibody therapy has its own limitations; therefore, the paradigm shifted to the non-immunoglobulin binding proteins. The advantages of protein scaffolds overpower the limitations of the antibody-based therapies; make them promising candidates for clinical applications. Their independence of disulfide bonds concurs with their ability to express in reducing environment such as the cytoplasmic compartment of cells. Moreover, scaffold proteins are highly soluble and exhibit thermal stability. They are smaller than an antibody molecule which is an advantage for tissue penetration and accumulation. In addition, the production or synthesis of scaffold proteins are less

expensive compared to antibody production (83, 86, 87, 120). We have recently designed and characterized two intracellular inhibitors of HIV-1, 2LTRZFP (121) and Ank^{GAG}1D4 (122). Both 2LTRZFP and Ank^{GAG}1D4 were classified as family of stable modular repeat protein scaffolds. 2LTRZFP is a zinc finger protein (ZFP) which has been designed to target the IN recognition sequence at the 2-LTR circle junctions, and which blocks the integration of the HIV-1 circular DNA into the host cell genome. Ank^{GAG}1D4 is an artificial ankyrin-repeat protein which has been selected through its affinity to the N-terminal domain of HIV-1 CA or p24, and which negatively interferes with viral assembly in HIV-1-infected SupT1 cells. The combined expression of the two antiviral molecules, 2LTRZFP and Ank^{GAG}1D4 molecular scaffolds in SupT1 cells resulted in a significant negative effect towards HIV-1 replication (121-124).

In the present study, we designed another type of HIV-targeted scaffolds called α Rep, which are based on a natural family of modular proteins constituted of alpha-helical HEAT repeats (13). Our viral target for the α Rep screen, abbreviated CA₂₁-SP1-NC, consisted of the carboxy terminal portion of the Gag polyprotein comprising of the full-length NC protein with its two ZFs, the SP1 domain (14 residues) and the last 21 residues of the CA C-terminal domain (L343-L363). CA₂₁-SP1-NC served as the viral bait in a phage display screen of our α Rep protein library. We isolated two α Rep proteins with a high affinity for CA₂₁-SP1-NC, called α Rep4E3 32 (kDa) and α Rep9A8 (28kDa) by phage display technique. α Rep4E3 contains 7 repeat motifs and α Rep9A8 consists of 6 repeat modules. These two α Rep proteins also showed the high binding efficacy to their target CA₂₁-SP1-NC *in vitro*. The first antiviral effect of α Rep4E3 and α Rep9A8 were observed from the experimental designed to study the effect of α Rep proteins on viral like particle (VLP) assembly in an insect cell expression system (73). We showed the quantitative effects of α Rep4E3 and α Rep9A8 on the amount of VLPs production in both western blotting and luciferase-based VLP production assay, and using a qualitative assay by electron microscopy. Sf9 cells stable expressing α Rep4E3-GFP and α Rep9A8-GFP mediated the negative effects to the VLPs production. Particles release from these two cell types displayed aberrant particle formation. Oval, irregular, bi-, triple-, or multi-particles budded in the same membrane envelope were mostly observed from the α Rep4E3 expressing cells. It is possibly that interaction of α Rep4E3 to CA₂₁-SP1-NC may interfere Gag-Gag interaction, Gag oligomerization, and/or Gag- polymerization.

Due to the target CA₂₁-SP1-NC is covered a part of C-terminal domain of CA, SP1 region, and NC domain. The evidence showed that CA_{CTD} is critical for both core formation and Gag oligomerization/polymerization in the particle assembly process (28, 37, 122). Moreover, SP1 region is required for the immature particle assembly by promoting the strength of Gag-Gag interaction and regulating the formation of the mature HIV-1 CA which is essential for virus infectivity (42, 44). The studies also reviewed that SP1 region especially first six residues are necessary for the normal-regular particle assembly. NC domain not only is involved in the viral genome packaging, the formation of NC-RNA tether complexes promote the increasing of Gag concentration at the assembly site, resulting in enhanced CA-CA interaction (125). Furthermore, CA-NC contains two PR cleavage sites, interact with α Rep proteins which may interfere with Gag-PR interaction or accessibility of an enzyme. All these suggested that the aberrant particle formations may be the cause of the reasons mention above (20, 29, 125). Subtle differences observed in the α Rep9A8-GFP expressing Sf9 cells is the fringe pattern, the accumulation of Gag protein at the plasma membrane without ability to generate the new particles. This maybe because of their interaction with α Rep9A8-GFP resulting in the failure of Gag polymerization. However, we are able to observed Gag on the cell membrane because Gag itself are able to address to the plasma membrane *via* the myristic signal at its N-terminus. With this experiment, the results showed the promising negative effect of α Rep4E3 and α Rep9A8 in terms of the quality of VLPs production but not effect on the amount of VLPs. Based on the baculovirus expression system used in this study is which known as the most powerful and versatile protein expression system, it could be that the level of Gag protein expression are saturated, α Rep proteins are therefore not enough to compete with these high level of Gag expression. In addition, AcMNPV^{gag} can re-infect cells overtime to produce more Gag protein. Meanwhile, α Rep proteins are constitutively expressed from absolute number of genome copies integrated in the Sf9 cells host chromosome.

It was very interesting that aberrant VLPs were released by the α Rep4E3 and α Rep9A8 expressing Sf9 cells. One hypothesis was that the abnormal particle morphology was caused by the incorporation of α Rep proteins into the VLPs and bud out together. To test this hypothesis, sucrose gradient ultracentrifugation were performed, and the results confirmed that both α Rep4E3-GFP and α Rep9A8-GFP were encapsidated inside the

particles as we observed the α Rep4E3-GFP and α Rep9A8-GFP at the same fractions of Gag protein in a dose dependent manner.

Consequently, after we confirmed the inhibitory effects of the two α Rep proteins on the viral like particle formation, the next study was to test the antiviral effects against the laboratory virus strain, HIV-1_{NL4-3}. SupT1 stable cell lines expressing α Rep4E3-EGFP and α Rep9A8-EGFP were constructed using SIN CGW third generation lentiviral vector as vehicle for gene delivery system. SupT1 cells expressing each of the α Rep proteins were challenged with the HIV-1_{NL4-3} at 1 MOI. Viral replication inhibition were observed from both α Rep4E3 and α Rep9A8 as presented by the level of CAp24 antigen in the culture supernatant of infected SupT1 stable line cells as same as the level of genomic RNA copies. The phase of action of α Rep4E3 and α Rep9A8 took place at the late step of replication cycle as the SYBR RT-PCR based integration assay presented the same integration level in all α Rep4E3, α Rep9A8, SupT1 control, and α Rep9C2 irrelevant α Rep control. These data are assayed at D14 pi, the day that we can clearly see the negative effects of α Rep4E3 and α Rep9A8. D7 pi was not the suitable day for investigating the function of α Rep protein because at the beginning or early infection virus does not cause effect much on cellular homeostasis. The level of CAp24 and viral genome copies in culture supernatant are less as well as the cells morphology, there is no cytopathic effect observed on this day except one giant cell in many field of 100x magnification. Meanwhile, D21 pi seems to be too late to interpret the results on this day. Since the control set which included SupT1 control and α Rep9C2 irrelevant α Rep control were faced with the heavy infection according to they do not contain any antiviral scaffold molecule and became giant cells consequently lysis. By the time of subculture, new fresh media added into the well will dilute the level of CAp24 in the culture supernatant.

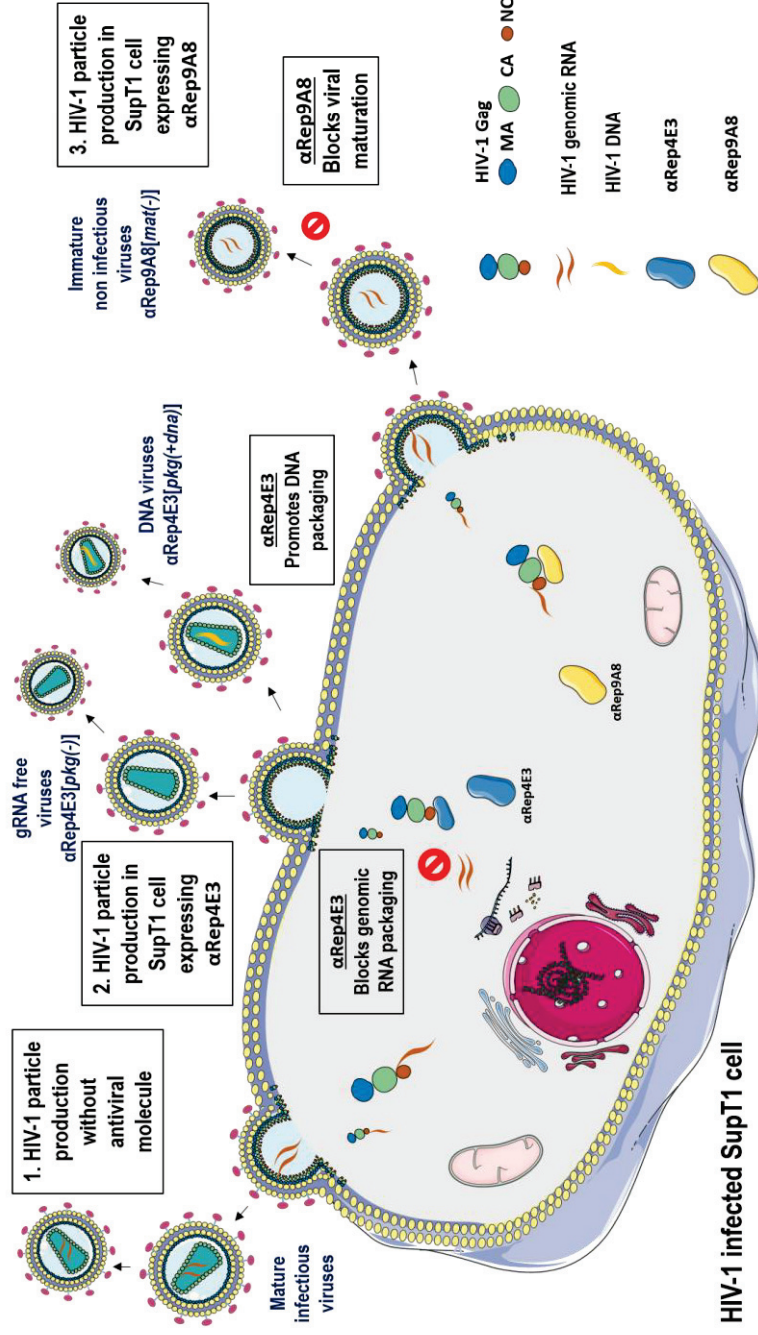
Although α Rep4E3 and α Rep9A8 were able to inhibit the virus replication at the same level as measured using CAp24, the level of viral genome copies were 3.4-fold difference. This implied that the molecular mechanism of the two α Rep proteins are not the same. The results obtained from VLPs assembly assay confirm this hypothesis. The late phase of HIV-1 life cycle, can be subdivided into many phases including; (i) particle assembly, (ii) particle budding, (iii) particle maturation and infectivity. The α Rep4E3 and α Rep9A8 may be able to inhibit or negatively interfere one or more of these phases during the virus

infection. We therefore, further analyzed the maturation and infectivity of the HIV-1 viruses released from α Rep4E3 and α Rep9A8 expressing SupT1 cells. ELISA-based maturation assay revealed that at the equal amount of CAp24, α Rep4E3 is likely not to be able to interfere or display a negative effect on the virus maturation as its percentage maturation was nearly 80% which is in the same level of SupT1 and SupT1 α Rep9C2 irrelevant control. It could be presumed that these virus particles are able to undergo maturation and become mature form. However, the viral infectivity assay of HIV-1 viruses released from α Rep4E3 contradictory. We could expect that the mature form of particles could have a high viral infectivity. But the results showed that their infectivity were significantly lower than the controls, suggesting that α Rep4E3 has no effect on viral maturation but interfered at the late phase of HIV-1 life cycle by another pathway. According to the viral load assay, it was shown that the genome copies detected in the culture supernatant of SupT1/ α Rep4E3-EGFP at D14 pi was the lowest level. Therefore, the mode of action of α Rep4E3 may involve the genome packaging. Another plausible hypothesis could be that α Rep4E3 may interfere the late stage reverse transcription regulation of NC (126). Binding of α Rep4E3 to the NC domain may promote the reverse transcription at the viral assembly step, following packing the viral DNA and egress.

Interestingly, α Rep9A8 expressing SupT1 cells produced immature virus particles higher than other SupT1 stable cell lines and SupT1 cell control. This antiviral effect was confirmed by subjecting viruses released from α Rep9A8 expressing SupT1 cells to the viral infectivity assay. The results indicated that they were able to re-infect the Jurkat-GFP at very low levels compared to the SupT1 and SupT1/ α Rep9C2-EGFP irrelevant control, suggesting that α Rep9A8 has antiviral effects against viral maturation and viral infectivity. The data obtained from the percentage viability and total cell number strongly supported the antiviral effect of α Rep9A8. After SupT1/ α Rep9A8-EGFP cells were infected with a high amount of viruses and most of infected cells in the culture well died, resulting in few HIV-1 producer cells. Subsequently, SupT1 cells expressing α Rep9A8 were able to resist by releasing immature virus particles every time that new virions are produced, resulting in no new infections. Therefore, SupT1/ α Rep9A8-EGFP were able to grow and the cell viability as well as number increased as shown in D38 pi. However, background level of virus particle production were found, but more interestingly, the viral

infectivity assays showed that the extracellular HIV-1 particles released by SupT1/ α Rep9A8-EGFP at D38 pi were noninfectious.

All together we can conclude that both α Rep4E3 and α Rep9A8 displayed antiviral effects against HIV-1 replication by reducing and delayed the virus production as same as level of HIV-1 genome in culture supernatant. In addition, they were able to interfere with the infectivity of the virus. However, the molecular mechanism of action of these two α Rep proteins are different as the schematic showed in Figure 4.1. The α Rep4E3 is likely to interfere with the viral genome packaging while α Rep9A8 acts like a maturation inhibitor to interfere or prevent the PR processing in the maturation step leading to the production of immature virus. In our future study, the main goal would be to elucidate the molecular mechanism of α Rep4E3 in the interference of genomic RNA packaging. High resolution and/or super resolution microscopy combined with florescence *in situ* hybridization will be the efficient tools to explore this hypothesis



HIV-1 infected SupT1 cell

Figure 4.1 Schematic representation of the distinct antiviral effects of α Rep4E3 and α Rep9A8 in HIV-1-infected SupT1 cell.

The normal pathway of HIV-1 assembly and egress is represented in (1); the molecular mechanisms of the α Rep4E3- and α Rep9A8-mediated antiviral effects are displayed in pathways (2) and (3). α Rep4E3 (blue symbol) negatively interferes with Gag-RNA interaction, genome packaging and promotes late phase reverse transcription and viral DNA packaging; α Rep9A8 (yellow symbol) acts as a maturation inhibition

CHAPTER 5

CONCLUSION

In the present study, we first designed another type of HIV-targeted scaffolds called α Rep protein, which are based on a natural family of modular proteins constituted of alpha-helical HEAT repeats. The two strong binders α Rep repeat protein scaffolds isolated and characterized from a large and diverse library by affinity screening on a critical C-terminal region of the HIV-1 Pr55Gag poly protein precursor, called α Rep4E3 (32kDa; 7 repeat motifs) and α Rep9A8 (28kDa; 6 repeat motifs). The high level of the two α Rep protein expression yielded from the bacterial expression system. Consequently, the potential antiviral activity of α Rep4E3 and α Rep9A8 was first observed on viral-like particle (VLP) assembly in the baculovirus-insect cell expression system. There is no quantitative difference in the level of extracellular VLPs production between the three AcMNPV^{gag}-infected cell types, control Sf9 cells, Sf/(Myr+)9A8-GFP and Sf/(Myr+)9A8-GFP cells. However, qualitative analysis of VLPs particle formation by electron microscope revealed that both α Rep4E3 and α Rep9A8 exerted a negative effect on the morphogenesis of the VLPs. VLPs released from the AcMNPV^{gag}-infected, α Rep-expressing displayed aberrant shape and structure. Oval, irregular, bi-, triple-, or multi-particles enveloped in the same membrane budded at the surface of the α Rep4E3-expressing cells. The different EM pattern was observed with α Rep9A8-expressing cells, with the occurrence of aberrant particles budding from the cell surface, but also with the accumulation of Pr55Gag polyprotein precursor at the inner leaflet of the plasma membrane of infected Sf9 cells, without formation of VLPs. In SupT1 cells, the human T cell line was used as a model to study anti-HIV-1 activity of both α Rep proteins, α Rep4E3 and α Rep9A8. These two α Rep scaffolds displayed antiviral effects against the HIV-1 replication, by reducing and delaying the new virus production with a similar efficiency, and by decreasing the infectivity of the egressed virions. Nevertheless, the molecular mechanism of the antiviral activity was different between these two α Rep

proteins: α Rep4E3 mainly interferes with the packaging of the viral genome, while α Rep9A8 interferes with the Pr55Gag processing by HIV-1 protease enzyme, and acts as a maturation inhibitor to prevent the PR cleavage required for the production of mature, infectious virus. More importantly, α Rep9A8-expressing SupT1 cells acquired a long-term resistance to HIV-1. Further analysis of the culture medium of α Rep9A8-expressing SupT1 cells collected five weeks after HIV-1 challenge revealed that it contained background levels of virus particles and viral genomes, but that these viral particles were noninfectious, as demonstrated by their infectivity titration on Jurkat-GFP reporter cells. The mapping of the α Rep4E3 and α Rep9A8 binding sites on the viral target provided some clues to explain their functional differences as antivirals. The most plausible hypothesis for the inhibitory effect of α Rep9A8 protein on virus maturation would be that α Rep9A8 would block the PR-mediated maturation cleavage of the Gag precursor indirectly, by steric hindrance, and not via a direct masking of the SP1 sites. Meanwhile, α Rep4E3 would interact with amino acid residues belonging to the two adjacent zinc fingers of NC which resulting in the reducing of genomic RNA packaging.

REFERENCES

1. Montessori V, Press N, Harris M, Akagi L, Montaner JS. Adverse effects of antiretroviral therapy for HIV infection. *CMAJ : Canadian Medical Association journal = journal de l'Association medicale canadienne*. 2004;170(2):229-38.
2. Carr A. Toxicity of antiretroviral therapy and implications for drug development. *Nature reviews Drug discovery*. 2003;2(8):624-34.
3. Van den Eynde E, Podzamczar D. Switch strategies in antiretroviral therapy regimens. *Expert review of anti-infective therapy*. 2014;12(9):1055-74.
4. Spreen WR, Margolis DA, Pottage JC, Jr. Long-acting injectable antiretrovirals for HIV treatment and prevention. *Current opinion in HIV and AIDS*. 2013;8(6):565-71.
5. Manjunath N, Yi G, Dang Y, Shankar P. Newer gene editing technologies toward HIV gene therapy. *Viruses*. 2013;5(11):2748-66.
6. Tang MW, Shafer RW. HIV-1 antiretroviral resistance: scientific principles and clinical applications. *Drugs*. 2012;72(9):e1-25.
7. Pennings PS. HIV Drug Resistance: Problems and Perspectives. *Infectious disease reports*. 2013;5(Suppl 1):e5.
8. Arenas M. Genetic Consequences of Antiviral Therapy on HIV-1. *Computational and mathematical methods in medicine*. 2015;2015:395826.
9. Simeon R, Chen Z. In vitro-engineered non-antibody protein therapeutics. *Protein & cell*. 2017.
10. Ewert S, Honegger A, Pluckthun A. Stability improvement of antibodies for extracellular and intracellular applications: CDR grafting to stable frameworks and structure-based framework engineering. *Methods*. 2004;34(2):184-99.
11. Vazquez-Lombardi R, Phan TG, Zimmermann C, Lowe D, Jermutus L, Christ D. Challenges and opportunities for non-antibody scaffold drugs. *Drug discovery today*. 2015;20(10):1271-83.
12. Cho US, Xu W. Crystal structure of a protein phosphatase 2A heterotrimeric holoenzyme. *Nature*. 2007;445(7123):53-7.

13. Urvoas A, Guellouz A, Valerio-Lepiniec M, Graille M, Durand D, Desravines DC, et al. Design, production and molecular structure of a new family of artificial alpha-helical repeat proteins (alphaRep) based on thermostable HEAT-like repeats. *Journal of molecular biology*. 2010;404(2):307-27.
14. Chevrel A, Urvoas A, de la Sierra-Gallay IL, Aumont-Nicaise M, Moutel S, Desmadril M, et al. Specific GFP-binding artificial proteins (alphaRep): a new tool for in vitro to live cell applications. *Bioscience reports*. 2015;35(4).
15. Gilbert PB, McKeague IW, Eisen G, Mullins C, Gueye NA, Mboup S, et al. Comparison of HIV-1 and HIV-2 infectivity from a prospective cohort study in Senegal. *Statistics in medicine*. 2003;22(4):573-93.
16. Popper SJ, Sarr AD, Travers KU, Gueye-Ndiaye A, Mboup S, Essex ME, et al. Lower human immunodeficiency virus (HIV) type 2 viral load reflects the difference in pathogenicity of HIV-1 and HIV-2. *The Journal of infectious diseases*. 1999;180(4):1116-21.
17. Engelman A, Cherepanov P. The structural biology of HIV-1: mechanistic and therapeutic insights. *Nature reviews Microbiology*. 2012;10(4):279-90.
18. Barre-Sinoussi F, Chermann JC, Rey F, Nugeyre MT, Chamaret S, Gruest J, et al. Isolation of a T-lymphotropic retrovirus from a patient at risk for acquired immune deficiency syndrome (AIDS). 1983. *Revista de investigacion clinica; organo del Hospital de Enfermedades de la Nutricion*. 2004;56(2):126-9.
19. Barre-Sinoussi F, Chermann JC, Rey F, Nugeyre MT, Chamaret S, Gruest J, et al. Isolation of a T-lymphotropic retrovirus from a patient at risk for acquired immune deficiency syndrome (AIDS). *Science*. 1983;220(4599):868-71.
20. Gheysen D, Jacobs E, de Foresta F, Thiriart C, Francotte M, Thines D, et al. Assembly and release of HIV-1 precursor Pr55gag virus-like particles from recombinant baculovirus-infected insect cells. *Cell*. 1989;59(1):103-12.
21. Liang C, Hu J, Russell RS, Roldan A, Kleiman L, Wainberg MA. Characterization of a putative alpha-helix across the capsid-SP1 boundary that is critical for the multimerization of human immunodeficiency virus type 1 gag. *Journal of virology*. 2002;76(22):11729-37.
22. Henderson LE, Sowder RC, Copeland TD, Oroszlan S, Benveniste RE. Gag precursors of HIV and SIV are cleaved into six proteins found in the mature virions. *Journal of medical primatology*. 1990;19(3-4):411-9.
23. Gelderblom HR. Assembly and morphology of HIV: potential effect of structure on viral function. *Aids*. 1991;5(6):617-37.

24. Wilk T, Gross I, Gowen BE, Rutten T, de Haas F, Welker R, et al. Organization of immature human immunodeficiency virus type 1. *Journal of virology*. 2001;75(2):759-71.
25. Monroe EB, Kang S, Kyere SK, Li R, Prevelige PE, Jr. Hydrogen/deuterium exchange analysis of HIV-1 capsid assembly and maturation. *Structure*. 2010;18(11):1483-91.
26. Freed EO. HIV-1 assembly, release and maturation. *Nature reviews Microbiology*. 2015;13(8):484-96.
27. Sundquist WI, Krausslich HG. HIV-1 assembly, budding, and maturation. *Cold Spring Harbor perspectives in medicine*. 2012;2(7):a006924.
28. Ono A. Relationships between plasma membrane microdomains and HIV-1 assembly. *Biology of the cell*. 2010;102(6):335-50.
29. Ganser-Pornillos BK, Yeager M, Sundquist WI. The structural biology of HIV assembly. *Current opinion in structural biology*. 2008;18(2):203-17.
30. Hill CP, Worthylake D, Bancroft DP, Christensen AM, Sundquist WI. Crystal structures of the trimeric human immunodeficiency virus type 1 matrix protein: implications for membrane association and assembly. *Proceedings of the National Academy of Sciences of the United States of America*. 1996;93(7):3099-104.
31. Gottlinger HG, Sodroski JG, Haseltine WA. Role of capsid precursor processing and myristoylation in morphogenesis and infectivity of human immunodeficiency virus type 1. *Proceedings of the National Academy of Sciences of the United States of America*. 1989;86(15):5781-5.
32. Ono A, Ablan SD, Lockett SJ, Nagashima K, Freed EO. Phosphatidylinositol (4,5) biphosphate regulates HIV-1 Gag targeting to the plasma membrane. *Proceedings of the National Academy of Sciences of the United States of America*. 2004;101(41):14889-94.
33. Chukkapalli V, Hogue IB, Boyko V, Hu WS, Ono A. Interaction between the human immunodeficiency virus type 1 Gag matrix domain and phosphatidylinositol-(4,5)-biphosphate is essential for efficient gag membrane binding. *Journal of virology*. 2008;82(5):2405-17.
34. Borsetti A, Ohagen A, Gottlinger HG. The C-terminal half of the human immunodeficiency virus type 1 Gag precursor is sufficient for efficient particle assembly. *Journal of virology*. 1998;72(11):9313-7.
35. Mateu MG. The capsid protein of human immunodeficiency virus: intersubunit interactions during virus assembly. *The FEBS journal*. 2009;276(21):6098-109.

36. McDermott J, Farrell L, Ross R, Barklis E. Structural analysis of human immunodeficiency virus type 1 Gag protein interactions, using cysteine-specific reagents. *Journal of virology*. 1996;70(8):5106-14.
37. Maldonado JO, Martin JL, Mueller JD, Zhang W, Mansky LM. New insights into retroviral Gag-Gag and Gag-membrane interactions. *Frontiers in microbiology*. 2014;5:302.
38. Didierlaurent L, Houzet L, Morichaud Z, Darlix JL, Mougel M. The conserved N-terminal basic residues and zinc-finger motifs of HIV-1 nucleocapsid restrict the viral cDNA synthesis during virus formation and maturation. *Nucleic acids research*. 2008;36(14):4745-53.
39. Jalaguier P, Turcotte K, Danylo A, Cantin R, Tremblay MJ. Efficient production of HIV-1 virus-like particles from a mammalian expression vector requires the N-terminal capsid domain. *PloS one*. 2011;6(11):e28314.
40. Lapadat-Tapolsky M, Gabus C, Rau M, Darlix JL. Possible roles of HIV-1 nucleocapsid protein in the specificity of proviral DNA synthesis and in its variability. *Journal of molecular biology*. 1997;268(2):250-60.
41. Driscoll MD, Golinelli MP, Hughes SH. In vitro analysis of human immunodeficiency virus type 1 minus-strand strong-stop DNA synthesis and genomic RNA processing. *Journal of virology*. 2001;75(2):672-86.
42. Krausslich HG, Facke M, Heuser AM, Konvalinka J, Zentgraf H. The spacer peptide between human immunodeficiency virus capsid and nucleocapsid proteins is essential for ordered assembly and viral infectivity. *Journal of virology*. 1995;69(6):3407-19.
43. Datta SA, Temeselew LG, Crist RM, Soheilian F, Kamata A, Mirro J, et al. On the role of the SP1 domain in HIV-1 particle assembly: a molecular switch? *Journal of virology*. 2011;85(9):4111-21.
44. Morellet N, Druillennec S, Lenoir C, Bouaziz S, Roques BP. Helical structure determined by NMR of the HIV-1 (345-392)Gag sequence, surrounding p2: implications for particle assembly and RNA packaging. *Protein science : a publication of the Protein Society*. 2005;14(2):375-86.
45. Pettit SC, Moody MD, Wehbie RS, Kaplan AH, Nantermet PV, Klein CA, et al. The p2 domain of human immunodeficiency virus type 1 Gag regulates sequential proteolytic processing and is required to produce fully infectious virions. *Journal of virology*. 1994;68(12):8017-27.
46. Coren LV, Thomas JA, Chertova E, Sowder RC, 2nd, Gagliardi TD, Gorelick RJ, et al. Mutational analysis of the C-terminal gag cleavage sites in human immunodeficiency virus type 1. *Journal of virology*. 2007;81(18):10047-54.

47. Kafaie J, Dolatshahi M, Ajamian L, Song R, Mouland AJ, Rouiller I, et al. Role of capsid sequence and immature nucleocapsid proteins p9 and p15 in Human Immunodeficiency Virus type 1 genomic RNA dimerization. *Virology*. 2009;385(1):233-44.
48. Muller B, Anders M, Akiyama H, Welsch S, Glass B, Nikovics K, et al. HIV-1 Gag processing intermediates trans-dominantly interfere with HIV-1 infectivity. *The Journal of biological chemistry*. 2009;284(43):29692-703.
49. de Marco A, Heuser AM, Glass B, Krausslich HG, Muller B, Briggs JA. Role of the SP2 domain and its proteolytic cleavage in HIV-1 structural maturation and infectivity. *Journal of virology*. 2012;86(24):13708-16.
50. Gottlinger HG, Dorfman T, Sodroski JG, Haseltine WA. Effect of mutations affecting the p6 gag protein on human immunodeficiency virus particle release. *Proceedings of the National Academy of Sciences of the United States of America*. 1991;88(8):3195-9.
51. Garnier L, Ratner L, Rovinski B, Cao SX, Wills JW. Particle size determinants in the human immunodeficiency virus type 1 Gag protein. *Journal of virology*. 1998;72(6):4667-77.
52. Sakuma T, Barry MA, Ikeda Y. Lentiviral vectors: basic to translational. *The Biochemical journal*. 2012;443(3):603-18.
53. Hellmund C, Lever AM. Coordination of Genomic RNA Packaging with Viral Assembly in HIV-1. *Viruses*. 2016;8(7).
54. Lever A, Gottlinger H, Haseltine W, Sodroski J. Identification of a sequence required for efficient packaging of human immunodeficiency virus type 1 RNA into virions. *Journal of virology*. 1989;63(9):4085-7.
55. Abd El-Wahab EW, Smyth RP, Mailler E, Bernacchi S, Vivet-Boudou V, Hijnen M, et al. Specific recognition of the HIV-1 genomic RNA by the Gag precursor. *Nature communications*. 2014;5:4304.
56. McBurney SP, Ross TM. Viral sequence diversity: challenges for AIDS vaccine designs. *Expert review of vaccines*. 2008;7(9):1405-17.
57. Nkeze J, Li L, Benko Z, Li G, Zhao RY. Molecular characterization of HIV-1 genome in fission yeast *Schizosaccharomyces pombe*. *Cell & bioscience*. 2015;5:47.
58. Cohen MS, Gay CL. Treatment to prevent transmission of HIV-1. *Clinical infectious diseases : an official publication of the Infectious Diseases Society of America*. 2010;50 Suppl 3:S85-95.

59. Arts EJ, Hazuda DJ. HIV-1 antiretroviral drug therapy. *Cold Spring Harbor perspectives in medicine*. 2012;2(4):a007161.
60. Hutter G, Nowak D, Mossner M, Ganepola S, Mussig A, Allers K, et al. Long-term control of HIV by CCR5 Delta32/Delta32 stem-cell transplantation. *The New England journal of medicine*. 2009;360(7):692-8.
61. Novembre J, Galvani AP, Slatkin M. The geographic spread of the CCR5 Delta32 HIV-resistance allele. *PLoS biology*. 2005;3(11):e339.
62. Alkhatib G. The biology of CCR5 and CXCR4. *Current opinion in HIV and AIDS*. 2009;4(2):96-103.
63. Lalezari JP, Eron JJ, Carlson M, Cohen C, DeJesus E, Arduino RC, et al. A phase II clinical study of the long-term safety and antiviral activity of enfuvirtide-based antiretroviral therapy. *Aids*. 2003;17(5):691-8.
64. Das K, Arnold E. HIV-1 reverse transcriptase and antiviral drug resistance. Part 1. *Current opinion in virology*. 2013;3(2):111-8.
65. Metifiot M, Marchand C, Pommier Y. HIV integrase inhibitors: 20-year landmark and challenges. *Advances in pharmacology*. 2013;67:75-105.
66. Wensing AM, van Maarseveen NM, Nijhuis M. Fifteen years of HIV Protease Inhibitors: raising the barrier to resistance. *Antiviral research*. 2010;85(1):59-74.
67. Braun K, Frank M, Pipkorn R, Reed J, Spring H, Debus J, et al. HIV-1 capsid assembly inhibitor (CAI) peptide: structural preferences and delivery into human embryonic lung cells and lymphocytes. *International journal of medical sciences*. 2008;5(5):230-9.
68. Sticht J, Humbert M, Findlow S, Bodem J, Muller B, Dietrich U, et al. A peptide inhibitor of HIV-1 assembly in vitro. *Nature structural & molecular biology*. 2005;12(8):671-7.
69. Bukrinskaya AG. HIV-1 assembly and maturation. *Archives of virology*. 2004;149(6):1067-82.
70. Nguyen AT, Feasley CL, Jackson KW, Nitz TJ, Salzwedel K, Air GM, et al. The prototype HIV-1 maturation inhibitor, bevirimat, binds to the CA-SP1 cleavage site in immature Gag particles. *Retrovirology*. 2011;8:101.
71. DaFonseca S, Blommaert A, Coric P, Hong SS, Bouaziz S, Boulanger P. The 3-O-(3',3'-dimethylsuccinyl) derivative of betulinic acid (DSB) inhibits the assembly of virus-like particles in HIV-1 Gag precursor-expressing cells. *Antiviral therapy*. 2007;12(8):1185-203.

72. Dafonseca S, Coric P, Gay B, Hong SS, Bouaziz S, Boulanger P. The inhibition of assembly of HIV-1 virus-like particles by 3-O-(3',3'-dimethylsuccinyl) betulinic acid (DSB) is counteracted by Vif and requires its Zinc-binding domain. *Virology journal*. 2008;5:162.
73. Gonzalez G, DaFonseca S, Errazuriz E, Coric P, Souquet F, Turcaud S, et al. Characterization of a novel type of HIV-1 particle assembly inhibitor using a quantitative luciferase-Vpr packaging-based assay. *PloS one*. 2011;6(11):e27234.
74. Coric P, Turcaud S, Souquet F, Briant L, Gay B, Royer J, et al. Synthesis and biological evaluation of a new derivative of bevirimat that targets the Gag CA-SP1 cleavage site. *European journal of medicinal chemistry*. 2013;62:453-65.
75. Didigu C, Doms R. Gene therapy targeting HIV entry. *Viruses*. 2014;6(3):1395-409.
76. Deeks SG. HIV infection, inflammation, immunosenescence, and aging. *Annual review of medicine*. 2011;62:141-55.
77. Scherer L, Rossi JJ, Weinberg MS. Progress and prospects: RNA-based therapies for treatment of HIV infection. *Gene therapy*. 2007;14(14):1057-64.
78. Klimas N, Koneru AO, Fletcher MA. Overview of HIV. *Psychosomatic medicine*. 2008;70(5):523-30.
79. Gopinath SC. Antiviral aptamers. *Archives of virology*. 2007;152(12):2137-57.
80. Bennett MS, Akkina R. Gene therapy strategies for HIV/AIDS: preclinical modeling in humanized mice. *Viruses*. 2013;5(12):3119-41.
81. Hannon GJ, Rossi JJ. Unlocking the potential of the human genome with RNA interference. *Nature*. 2004;431(7006):371-8.
82. Scolnik PA. mAbs: a business perspective. *mAbs*. 2009;1(2):179-84.
83. Gebauer M, Skerra A. Engineered protein scaffolds as next-generation antibody therapeutics. *Current opinion in chemical biology*. 2009;13(3):245-55.
84. Binz HK, Amstutz P, Kohl A, Stumpp MT, Briand C, Forrer P, et al. High-affinity binders selected from designed ankyrin repeat protein libraries. *Nature biotechnology*. 2004;22(5):575-82.

85. Holliger P, Hudson PJ. Engineered antibody fragments and the rise of single domains. *Nature biotechnology*. 2005;23(9):1126-36.
86. Tamaskovic R, Simon M, Stefan N, Schwill M, Pluckthun A. Designed ankyrin repeat proteins (DARPs) from research to therapy. *Methods in enzymology*. 2012;503:101-34.
87. Boersma YL, Pluckthun A. DARPs and other repeat protein scaffolds: advances in engineering and applications. *Current opinion in biotechnology*. 2011;22(6):849-57.
88. Guellouz A, Valerio-Lepiniec M, Urvoas A, Chevrel A, Graille M, Fourati-Kammoun Z, et al. Selection of specific protein binders for pre-defined targets from an optimized library of artificial helicoidal repeat proteins (alphaRep). *PloS one*. 2013;8(8):e71512.
89. Burg M, Ravey EP, Gonzales M, Amburn E, Faix PH, Baird A, et al. Selection of internalizing ligand-display phage using rolling circle amplification for phage recovery. *DNA and cell biology*. 2004;23(7):457-62.
90. Hong SS, Boulanger P. Protein ligands of the human adenovirus type 2 outer capsid identified by biopanning of a phage-displayed peptide library on separate domains of wild-type and mutant penton capsomers. *The EMBO journal*. 1995;14(19):4714-27.
91. Rakonjac J, Bennett NJ, Spagnuolo J, Gagic D, Russel M. Filamentous bacteriophage: biology, phage display and nanotechnology applications. *Current issues in molecular biology*. 2011;13(2):51-76.
92. Petrenko V. Evolution of phage display: from bioactive peptides to bioselective nanomaterials. *Expert opinion on drug delivery*. 2008;5(8):825-36.
93. Pennock GD, Shoemaker C, Miller LK. Strong and regulated expression of *Escherichia coli* beta-galactosidase in insect cells with a baculovirus vector. *Molecular and cellular biology*. 1984;4(3):399-406.
94. Smith GE, Summers MD, Fraser MJ. Production of human beta interferon in insect cells infected with a baculovirus expression vector. *Molecular and cellular biology*. 1983;3(12):2156-65.
95. Jarvis DL. Baculovirus-insect cell expression systems. *Methods in enzymology*. 2009;463:191-222.
96. Murphy CI, Piwnica-Worms H. Overview of the baculovirus expression system. *Current protocols in protein science*. 2001;Chapter 5:Unit5 4.

97. McCarron A, Donnelley M, McIntyre C, Parsons D. Challenges of up-scaling lentivirus production and processing. *Journal of biotechnology*. 2016;240:23-30.
98. Helseth E, Kowalski M, Gabuzda D, Olshevsky U, Haseltine W, Sodroski J. Rapid complementation assays measuring replicative potential of human immunodeficiency virus type 1 envelope glycoprotein mutants. *Journal of virology*. 1990;64(5):2416-20.
99. Page KA, Landau NR, Littman DR. Construction and use of a human immunodeficiency virus vector for analysis of virus infectivity. *Journal of virology*. 1990;64(11):5270-6.
100. Akkina RK, Walton RM, Chen ML, Li QX, Planelles V, Chen IS. High-efficiency gene transfer into CD34+ cells with a human immunodeficiency virus type 1-based retroviral vector pseudotyped with vesicular stomatitis virus envelope glycoprotein G. *Journal of virology*. 1996;70(4):2581-5.
101. Zufferey R, Nagy D, Mandel RJ, Naldini L, Trono D. Multiply attenuated lentiviral vector achieves efficient gene delivery in vivo. *Nature biotechnology*. 1997;15(9):871-5.
102. Yu SF, von Ruden T, Kantoff PW, Garber C, Seiberg M, Ruther U, et al. Self-inactivating retroviral vectors designed for transfer of whole genes into mammalian cells. *Proceedings of the National Academy of Sciences of the United States of America*. 1986;83(10):3194-8.
103. Dull T, Zufferey R, Kelly M, Mandel RJ, Nguyen M, Trono D, et al. A third-generation lentivirus vector with a conditional packaging system. *Journal of virology*. 1998;72(11):8463-71.
104. Kim VN, Mitrophanous K, Kingsman SM, Kingsman AJ. Minimal requirement for a lentivirus vector based on human immunodeficiency virus type 1. *Journal of virology*. 1998;72(1):811-6.
105. Wright JK, Brumme ZL, Carlson JM, Heckerman D, Kadie CM, Brumme CJ, et al. Gag-protease-mediated replication capacity in HIV-1 subtype C chronic infection: associations with HLA type and clinical parameters. *Journal of virology*. 2010;84(20):10820-31.
106. Brockman MA, Brumme ZL, Brumme CJ, Miura T, Sela J, Rosato PC, et al. Early selection in Gag by protective HLA alleles contributes to reduced HIV-1 replication capacity that may be largely compensated for in chronic infection. *Journal of virology*. 2010;84(22):11937-49.
107. Lee VS, Tue-ngeun P, Nangola S, Kitidee K, Jitonnorn J, Nimmanpipug P, et al. Pairwise decomposition of residue interaction energies of single chain Fv

with HIV-1 p17 epitope variants. *Molecular immunology*. 2010;47(5):982-90.

108. Kitidee K, Nangola S, Hadpech S, Laopajon W, Kasinrerak W, Tayapiwatana C. A drug discovery platform: a simplified immunoassay for analyzing HIV protease activity. *Journal of virological methods*. 2012;186(1-2):21-9.
109. Wu CH, Liu JJ, Lu RM, Wu HC. Advancement and applications of peptide phage display technology in biomedical science. *Journal of biomedical science*. 2016;23:8.
110. Santiago-Tirado FH, Doering TL. All about that fat: Lipid modification of proteins in *Cryptococcus neoformans*. *Journal of microbiology*. 2016;54(3):212-22.
111. Zaccarelli M, Tozzi V, Lorenzini P, Trotta MP, Forbici F, Visco-Comandini U, et al. Multiple drug class-wide resistance associated with poorer survival after treatment failure in a cohort of HIV-infected patients. *Aids*. 2005;19(10):1081-9.
112. Perez-Pinera P, Ousterout DG, Gersbach CA. Advances in targeted genome editing. *Current opinion in chemical biology*. 2012;16(3-4):268-77.
113. Urnov FD, Rebar EJ, Holmes MC, Zhang HS, Gregory PD. Genome editing with engineered zinc finger nucleases. *Nature reviews Genetics*. 2010;11(9):636-46.
114. Joung JK, Sander JD. TALENs: a widely applicable technology for targeted genome editing. *Nature reviews Molecular cell biology*. 2013;14(1):49-55.
115. Perez-Pinera P, Kocak DD, Vockley CM, Adler AF, Kabadi AM, Polstein LR, et al. RNA-guided gene activation by CRISPR-Cas9-based transcription factors. *Nature methods*. 2013;10(10):973-6.
116. Chandrasegaran S, Carroll D. Origins of Programmable Nucleases for Genome Engineering. *Journal of molecular biology*. 2016;428(5 Pt B):963-89.
117. Leader B, Baca QJ, Golan DE. Protein therapeutics: a summary and pharmacological classification. *Nature reviews Drug discovery*. 2008;7(1):21-39.
118. Chames P, Van Regenmortel M, Weiss E, Baty D. Therapeutic antibodies: successes, limitations and hopes for the future. *British journal of pharmacology*. 2009;157(2):220-33.

119. Chiu ML, Gilliland GL. Engineering antibody therapeutics. *Current opinion in structural biology*. 2016;38:163-73.
120. Tobin PH, Richards DH, Callender RA, Wilson CJ. Protein engineering: a new frontier for biological therapeutics. *Current drug metabolism*. 2014;15(7):743-56.
121. Sakkhachornphop S, Jiranusornkul S, Kodchakorn K, Nangola S, Sirisanthana T, Tayapiwatana C. Designed zinc finger protein interacting with the HIV-1 integrase recognition sequence at 2-LTR-circle junctions. *Protein science : a publication of the Protein Society*. 2009;18(11):2219-30.
122. Nangola S, Urvoas A, Valerio-Lepiniec M, Khamaikawin W, Sakkhachornphop S, Hong SS, et al. Antiviral activity of recombinant ankyrin targeted to the capsid domain of HIV-1 Gag polyprotein. *Retrovirology*. 2012;9:17.
123. Khamaikawin W, Saoin S, Nangola S, Chupradit K, Sakkhachornphop S, Hadpech S, et al. Combined Antiviral Therapy Using Designed Molecular Scaffolds Targeting Two Distinct Viral Functions, HIV-1 Genome Integration and Capsid Assembly. *Molecular therapy Nucleic acids*. 2015;4:e249.
124. Sakkhachornphop S, Barbas CF, 3rd, Keawwichit R, Wongworapat K, Tayapiwatana C. Zinc finger protein designed to target 2-long terminal repeat junctions interferes with human immunodeficiency virus integration. *Human gene therapy*. 2012;23(9):932-42.
125. Muriaux D, Mirro J, Harvin D, Rein A. RNA is a structural element in retrovirus particles. *Proceedings of the National Academy of Sciences of the United States of America*. 2001;98(9):5246-51.
126. Racine PJ, Chamontin C, de Rocquigny H, Bernacchi S, Paillart JC, Mougél M. Requirements for nucleocapsid-mediated regulation of reverse transcription during the late steps of HIV-1 assembly. *Scientific reports*. 2016;6:27536.

LIST OF PUBLICATIONS

- 1.) Kitidee K, Nangola S, **Hadpech S**, Laopajon W, Kasinrerak W, Tayapiwatana C. A drug discovery platform: a simplified immunoassay for analyzing HIV protease activity. *Journal of virological methods*. 2012;186(1-2):21-9.
- 2.) Khamaikawin W, Saoin S, Nangola S, Chupradit K, Sakkhachornphop S, **Hadpech S**, et al. Combined Antiviral Therapy Using Designed Molecular Scaffolds Targeting Two Distinct Viral Functions, HIV-1 Genome Integration and Capsid Assembly. *Molecular therapy Nucleic acids*. 2015;4:e249.

APPENDIX A

LIST OF THE CHEMICALS AND INSTRUMENTS

1. Chemicals

All chemicals used as in this study were analytical grade reagents.

Chemical name	Source
4', 6-diamidino-2-phenylindole (DAPI)	Molecular Probes, Eugene, OR, USA
Acrylamide	Biorad, Hercules, CA, USA
Agarose (electrophoresis grade)	Sigma-Aldrich. St.Louis, MO, USA
Amersham Hybond TM -ECL	GE healthcare Bio-Sciences Co. Piscataway, NJ , USA
Ampiillin	Sigma-Aldrich. St.Louis, MO, USA
β -mercaptoethanol	Gibco, Grand Island, NY, USA
Basic fibroblast growth factor (bFGF)	R&D Systems, Minneapolis, MN, USA
Blasticidine	Gibco, Grand Island, NY, USA
Bovine Serum Albumin (BSA)	EMD Millipore Corp., Billerica, MA, USA

Chemical name	Source
COBAS [®] AMPLICOR HIV-1 Monitor Test, v1.5	Roche Molecular Systems, Branchburg, NJ, USA
Dulbecco's Modified Eagle's medium (DMEM)	Gibco, Grand Island, NY, USA
Dimethyl sulfoxide (DMSO)	Sigma-Aldrich, St.Louis, MO, USA
EDTA	Sigma-Aldrich. St.Louis, MO, USA
Ethanol	Merck, Darmstadt, Germany
Ethidium bromide	Sigma-Aldrich. St.Louis, MO, USA
Fetal bovine serum (FBS)	HyClone, Cramlington, UK
GeneJet [™] PCR purification kit	Thermo Scientific, Rockford, IL, USA
Genscreen ULTRA HIV Ag-Ab assay	Bio-Rad, Marnes-la-Coquette, France
Glacial acetic acid	BDH Laboratory Supplies, UK
Glycerol	Sigma-Aldrich. St.Louis, MO, USA
High Pure PCR Template Preparation Kit	Roach, Mannheim, Germany
KOD Hot Start DNA polymerase	Novagen, Madison, WI, USA
LB Broth Agar	Bio Basic inc., Ontario, Canada
Lipofectamine	Invitrogen, Carlsbad, CA, USA
Micro-BCA protein assay	Pierce, Rockford, IL, USA
Millipore Millex-HA filter unit, 0.45µm	Merck Millipore, Hessen, Germany
NaCl	Sigma-Aldrich. St.Louis, MO, USA

Chemical name	Source
NaOH	Sigma-Aldrich. St.Louis, MO, USA
Non-essential amino acid (NEAA)	Millipore Corporation, Billerica, MA, USA
Paraformaldehyde	Sigma-Aldrich. St.Louis, MO, USA
Penicillin	Gibco, Grand Island, NY, USA
Plus Reagent	Invitrogen, Carlsbad, CA, USA
Phosphate Buffered Saline (PBS)	EMD Millipore Corp., Billerica, MA, USA
Q5™ High-Fidelity DNA Polymerase	NEB Biolab, Ipswich, MA
QIAGEN Miniprep Kit	Qiagen, Hilden, Germany
Quick change® lightning site-directed mutagenesis kit	Stratagene, La Jolla, CA, USA
Triton X-100	Sigma-Aldrich. St.Louis, MO, USA
Trypan Blue 0.2%	Sigma-Aldrich. St.Louis, MO, USA
Tryptone water	Merck, Darmstadt, Germany
Tween 20	Fluka, Buchs, Switzerland
Yeast extract	Bio Basic inc., Ontario, Canada

Instruments

Instruments	Source
37 °C CO ₂ incubator EG 115 IR	Jouan GmbH, Unterhaching, Germany
37 °C incubator	JP Selecta, Barcelona, Spain
Bio-Plex 200	Bio-Rad, Hercules, CA, USA
BioRad Chemidoc XRS Gel Documentation System	BioRad, Hercules, CA, USA
BioTek Synergy™ 4 Hybrid Microplate Reader	BioTek Instruments, Winooski, VT, USA
BECKMAN L-60 ultracentrifuge	Beckman Coulter, Fullerton, CA, USA
Electrophoretic power supply 3000Xi	BioRad, Hercules, CA, USA
Flow cytometer (BD FACSCalibur™)	BD Biosciences, San Diego, CA, USA
Flow cytometer (BD Accuri™ C6)	BD Biosciences, San Diego, CA, USA
Shaking incubator (JSSI-100C)	JS Research Inc., Gongju-city, Korea
Inverted microscope	Olympus, Japan
Laminar Flow biological safety cabinet	NUAIRE, Plymouth, MN, USA
Microcentrifuge	Eppendorf AG, Hamburg, Germany
Microplate	NUNC, Roskilde, Denmark

Instruments	Source
MJ Mini™ Thermal Cycler and MiniOpticon™ Real-Time PCR System	BioRad, Hercules, CA, USA
MRX-150 Refrigerated microcentrifuge	Tomy Tech USA Inc., CA, USA
MTP-120 ELISA plate reader	Corona Electric, Japan
NanoDrop 2000	ThermoScientific, Rockford, IL, USA
Ultrasonic Processor UP100H	Hielscher, Teltow, Germany
UV spectrophotometer	Shimadzu Scientific Instruments Inc, Kyoto, Japan
UV-2450/2550 spectrophotometer	Shimadzu, Columbia, MD, USA
Vortex-Genie K-550-GE	Scientific Industries Inc, Bohemia, NY, USA

APPENDIX B

LIST OF CELL LINES AND MICROORGANISMS

1. Cell lines

Name	Type of cell lines
Jurkat-GFP	Human T cell lymphocytic cell line
HeLa	Cervical carcinoma cells
HEK293T	Human embryonic kidney cells
Sf9	Insect cell line
SupT1	Human T cell lymphocytic cell line

2. Microorganisms

Name	Genotype
<i>Escherichia coli</i> XL-1 Blue MRF'	Genotype: $\Delta(mcrA)183 \Delta(mcrCB-hsdSMR-mrr)173 endA1 supE44 thi-1 recA1 gyrA96 relA1 lac [F' proAB lacI^qZ\Delta M15 Tn10 (Tet^r)]$
<i>Escherichia coli</i> M15 [pREP4]	Genotype: <i>Lac ara gal mtl recA+ uvr+ [pREP4 lacI kanar]</i>
<i>Escherichia coli</i> BL21(DE3)	Genotype: <i>fhuA2 [lon] ompT gal (λ DE3) [dcm] $\Delta hsdS \lambda$ DE3 = λ sBamHIo $\Delta EcoRI-B int::(lacI::PlacUV5::T7 gene1) i21 \Delta nin5$</i>

APPENDIX C

REAGENT PREPARATIONS

1. Reagents for gel electrophoresis

1.1 10× Tris-acetate/EDTA electrophoresis buffer (TAE)

Tris-base	48.40	gm
Glacial acetic acid	11.42	ml
0.5 M EDTA, pH 8.0	20	ml

Dissolved all ingredients in deionized distilled water and filled up to 1,000 ml.
Sterilized by autoclave and kept at room temperature.

1.2 1% or 2 % Agarose gel

Agarose	1 or 2	gm
1× TAE	100	ml

Melted by microwave oven until the agarose was completely dissolved.

1.3 Ethidium bromide working solution (10 mg/ml)

Ethidium bromide	1.0	gm
Distilled water	100	ml

Dissolved and kept in dark bottle at 4 °C

1.4 6X gel loading buffer

Bromphenol blue	0.25	%
Glycerol	30	%

Mixed thoroughly and stored at -20 °C

2. Medium for bacterial culture

2.1 50% glucose

D-glucose	5 gm
-----------	------

Added distilled water to 10 ml and boiled in boiling water.

Filtered through 0.2 µm Millipore filter and stored at 4 °C

2.2 2XTY broth

Yeast extract	1.0 gm
---------------	--------

Tryptone	1.60 gm
----------	---------

NaCl	0.5 gm
------	--------

Dissolved all ingredients in 100 ml distilled water

Sterilized by autoclave, and kept at 4 °C

2.3 LB broth

Yeast extract	5.0 gm
---------------	--------

Tryptone	10.0 gm
----------	---------

NaCl	10.0 gm
------	---------

Dissolved all ingredients in 1,000 ml distilled water

Sterilized by autoclave, and kept at 4 °C

2.4 LB agar

LB agar	15 gm
---------	-------

Dissolved all ingredients in 1,000 ml distilled water.

Sterilized by autoclave, poured on Petri dish (plate) and stored at 4 °C

2.5 Super broth

Yeast extract	2.0	gm
Tryptone	3.0	gm
Morpholinepropanesulphonic acid (MOPS)	1.0	gm

Added distilled water to 10 ml and boiled in boiling water.

Filtered through 0.2 μ m Millipore filter and stored at 4 °C

2.6 Terrific broth

Yeast extract	24.0	gm
Tryptone	12.0	gm
Glycerol	4	ml
dH ₂ O up to	900	ml

Autoclaved and kept at 4 °C

Added filtered buffer 100 ml

TR Buffer 500 ml

0.17 M KH ₂ PO ₄	11.57	gm
0.72 M K ₂ HPO ₄	62.17	gm
dH ₂ O	500	ml

3. Reagents for fluorescence microscopy and flow cytometry analysis

3.1 4% Paraformaldehyde in PBS

Paraformaldehyde	4	gm
PBS pH 7.2	100	ml

Heat at 56°C until dissolved

Filtered with 0.2 μ m Millipore filter, stored at 4°C

3.2 1% BSA-PBS- NaN_3

BSA	1	gm
NaN_3	0.09	gm
Dissolved in PBS 100 ml		

3.3 0.2% Triton X-100

Triton X-100	0.2	ml
Dissolved in PBS 100 ml		

4. Reagents for cell culture

4.1 RPMI-1640 medium

RPMI powder	1	pack
NaHCO_3	2	gm
ddH ₂ O	800	ml
Penicillin (100 U/ml)/Streptomycin (100 $\mu\text{g/ml}$)	1	ml

Stirred until dissolved and adjusted volume into 1,000 ml.

Filtered through 0.2 μm Millipore membrane filter.

Mixed and stored at 4 °C.

4.2 Complete RPMI culture medium

RPMI 1640 medium	90	ml
Fetal bovine serum (FBS)	10	ml

Checked sterility before use.

4.3 DMEM medium

DMEM powder	1	pack
NaHCO_3	3.7	gm
ddH ₂ O	800	ml
Penicillin (100 U/ml)/Streptomycin (100 $\mu\text{g/ml}$)	1	ml

Stirred until dissolved and adjusted volume into 1,000 ml.

Filtered through 0.2 μm Millipore membrane filter.

Mixed and stored at 4 °C.

4.4 Complete DMEM culture medium

DMEM medium	90	ml
Fetal bovine serum (FBS)	10	ml

Checked sterility before use.

4.5 Freezing medium (10%DMSO in 90%FCS)

Fetal bovine serum (FBS)	9	ml
DMSO	1	ml

Fresh preparation before use.

4.6 Trypan blue (0.2%)

Trypan blue powder	0.2	gm
PBS pH 7.2	100	ml

Filtered by Whatman filter paper No. 1 and

Stored at room temperature.

5. Reagents for Calcium Phosphate co-transfection

5.1 2x HBS

NaCl	8	gm
KCL	0.37	gm
Na ₂ HPO ₄	106.5	gm
Dextrose	1	gm
HEPES	5	gm
ddH ₂ O	400	ml

Stirred until dissolved and adjusted pH into to 7.05 with NaOH

Added volume with ddH₂O into 500 ml.

Filtered through 0.2 µm Millipore membrane filter.

Mixed and stored at -20 °C.

5.2 2.5 M CaCl₂

CaCl ₂ (Mw. 111 g)	13.88	gm
ddH ₂ O	30	ml

Stirred until dissolved and adjusted volume into 50 ml.

Filtered through 0.2 µm Millipore membrane filter.

Mixed and stored at -20 °C.

5.3 0.1% TE buffer

TE buffer	100	µl
-----------	-----	----

Added ddH₂O to 100 ml

Filtered through 0.2 µm Millipore membrane filter.

Mixed and stored at 4 °C.

6. Reagents for luciferase activity assay

6.1 Cell lysis solution for luciferase assay (Clontech)

100 mM Potassium phosphate pH 7.8, 0.2% TritonX-100

K ₂ HPO ₄ 100 mM	9.15	ml
KH ₂ PO ₄ 100 mM	0.85	ml
Triton X-100 (0.2% final)	20	µl
DTT 1 M	10	µl

Added DTT just prior to use

Kept on ice until to use

6.2 Luciferase assay substrate

Tris acetate pH 7.8 0.1 M	2.5	ml
DTT 1 M	410	μl
EDTA 0.5 M	2.5	μl
MgSO ₄ 1 M	46.7	μl
CoA 10 mM	340	μl
ATP 50 mM	125	μl
Luciferin 10 mM	590	μl
dH ₂ O	5.98	ml

CURRICULUM VITAE

Name	Miss Sudarat Hadpech
Date of birth	September 20 th , 1988
Place of birth	Nan Province, Thailand
Education	
2011	B.Sc. (Medical Technology), Faculty of Associated Medical Sciences, Chiang Mai University, Thailand.
Experiences	
2011-2012	Research assistance
Publications	
1. Kitidee K, Nangola S, Hadpech S , Laopajon W, Kasinrerker W, Tayapiwatana C. A drug discovery platform: a simplified immunoassay for analyzing HIV protease activity. Journal of virological methods. 2012;186(1-2):21-9.	
2. Khamaikawin W, Saoin S, Nangola S, Chupradit K, Sakkhachornphop S, Hadpech S , et al. Combined Antiviral Therapy Using Designed Molecular Scaffolds Targeting Two Distinct Viral Functions, HIV-1 Genome Integration and Capsid Assembly. Molecular therapy Nucleic acids. 2015;4:e249.	

Presentations

1. Antiviral effects of alpha-helicoidal HEAT-like repeat protein scaffolds (α Rep) targeting the SP1-NC (spacer peptide-nucleocapsid) domain of the HIV-1 Gag polyprotein. RETROPATH 2015: The 27th International workshop on Retroviral Pathogenesis, Universität Duisburg-Essen, Institut für virologie, Die Wolfsburg, Falkenweg 6, 45478 Mülheim an der Ruhr, Germany, August, 2015. (Poster presentation)
2. Design and functional studies of alpha-repeat protein scaffolds targeting domains of HIV-1 Gag polyprotein. 11th International Symposium of the Protein Society of Thailand, Protein Society of Thailand, Chulabhorn Research Institute Convention Center Bangkok, August, 2016. (Oral presentation)
3. Development of Alpha-Helicoidal HEAT-like Repeat Protein Scaffolds (α Rep) for HIV-1 Assembly Inhibition Targeting Capsid-Nucleocapsid Domain of Pr55Gag Polyprotein. วันวิชาการ มหาวิทยาลัยเชียงใหม่ ครั้งที่ 11, Chiang Mai University, Chiang Mai, Thailand, November 2016. (Poster presentation)

